Universidad del País Vasco Euskal Herriko Unibertsitatea

KIMIKA FAKULTATEA

FACULTAD DE QUÍMICA

Universidad del País Vasco/Euskal Herriko Unibertsitatea

Facultad de Química/Kimika Fakultatea

Grado en Química

TRABAJO FIN DE GRADO

3D printed hydrogels for oral personalized medicine

Autor/a: Itziar Insua Castellanos

Dirigido por: Robert Aguirresarobe Hernández

San Sebastián, Junio de 2021

GIPUZKOAKO CAMPUSA

CAMPUS DE GIPUZKOA

Pº. Manuel de Lardizabal, 3

20018 DONOSTIA-SAN SEBASTIAN

GIPUZKOA

1. PREFACE

The bachelor's degree thesis presented below is entitled "3D printed hydrogels for oral personalized medicine ". The basis of this research on rheology has been carried out in Donostia/San Sebastián. This paper has been written as part of the graduation requirements for the Chemistry degree of the UPV/EHU. The period of research and writing of this end-of-degree work has lasted from October to June 2021.

The project was carried out at the request of Polymat, where I did my thesis. The main focus of the work was decided with my tutor, Robert Aguirresarobe, as well as with a PhD student who was guided me through the thesis, Oliver Etzold. Fortunately, both have always been available and willing to help me with all my questions. The research process has been tedious, but conducting a thorough study has allowed me to learn more about both rheology and oral drug delivery.

I would therefore like to thank my supervisors for their excellent guidance and support throughout the process of carrying out my work. I would also like to thank my parents for giving me the opportunity to study and for being there whenever I needed them. Finally, I would also like to thank my boyfriend and friends who have cheered me in the process of writing this thesis.

2. ABBREVIATIONS

- 2D→ two dimensional
- 3D → three dimensional
- ALM→ additive layer manufacturing
- AM→ additive manufacturing
- API→ active pharmaceutical ingredient
- CAD→ computer-aided design
- CMC→ carboxymethyl cellulose
- DLP→ inkjet printing and digital light processing
- FDC→ fixed dose combination
- FDM→ fused deposition modelling
- G'→ storage modulus
- G''→ loss modulus
- GI→ gastrointestinal
- GIT→ gastrointestinal tract
- HCTZ → hydrochloric thiazide
- LVE→ linear-viscoelastic regime
- PAM→ pressure-assisted microsyringe
- PEG→ polyethylene glycol
- PEO→ polyethylene oxide
- SEM→ scanning electron microscope
- SLA→ stereolithography
- SLS→ selective laser sintering
- STL→ standard triangle language

3.1 ABSTRACT

3D printing has become a promising and revolutionary pill-making technique for the pharmaceutical industry, enabling a relatively low-cost personalized medicine. Fused deposition modelling, also known by its initials FDM, is the most affordable technology for this goal, printing the material by a layer-by-layer deposition. However, the pressure assisted microsyringe technique is more adequate for working with drug containing inks as it does not need high temperatures, preventing the drug degradation. However, to make this goal possible, high accuracy and reproducibility is required, avoiding trial and error procedures. Thus, a correlation between rheology, printing parameters and the printed object was investigated. This way predicting the printing process just by looking at the materials rheology can be achieved. In fact, even though there are a lot of oral drug delivery and 3D printing related articles, there are only a few that focus on the relation between the rheology and the printing conditions of the sample. Thus, this thesis will try to expand this research area.

As the basis of this thesis hydrogels containing different drugs were selected. Hydrogel formulations with two different bases have been prepared, one based in polyethylene glycol and the other one based in glycerol. In addition, carboxymethyl cellulose and water were present in all the mixtures prepared by mixing the components with different concentrations. The drugs contained within are atenolol and hydrochloric thiazide (HCTZ), both being antihypertensive drugs. The preparation of the formulations was simple and it could easily be translated to other drugs and scaled-up. It has been shown that glycerol-based compositions have better rheological properties for the pill making purpose. The effects of atenolol and HCTZ on the prepared hydrogels were studied as well as the relation between the drugs and the polymeric matrix with the final objective of printing a multicomponent formulation, also called polypill.

Finally, the morphology of the 3D printed objects has been examined after the consolidating process and after a pH test and lyophilization. This way the effect of the stomach's acidic environment on the drug delivery systems has been studied. The contained carboxymethyl cellulose (CMC) was supposed to have a pH responsive behaviour collapsing under acidic environments. But it has been shown by morphological characterization that it is not suitable for this purpose. Even though they showed that they do not fit their purpose of protecting the drug at acidic conditions, rheological studies and the 3D printing process for glycerol-based formulations showed that they have good shape fidelity to the CAD design.

Improving such formulations could lead to good resolution pills that fit the purpose of protecting the incorporated drug from degrading at the acidic pH of the stomach. A personalized medicine could be achieved by such formulations.

3.2 RESUMEN

La impresión 3D se ha convertido en una técnica prometedora y revolucionaria para la fabricación de pastillas en la industria farmacéutica, lo que permite una medicina personalizada de costo relativamente bajo. El modelado de deposición fundida, también conocido por sus iniciales FDM, es la tecnología más asequible para este objetivo, imprimiendo el material mediante una deposición capa por capa. Sin embargo, la técnica de microjeringa asistida por presión es más adecuada para trabajar con tintas que contienen fármacos, ya que no necesita altas temperaturas y previene la degradación de los mismos.

Se han preparado formulaciones de hidrogel con dos bases diferentes, una a base de polietilenglicol y otra a base de glicerol. Los fármacos implementados en ellos son atenolol e hidroclorotiazida (HCTZ), ambos fármacos antihipertensivos. La carboximetilcelulosa y el agua estaban presentes en las nueve mezclas preparadas y se mezclan los componentes con diferentes concentraciones en cada mezcla. De hecho, su preparación es muy sencilla, requiriendo únicamente mezclar los componentes en las cantidades necesarias. Por lo tanto, podría traducirse fácilmente a otros medicamentos y ampliarse su uso.

Se estudia el efecto de atenolol y HCTZ sobre los hidrogeles preparados, así como la relación entre los fármacos y la matriz polimérica con el objetivo de imprimir un fármaco multicomponente, también llamado polipíldora.

Se investiga también una correlación entre la reología, los parámetros de impresión y el objeto impreso. De esta manera se podría lograr predecir el proceso de impresión con conocer la reología de los materiales. De hecho, a pesar de que hay una gran cantidad de artículos sobre fármacos orales y artículos relacionados con la impresión 3D, sólo hay unos pocos que se centran en la relación entre la reología y las condiciones de impresión de la muestra. Así, esta tesis tratará de ampliar esta área de investigación.

Finalmente, se ha analizado la morfología del objeto impreso tras el proceso de consolidación y tras un test de pH y liofilización. De esta manera se ha estudiado el efecto del ambiente ácido estomacal sobre los sistemas de administración de fármacos. La carboximetil celulosa (CMC) contenida debería mostrar un comportamiento responsivo al

pH, colapsando en ambientes ácidos. En cambio, se ha observado por caracterización morfológica que no es adecuada para este propósito.

Se ha demostrado que las composiciones a base de glicerol tienen mejores propiedades reológicas para el propósito de fabricación de píldoras, a pesar de no ajustarse a su propósito de proteger el medicamento en condiciones ácidas, ya que los estudios reológicos y el proceso de impresión 3D mostraron que tienen una buena fidelidad al diseño CAD.

La mejora de tales formulaciones podría conducir a píldoras de buena resolución que se ajustan al propósito de proteger el fármaco incorporado de la degradación en el pH ácido del estómago. Finalmente, una medicina personalizada se puede lograr mediante estas formulaciones si se desarrollan lo suficiente para ser asequibles.

4. INDEX

5. INTRODUCTION

With the advent of modern medicine, people all over the world have been looking for effective ways to treat medical conditions in a minimally invasive and even non-invasive way to improve patient compliance, thus contradicting the Latin proverb *Aegrescit medendo* - remedies are often worse than the disease. Efficient oral delivery could be the answer sought, as it is very complaint, especially with chronic patients, due to being non-invasive.

Oral drug delivery also opens a new door for personalized medicine as formulations for individual patients have potential to improve adherence to medication and reduce side effects by setting a dose suitable for each individual. Even though 3D printing was not an option until the past two decades for personalized medicine, nowadays it offers the possibility to fabricate pills on an individual scale at acceptable costs.

Thus, tailoring formulations to a patient is no longer a fiction; lot of research has been done in the past decades to progress. Finally, this thesis will try to contribute its little grain of sand in the mentioned topic.

5.1 3D PRINTING

3D printing is an advanced manufacturing technology that typically works by layer-by-layer deposition of the material to prototype computer designed models. [1] Additive manufacturing (AM) or additive layer manufacturing (ALM) is the industrial production name for the 3D printing method. [2] Conveniently, it does not need any kind of moulds or unit operations and minimum human interaction is needed. In addition, 3D printing creates less material waste as it works the opposite way to subtractive manufacturing processes, where the material is cut from a larger material block. [3] Trained personal is not needed either when the used ink is completely characterized. [4]

Those are the reasons why this method is low-cost compared with other forms of personalized medicine. It allows to design and develop complex dosage forms, suitable for tuning drug release.[5] Recently, 3D printing has gained interest for pharmaceutical manufacturing.

Most 3D printing processes follow the same procedure for the manufacturing, even though each method has its own operating principles. [4] The design of the material in the software is the same for all the methods; it can be rendered either in 3D as a final product

or in 2D as the layers needed for the printing process. In all the layer-by-layer printing methods the final design should be in 2D in order to obtain the layer-by-layer instructions for the printer. In addition, the printed material should consolidate once it is printed to obtain the desired product. [6]

With this method, innovative medical devices and customized drug delivery systems can be achieved. 3D printing technology offers the option of loading multiple drugs into a single matrix that could act like a multifunctional polypill having different release profiles for each drug. [7] It also allows to make a variety of quality products in minutes, which is a huge advance compared with traditional manufacturing. [4] Furthermore, the same 3D printing equipment can print a limitless variety of products. This technique is unique in terms of product complexity, flexibility and throughput. [8] As a highly automated process with minimal operating cost, 3D printing has a future for on-demand production. [2]

Some of the characteristics where 3D printing distinguishes itself from traditional manufacturing processes are product complexity, personalization, and on-demand manufacturing, as mentioned before (Figure 1). In terms of complexity and on-demand fabrication, 3D printing allows using low-stability drugs for immediate consumption. [9] In general, there are more personalized options with 3D printing than with traditional drug manufacturing. First, 3D printing works with a digital design that can be more easily modified than a physical equipment. Second, this method allows to tailor the specific amount of drug needed by each subject which varies with patients mass and metabolism. [10] It is especially important to ensure accurate dosing in children and for the dosing of highly potent drugs. [11] Finally, multi-drug polypills can be made to combine all of a patient's medications into a single daily dose, which fits both in complexity improvement and personalization. These preparations could improve patients adherence to medication. [12] All the potential benefits of 3D printed products are resumed in Table 1.

Figure 1. Representation of a traditional mass manufacturing system vs the 3D printing method. [111], [112]

Table 1. Resume of the potential benefits of 3D-printed drug products adapted from [4].

BENEFIT CATEGORY	3D PRINTING CAPABILITIES	EXAMPLE USES FOR DRUG DELIVERY	POTENTIAL MEDICAL AND ECONOMIC BENEFITS
INCREASED PRODUCT COMPLEXITY	Un-mouldable. Difficult-to-make shapes.	Highly porous products that orally disintegrate. Products with approximately zero-order release.	Improved adherence. Improved drug effectiveness. Reduced side effects. New therapies based on combination products.
	Digitally controlling the arrangement of matter.	Excipient gradients that modify drug release. Control over API form during printing. Complex drug-device combination products.	
PERSONALIZATION	Infinite variety of shapes with same equipment.	Personalized dosing for potent drugs. Personalized dosing for growing children. Drug-loaded implants that match the anatomy of individual patients. Custom shapes for children.	Reduced side effects. Appropriate doses for children. Reduced complications after implantation. Improved paediatric adherence.
	Varying composition within simple designs.	"Polypills" that combine different drugs and release mechanisms into single doses. Hollow products with variable in-fill to control drug release rate.	Reduced medical burden for the elderly. Appropriate drug release based on a patient's anatomy and drug metabolism.
ON-DEMAND MANUFACTURING	Rapid printing from digital designs. No intermediate machining.	Printing in emergency settings. Printing directly onto patients. Reducing barriers to experimentation during drug product development.	Expanded capabilities for surgery and emergency medicine. Reduced time to market for new drugs.
	Printing at the point-of-care.	Drugs with limited shelf lives.	New drugs.

As manufacturers and researchers gain experience with this innovative method, ways to increase speed and resolution and to print new materials are being discovered, as well as more complex inks for specific purposes. [13]

Despite the promising benefits of the technique, there are some challenges involving the 3D printing for the fabrication of drug delivery systems. Traditional mass manufacturing cannot be replaced by 3D printing due to its disability to print large quantities. [14] The material plays an important role in a successful print; hence, it needs to have appropriate physical and rheological characteristics. Moreover, low concentrations of drug are needed in order to prevent clogging of the tip, limiting the 3D printing method for

drugs that need high therapeutic doses. However, for drugs with narrow therapeutic windows, precise, accurate and reproducible doses can be obtained. [15]

Another problem is that obtaining a functional ink is quite difficult where good features like bioadhesion and suitable release profiles are needed for the ink to be valid for this technique. Polymers are key materials for this purpose. [16] There are an increasing number of reports of 3D printing being used to manufacture medicines, but for its use to become widespread, consideration must be given to the specific requirements and problems briefly described.

5.1.1 METHODS FOR 3D PRINTING

The most common methods used for drug printing can be categorized in three main ones: powder based, light assisted printings and material extrusion printing. **Powder-based printing** splits in two: powder bed and powder jetting. **Light assisted printings** include stereolithography (SLA), selective laser sintering (SLS), inkjet printing and digital light processing (DLP) while **material extrusion**, can be divided into fused deposition modelling (FDM) and pressure-assisted microsyringes (PAM)) [17], [18]

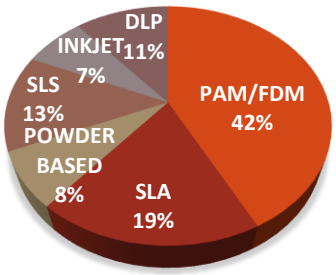

Figure 2. Number of articles referred to each method for drug delivery published from 2020 on. Data: Scifinder scholar.

On one hand, powder-based technologies are fundamentally using a thin layer of binder to "glue" the printed layers to each other. It is used for materials such as steel. [19] On the other hand, light assisted methods work by exposing liquid polymers (resins) to ultraviolet (UV) light to turn liquid into solids by curing the polymer. [20]

However, from all the methods mentioned, material extrusion-based printing (both FDM and PAM) has shown a growing interest, as can be seen in Figure 2, among researchers due to its advantages. Even if 2020 is not the most representative year because of the pandemic, the importance of PAM and FDM techniques can still be seen. Extrusion based printing is a relatively low-cost method which can fabricate hollow objects and works with a decent range of polymers (with or without drug). It also has the ability to obtain different drug release profiles by modifying the geometry and polymer used in the printing process. PAM, specifically, also has the advantage of printing at room temperature. [16] As PAM has been the chosen printing method for the experimental work, extrusion-based 3D printing methods will be explained more deeply.

5.1.1.1 MATERIAL EXTRUSION PRINTING

As mentioned before, material extrusion printing can be categorized in FDM and PAM. Extrusion printing works the same way as other layer by layer printing methods where a computer design is prepared to obtain a 3D object; each layer of a 3D product is built line-by-line. [21]

The process starts with choosing the dosage, searching a specific application that works as a goal, then designing the object by using Computer-Aided Design (CAD), translating it to machine language (generally (standard triangle language) STL format), deciding and preparing materials as well as optimizing parameters, and, finally, printing the formulation. [22] The layer thickness depends on printing speed, temperature, extrusion flow rate or pressure and nozzle diameter, which conform the printing parameters. [23] It also depends on the material that is being printed and its rheological properties. [24] Despite the number of parameters that should be taken into account for the printing process, this method is useful for many different types of materials.

However, it often requires excess support material as "rafts" (Figure 3) to build surfaces or scaffolding to hold up in-process products. [10] Oral drug delivery specifically does not generally require such supports as the geometry used id easier.

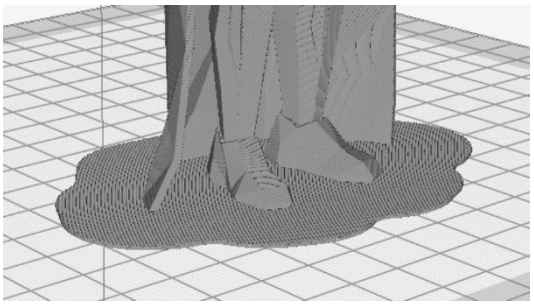

Figure 3. Rafts for a 3D printed object with a difficult geometry. [113]

In addition, several issues such as product quality changes that the material could suffer (shrinkage, warpage and residue, for example), mechanical instability, low drug loading and long post-processing cycle need improvement in order to obtain reproducible high-quality products. [25] Anyways, the equipment needed is simpler than for other methods.

FDM: FUSED DEPOSITION MODELING

On one hand, there is fused deposition modelling, which is the most widely used 3D printing technology for rapid prototyping and preparation of special drug dosage forms. [26] In this method, a thermoplastic filament is directed into a heating block where it is

heated to a molten state. The filament is moved by two rollers that make the cold filament push the molten material like represented in Figure 4. [27]

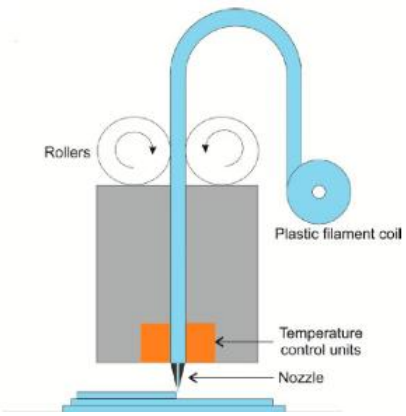

Figure 4. Scheme of a FDM printer where a plastic filament is extruded by melting it at high temperatures.. [114]

The molten material is then printed onto an adjustable stage to form a layer of the designed object, usually generating the outline first and then filling it in. The stage is adjusted (lowered) and another layer is printed. In this case, the material needs to solidify as soon as it is deposited by cooling the material. [2]

An advantage of FDM technique is that it can create objects fabricated from multiple material types by printing first with one material and then changing it, which enables more possibilities for the printing. [28]

PAM: PRESSURE-ASSISTED MICROSYRINGE

On the other hand, PAM is a printing method for gels or pastes that has recently gained popularity in pharmaceutical applications. [21] Semi-solid materials are extruded continuously layer-by-layer through a tool-head that simulates a syringe which is represented in Figure 5. The extrusion is usually based on a pneumatic piston or a rotating screw. [29], [30] The PAM printing technology doesn't need high temperatures for printing but it is neccesary to have a post-print processing time (drying) for the sample. [29]

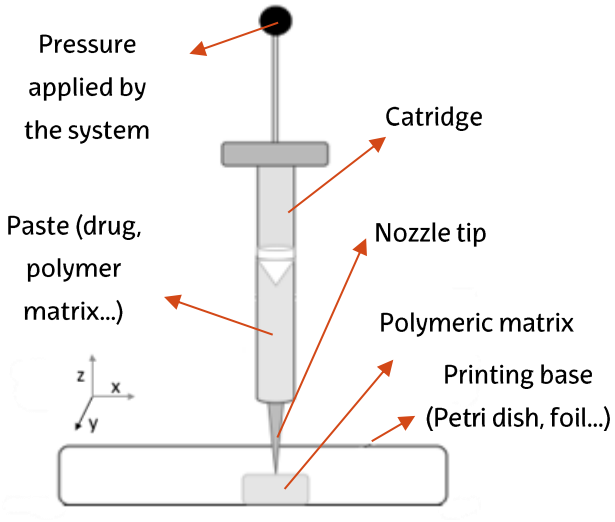

Figure 5. Schematic representation of PAM printing equipment. Adapted from [16].

It is necessary to be careful with defects that can appear after printing due to relaxation of residual stress or due to the drying process that could cause shrinking or

deformation. If the layers aren't structured enough, it could also lead to the collapse of the printed object. [31]

A comparison between both printing technologies (FDM and PAM) is done in .

Table 2 in order to understand each methods advantages and disadvantages.

Table 2. Comparison between FDM and PAM. Adapted from [16].

TECHNOLOGY	**FDM**	**PAM**
ADVANTAGES	∴ Low cost ∴ No post processing ∴ Better drug uniformity	∴ Room temperature ∴ High drug loading ∴ Suitable for polypills
DISADVANTAGES	∴ High temperature (not suitable for thermosensitive drugs) ∴ Pre-processing of filaments ∴ No biocompatible/ biodegradable polymers ∴ APIs could degrade	∴ Drying (post-processing) needed ∴ Polymer's rheology impact on structure and printing ∴ Resolution dependent on parameters ∴ Solvents needed

5.2 ORAL DRUG DELIVERY

Oral administration of drugs is preferred over other methods of therapeutic administration because, compared with subcutaneously administered drugs, oral formulations show greater chemical stability at high temperatures, and biohazardous needle waste is not created. [32] Furthermore, it is simple and convenient, being a less invasive method that causes the minimum amount of pain possible, being especially convenient for chronic patients that require frequent administration. [33], [34]

Thus, an oral dosage form for medications is ideal, however, macromolecular drugs are not easily absorbed into the bloodstream through the gastrointestinal tract. This is why polymeric carriers play an important role to achieve therapeutic results as they can improve drug penetration of macromolecular drugs. [35]

However, there are challenges around this type of administration as well. The gastrointestinal (GI) tract (Figure 6) comes with an acidic environment that can degrade the therapeutics that are taken in, and the pH changes through it. [34] We should also take into account the digestive enzymes that are present in it.

Peptides and proteins, for example, cannot be present in this environment without a protective barrier because they are easily degraded. [36] Therefore, in order to obtain therapeutic activity, frequent administration of these drugs becomes essential, and oral methods gain interest as mentioned previously. For this purpose, an outer layer is needed for the drug and polymers can adapt properly to the needs for an oral administration. [37]

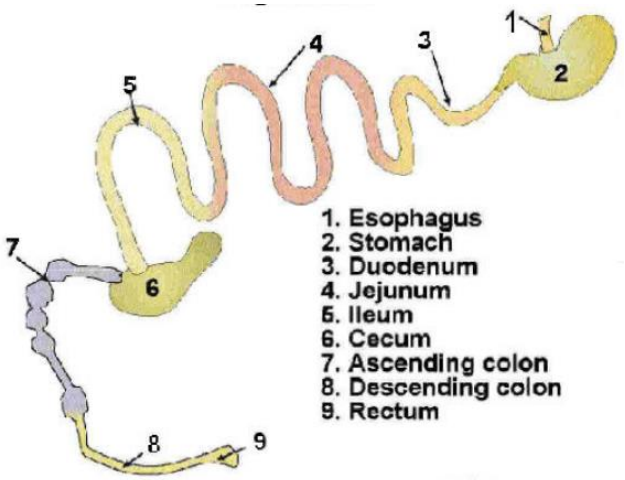

Figure 6. Schematic representation of the GI tract and its parts. [121]

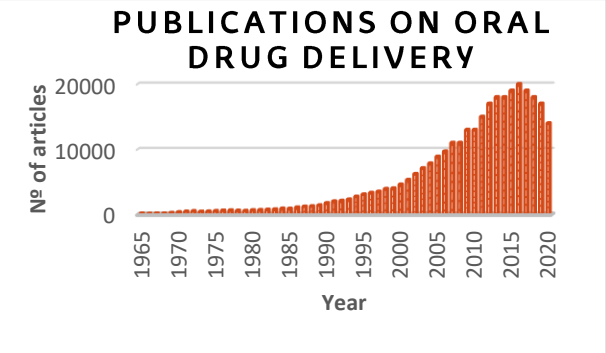

Figure 7. Representation of the annual number of articles published referring to oral drug delivery from 1965 to 2019.

Therefore, in the last 50 years the interest in oral drug delivery has increased as we can see reflected on the number of scientific articles published. In Figure 7 the annual number of articles available in SciFinder-n by searching "*oral drug delivery*" as a general search entry is represented.

5.2.1 PH VARIATION AT THE BODY

Regardless of the benefits offered by the oral route, drug delivery can be a challenge as the human GI tract is complex and has physiological barriers that influence the delivery. Some of the mentioned difficulties are poor drug solubility and stability, low drug permeability across mucosal barriers and variability of the GI tract of each subject. [38] It is necessary to fully understand the transport conditions, the

Table 3. pH variation in the GI tract adapted from [43].

	pH
Mouth	6.2-7.04 *5 (bacteria)
Stomach	1 - 2.5 *5 when fed
Proximal intestine	6.15 - 7.35
Distal intestine	5.26 - 6.72
Descending colon	5.20 - 7.02
Ascending colon	5.26 - 6.72

drug release and the absorption process of oral formulations in the body as it is known that the local pH difference and transit time along the human gastrointestinal tract will change the release of solid oral formulations. [10]

The value of the pH changes along the GI tract. In fact, it is the tract where the pH has the greatest variation in the body. [39] It starts slightly acidic in the oral cavity, continues highly acidic in the stomach and then changes to neutral/alkaline in the duodenum, jejunum and ileum as we can see in Table 3 and Figure 8. The exposure of the drug to these changes could lead to hydrolysis, oxidation or deamination of the drug that can be deactivated by such changes. [40]

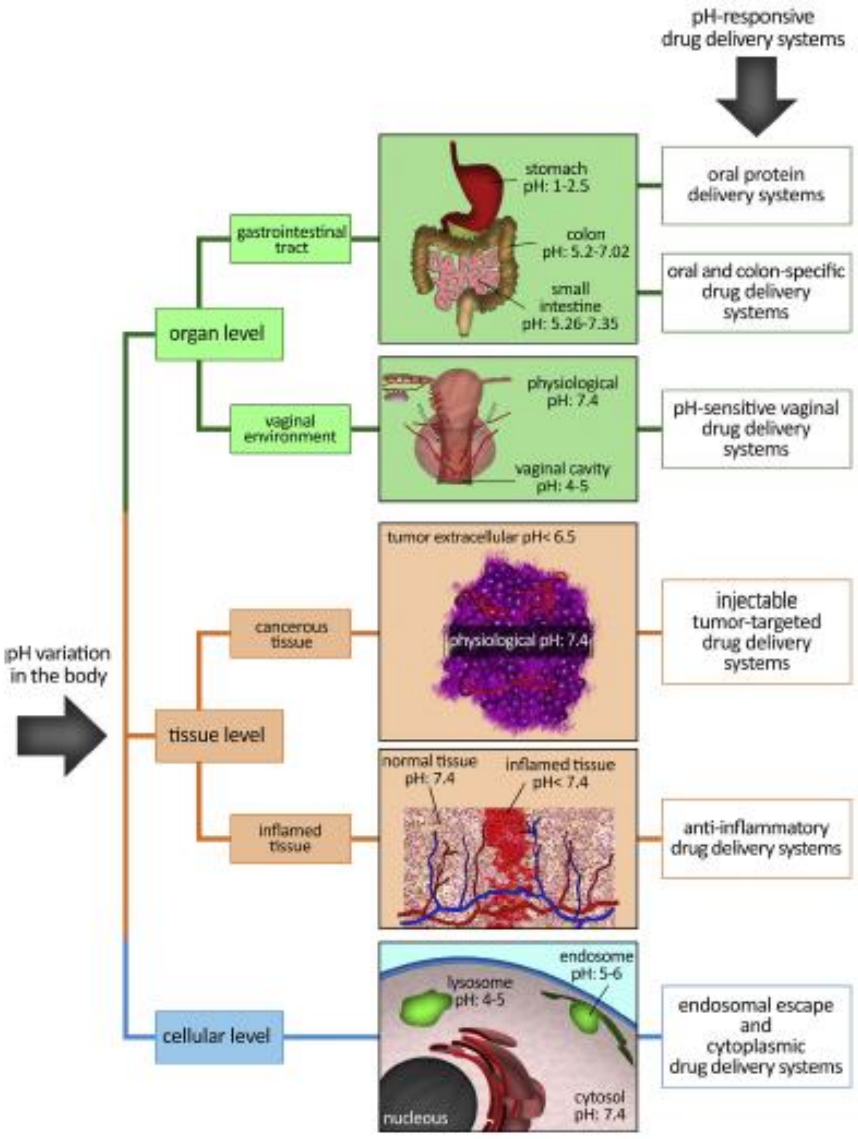

Figure 8. pH variation in the body at different levels. [43]

At the tissue level the pH of healthy tissues is not the same one as the cancerous or inflamed tissues. As they have elevated metabolisms compared to the normal tissues, the

pH decreases a bit. This is due to three mechanisms to keep the fast growth of this kind of tumorous tissues, the first one is absorbing all the oxygen that they can find around them therefore lactic acid is produced which lowers the pH level. [41] The second one is the hydrolysis of ATP as an energy source which also contributes to the lower pH level and the last one is that leukocytes are capable of pumping lactic acid into the exudate. [42]

At a cellular level each of the subcomponents of a cell have their own characteristic pH value. The range varies from pH 8 in mitochondria to 5.5 in the secretory granule. [43]

5.2.2 BARRIERS FOR ADSORPTION

The absorption of drugs by oral drug delivery is limited by the GI tract (Figure 9) and its anatomy, physiology and biochemistry due to its physical and chemical restrictions.

The gastrointestinal tract (GIT) is divided in upper and lower GIT and consists of the following: starting with the upper GIT it includes the mouth, pharynx, oesophagus, stomach, and the first part of the small intestine: the duodenum. The lower GIT involves the rest of the parts of the small intestine, which are jejunum and ileum, and the large intestine: cecum, colon, and rectum. [44]

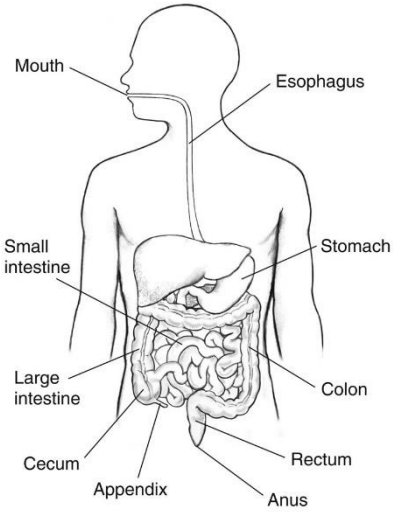

Figure 9. Schematic representation of the GI tract with the most important parts labelled. [115]

The first place in oral drug delivery is the mouth. The main function of the oral cavity is protecting the intestines by wetting the food to form a mass. Saliva is a viscous water-containing liquid, which is less permeable than plasma. One or two litres are discharged into the mouth every day and its composition and pH value vary with secretion rate. The pH value varies between 7.4 and 6.2, but sometimes it drops to 5 due to the influence of bacteria. [45]

Then, food and orally dosed drugs are transported due to peristaltic contractions through the oesophagus to the stomach, which acts like a temporary storage before it is delivered to the duodenum. Most of the digestion takes place under the action of gastric acid and enzymes, especially peptidases. Due to the small surface area of the stomach compared with the small intestine and mostly due to its environment, drug absorption rarely occurs in it.[36]

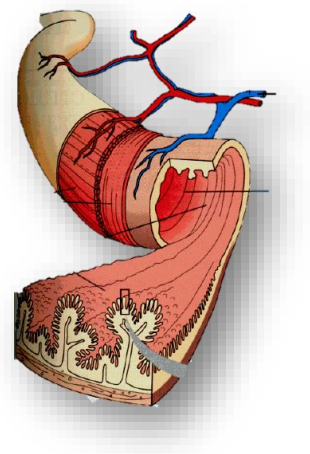

Figure 10. Scheme of the small intestine. Example of the increase of surface area. Adapted from. [116]

Finally, food and drugs reach the small intestine where the majority of digestion is completed with enzymes from the liver and the pancreas, and most of the absorption of nutrients then takes place due to its large surface area (Figure 10). [46] The large intestine is the final major part of the GI tract which function is processing the waste products generated and absorbing any remaining nutrients and water back into the system. Its surface isn't as large as the small intestine's but it forms crypt structures in order to amplify it. [47]

When a drug formulation is swallowed it enters the GI tract; the drug has to be delivered through the mucus layer and starts to diffuse in the mucus layer of the small intestine. The GIT has a low permeability to the bloodstream, which affects in case of orally formulated drugs. [7] When studying different drug release mechanisms, it is mandatory to take into account the different properties and characteristics that are shown in Table 4, referred to different parts of the GI tract.

Table 4. Physiological properties of different segments of the human GI tract. Adapted from [48].

	pH	Length (cm)	Diameter (cm)	Mucus thickness (μm)
Stomach	0.8-5	20	-	245 ± 200
Duodenum	~7	17-56	4	15.5
Jejunum + Ileum	≥7	280-1000	2-3	15.5
Colon	7-8	80-313	4-4.8	135 ± 25

There are three main barriers that impede oral drug delivery which are biochemical barriers (pH and enzymes), the mucosal diffusion barrier and the intestinal epithelium. First, degradation of the drug could happen through pH and specific enzymes that cleave amino and glycosidic bonds. [7], [49] Thus, it is necessary to protect the drug from the acidic environment. For that, oral drug delivery systems have been designed in order to achieve a successful delivery in the correct place of the GIT. Second, an inhibition of diffusion occurs due to viscous mucus. [34], [50] Finally, tight junctions found in the intestinal epithelium inhibit the uptake into the bloodstream. [49], [51]

5.2.3 PH RESPONSIVE FORMULATIONS FOR ORAL DRUG DELIVERY

In order to overcome the challenges of oral drug delivery, pH-responsive carriers have been investigated. They are a good alternative to achieve the absorption of the drug

through the GIT. Their function is to stabilize the drug delivery in the stomach protecting the drug and achieve a controlled release in the intestines. [52]

pH sensitive materials can be divided in anionic and cationic and their behaviour depends on this classification. Anionic materials, one of which are carboxymethyl cellulose (CMC) containing hydrogels used in the experimental part of the thesis, are charged when the pH is above the pK_a of the network. The polymer is swollen when the pH is high enough. [43] This kind of hydrogels protect the drug when the pH is low and they release it in specific locations taking advantage of the pH responsive behaviour. If the pH is not high enough, the hydrogel stays in a collapsed state that does not release the drug. Anionic hydrogels are suited for target delivery to the small intestine and colon. [37] In case of cationic materials, their behaviour is the inverse one. They release the drug in acidic environments and protect it by collapsing at basic environments.

5.3 HYDROGELS

The concept of a hydrogel refers to polymeric 3D networks that are based on hydrophilic macromonomers and that can retain a large amount of water. [53] Hydrogels are materials that can be used for the controlled release of therapeutics. They can contain therapeutics inside their network, allowing the release of the therapeutics in a controlled way. [35] In the last decades they have been used as a strategy to lower the amount of drugs administered to the patients. [52]

Their structure prevents irritations by an oral intake. When hydrogels are being used for oral drug delivery, it is important that they preserve the therapeutic efficacy of the drug. [37] Additionally, their structure can change depending on the environment they are in, if they contain specific functional groups. There are different parameters that can be controlled to achieve this behaviour, like pH or temperature changes. [54]

Initially only simple hydrogels were investigated, but as they are being more and more studied, new technologies are developed, such as multicomponent hydrogels, stimuli-responsive hydrogels (pH responsive hydrogels are among this group), nanogels, etc. This means that a dose given to a patient can be sustained for a long period of time, having a more efficient way to medicate patients. [55] The more complicated hydrogels are the ones that allow the stimuli-responsive behaviours of the hydrogels.

5.3.1 HYDROGEL CHARACTERISTICS

Hydrogels are 3D crosslinked networks of polymers that can be classified depending on the source they are obtained as natural, synthetic or hybrid. They can be physically or chemically crosslinked, as well as by a combination of both effects (Figure 11). If the hydrogel is physically crosslinked non-covalent bonds take part, whereas if it is chemically crosslinked, actual covalent bonds are formed within the hydrogel. Yet, the chemical bond is usually stronger than the physical bond. [52]

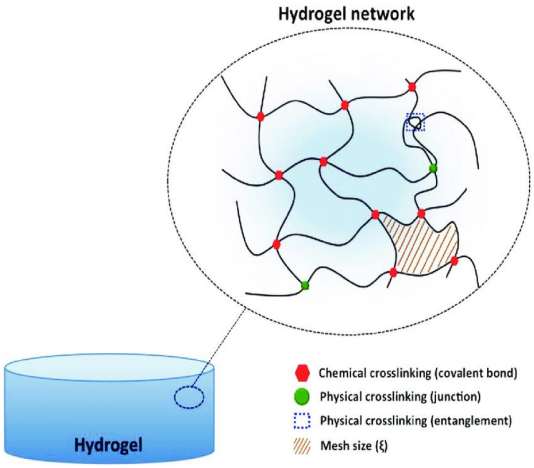

Figure 11. Schematic representation of different crosslinks in hydrogel networks. [117]

In addition, the density of the crosslinking and the chemical structure determine the mesh size, which is a key parameter to control the behaviour of the hydrogel. [56] If the formulation is above the solubility limit, depending on the mesh size, the water-soluble groups contained within the hydrogel can be more or less easily liberated. The mesh size is a parameter that can be optimized depending on the desired behaviour. Greater mesh sizes allow a more rapid liberation whereas smaller mesh sizes lead to drug retention. [57] The reason for that are the hydrodynamic radii of the drug particles and if they can pass through the mesh, which size is normally around 5 to 100 nm. [58] It affects the physical properties such as degradation, diffusion and mechanical strength as well. [59]

5.3.2 HYDROGEL BASED DRUG DELIVERY

Hydrogels can be used for a more efficient medication treatment for the patients. Using a hydrogel to deliver the drug could protect it from degradation by enzymes and acids present in the GI tract. [52] Furthermore, crosslinked hydrogel networks can be used as a protection layer for the hostile environment that is the GI tract for many drugs, proteins and microorganisms. [37]

On one hand, comparing with the same hydrogel with lower crosslink density, higher crosslink density obstructs the mobility of the polymeric chains. Hence, it reduces the swelling rate and protects drugs from harmful environments. [53]

On the other hand, hydrogels containing hydrophobic groups collapse in the presence of water. Introduction of hydrophilic groups in the crosslinking agent can result in

a higher degree of swelling. [60] In order to achieve this type of protection, modifications can be made in the hydrogels structure.

Hydrogel modification to achieve pH responsive materials is an interesting topic of research, as it allows to protect drugs from the pH changes occurring along the gastrointestinal tract. By adding carboxymethylcellulose (CMC) for example, a hydrogel could collapse under acidic pH. Sustained release and drug protection can be achieved by such an addition. [61]

Other methods will not be explained because they are not of especial interest for this overview, but to have a reference there are methods like raft forming systems, magnetic systems, high and low density or sinking system (non-floating or floating systems), expandable, unfoldable, and swellable systems... [33]

5.3.4 POSSIBILITIES OF 3D PRINTING FOR ORAL DOSAGE FORMS: POLLYPILLS

Polypill is a term that refers to a single dosage form that could be conventional pills or hydrogels for example, that contains two or more APIs in the same system. [62] Several fixed-dose combination (FCD) are already sold in the market for different therapies such as bacterial infections, severe pains, etc. [63] They are especially interesting for poly-medicated patients to enhance the probability of the patient adhesion to medication due to the easier intake. [64] Polypills (Figure 12) can modify the in vivo behaviour of the APIs, so several tests need to be carried out in order to understand how the matrix or the mixture of APIs affects each APIs intrinsic behaviour. They could alter kinetic and dynamic profiles affecting the APIs release profile, for example. [65]

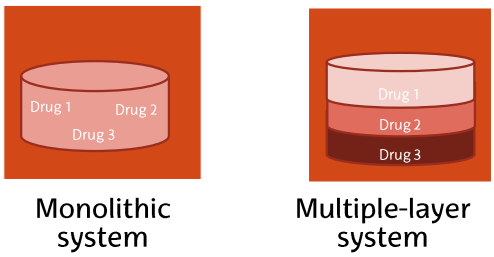

Figure 12. Representation of the main types of polypills. Adapted from [64].

Additionally, the mixture of APIs and the matrix could show a synergistic activity (higher activity than the summative effect of each API by themselves) which could allow the possibility to administer lower doses of drugs, reducing the risk of adverse effects. [66] The contrary could also happen if the interaction is antagonistic. Furthermore, stability, absorption, distribution, metabolism, and excretion of the mixture of drugs could lead to incompatibilities. [64]

However, one problem concerning hydrogels is that they contain water. This is not a disadvantage when the drug to be incorporate is hydrophilic, but it is when the drug is hydrophobic. The solubility of the drug decreases, generating a potential problem. [67] For these situations, hybrid hydrogels could present some advantages. Drug particles can be loaded into the hydrogel matrix without being linked. [68] This method can increase the release time of the drug, as it should be released from the hydrogel to be absorbed into the body. This behaviour depends on parameters as hydrogel mesh size, solubility, hydrophilicity, concentration of drug and particle size. [52]

Other disadvantages could be the challenge to identify negative effects when they occur due to having more than one drug together as well as the difficulty to select the needed dose of each of the drug for every patient. [64] Actually, this argument seems especially important for all personalized drug formulations. Searching for the appropriate amount of drug for each patient could require a considerable amount of time. Finally, segregation is another possible problem in this kind of systems that could have the need of additional manufacturing steps, making this method more expensive. [69]

Even though there are disadvantages, the potential of synergistic interactions is huge, and further investigation into this field is required in order to fully understand the systems and obtain the maximum of their advantages. [70]

5.4 RELATIONSHIP OF RHEOLOGY AND 3D PRINTING

Rheology plays an important role in the process of polypill fabrication as represented in Figure 13. The processing of the material could lead to transformations of properties due to thermomechanical processes, such as, orientation of polymer chains, phase separations, gelation, crystallization and degradation. Rheology is the science that studies polymer flow and matter deformation.

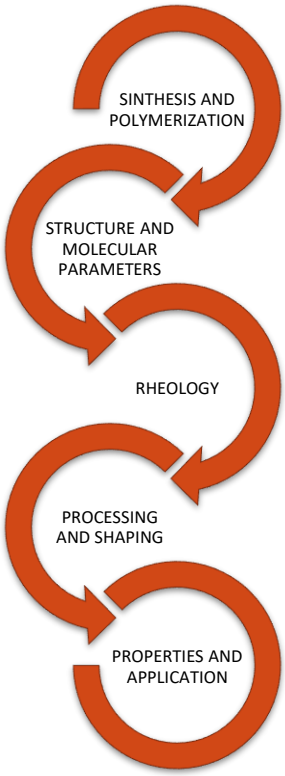

Figure 13. Scheme of the process to obtain a product. Rheology plays an important role in it.

Polymers show peculiar behaviours in solution and flow due to their macromolecular nature. [71] In general, to have a polymer flowing it needs to have a predominantly liquid behaviour, meaning that higher values of the viscous modulus, G'', rather than the elastic modulus, G', are needed. [72]

However, the rheological behaviour of hydrogels differs from molten polymers. The 3D network structure prevents hydrogels from flowing and, therefore, they present a predominantly elastic behaviour (G'›G''). This characteristic is the key feature of a gel, in contrast to a highly viscous liquid (G''›G'). Even though, this characteristic is different in chemically and physically crosslinked hydrogels: while in chemically crosslinked gels the 3D structure is independent on the stress applied, physical gels show a yield stress point, where the structure is destroyed and the material can flow (G''›G'). Although there is a controversy in academia about the definition of the yield stress, in this work we will take the crossover point G'=G'' as representative of the yield stress.

Even though there are plenty of articles about 3D printing there are not much that explain polymers rheology impact on the printing process, and the required characterization for the 3D printed pharmaceuticals. In addition, the behaviour of polymer–active pharmaceutical ingredient combination also impacts the printing process. [16] The objective is being able to correlate the rheological parameters and behaviours studied in the experimental part in order to simulate the 3D printing process with rheology, as it is a faster and more convenient tool. If correlations are successfully achieved, rheology could be a solution for problems related to 3D printing as well as a previous step to the process.

Looking at the PAM manufacturing process, the hydrogel needs to change from a solid-like behaviour (G'›G'') to a fluid-like one when pressure is applied in order to extrude the material from the cartridge in the 3D printing method. [16]

Then, once the ink is printed, it needs to restore the network, becoming again more solid-like for the shape to be maintained. The inks properties could also be affected in this process even though high temperatures are not involved.

Such manufacturing conditions can be simulated by selecting the appropriate conditions in rheological tests. In the linear-viscoelastic regime (LVE), the frequency-dependence of the dynamic moduli, the storage modulus (G') and loss modulus (G'') may be used to investigate some aspects of the gel structure and mechanical behaviour. [72] For example, with frequency sweeps we can detect the hydrogel character and some details of the groups that form the chains. [73] In contrast, changing the strain (or stress) applied over the LVE conditions we can detect the yield stress and analyse the flow characteristics of the gel. By sweeping from linear to non-linear viscoelastic conditions over time, we can reflect the gel formation kinetics once the 3D structure is destroyed, and therefore, it is possible to investigate the reversibility of the gels (Figure 14).

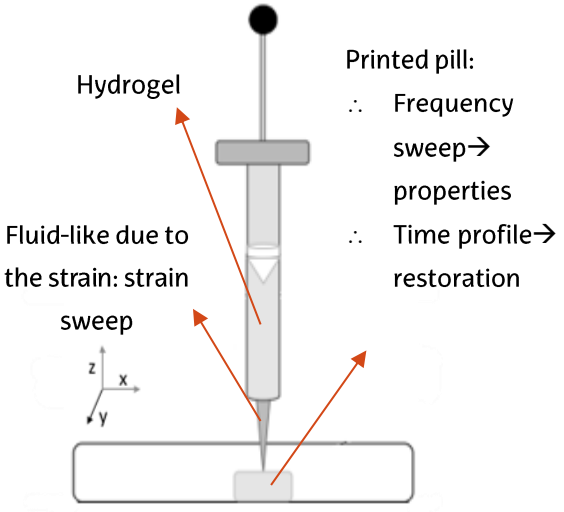

Figure 14. Selection of rheological characterization methods. Picture adapted from [16].

Having said that, it is possible to hypothesize the ideal characteristics of a 3D printable hydrogel. First, G' values need to be higher than G'' values, having a predominantly solid-like material to facilitate the fabrication of 3D pills. It also needs to present a yield stress value, where applying higher strain (or stress) the material flows in order to be able to extrude it. It is easier to have this type of behaviours in hydrogels with a physical network rather than a chemically crosslinked hydrogels, as the interactions are stronger in a

chemical network that needs to be broken in the printing process. Finally, the hydrogel formation needs to be reversible.

Rheology helps to determine if the prepared mixtures are printable or not by different tests (Figure 15). It is convenient specifically for measuring hydrogels mechanical properties since it is quick, sensitive and requires small sample sizes. [52] For extended information about the measuring specifics, refer to appendix *13.1 RHEOLOGICAL MEASUREMENTS.*

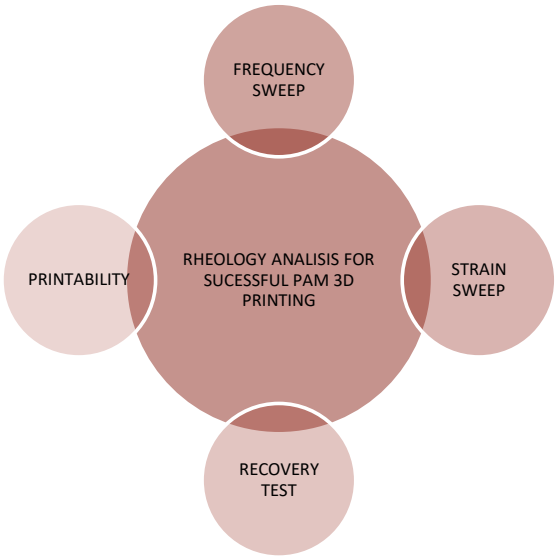

Figure 15. Rheological tests are required for drug containing hydrogels to ensure their suitability and processability for extrusion-based 3D printing.

5.4.1 FABRICATION CAPACITY OF HYDROGELS

As these systems are personalized to each patient, the fabrication capacity will never be as high as in traditional pill manufacturing. Anyways, for being so personalized they just need a couple of minutes to be printed if the ink and the digital design are already prepared. [4] For each patient, pills need to be highly reproducible in order to adjust the therapeutic dose to their needs. [69] Thus, process optimization studies are crucial for this objective.

On one hand monolithic systems are the easiest to manufacture as all the drugs are contained within the ink. However, they have the highest risk of drug segregation and interactions between the added APIs. [74] On the other hand, multiple-layer systems can be more challenging to design, thus it is only carried out when the APIs loaded into the ink are chemically incompatible or dissolution profiles are very different. [66]

To conclude, finding materials with the needed rheological requirements it is not so simple. In addition, the process and optimization of each drug could be a difficult and time-consuming process, so extrapolation to other drugs could be interesting. Maybe in the future and with enough investigation, theoretical models or simulation programs could be achieved in order to predict some APIs mixing interactions as well as API-matrix interactions. This way, time could be saved and the manufacturing process could be easier and more predictable.

6. OBJECTIVES

The objective of this bachelor's degree is establishing the key aspects that ensure successful printing of drug-containing hydrogels by the PAM technique. With this purpose, some inks have been developed. These inks contain polyethylene glycol (PEG), glycerol, CMC, water, atenolol and hydrochloric thiazide as their main components. Thus, the effect of the two drugs mentioned will be studied as well as the relation between the API and the polymeric matrix. Another objective is finding hydrogel mixtures, which incorporate more than one drug that can be 3D printed.

A correlation between rheology, printing parameters and the printed object will also be investigated with the objective of predicting the printing process just by looking at the material rheology. Good resolution pills are searched after the printing, meaning shape fidelity close to the CAD design created.

Finally, the morphology of the printed object will be analysed. First, after the consolidation process and later on after a pH test and lyophilization. This way the effect of the stomach acidic environment on the drug delivery systems will be studied.

7. HYPOTHESIS

In the process of obtaining functional inks, the materials chosen for preparing the hydrogel matrix in the experimental part are PEG, CMC and glycerol as they are suitable for oral drug delivery. It is expected, that a combination of these materials without chemical modifications by facile means can provide gel-like materials which can be employed in PAM 3D printing. Even though there is a lot of research done in this topic, none of the papers found speak specifically of the mixtures prepared in the project.

As representative APIs, atenolol and hydrochloric thiazide (HCTZ) will be the two drugs added to the hydrogels, both being antihypertensives. As the drugs are going to be added above their solubility limit in some of the hydrogels it is also expected to have solid drug particles, which should be visible by scanning electron microscopy (SEM) if the particles are large enough. atenolol is more water soluble than HCTZ. Hence, as the hydrogels contain water, those containing atenolol are expected to be more homogeneous than the hydrogels containing HCTZ. This could be due to the different size of the not solubilized drug particles as HCTZ particles are expected to be bigger than the atenolol ones. atenolol can crystalize if it is refrigerated and as the hydrogels are going to be stored in the fridge, so maybe some crystals could appear if there is not solubilized atenolol. The last hypothesis could also be confirmed by SEM.

Actually, hydrogel's rheology and printability are thought to be dependent on the hydrogels structure as well as the APIs concentration, but not on the APIs chemical structure. This theory is based on the poor solubility that both of the drugs show in water. It could be interesting in order to extrapolate the results obtained with this thesis to other not soluble APIs for the same hydrogels. However, the theory needs to be tested. With this objective, mixtures above and below the solubility limit of the API will be prepared, varying their concentration on each hydrogel.

The most probable affecting parameters are gels nature, the concentration in which the API is added and the pH response of the material. Thus, the variables mentioned will change the rheological properties, so, thinking about behaviour is expected, higher elastic modulus (G') of the mixtures should be related to pills that maintain the form better because of a more solid like behaviour. Is also expected that the printing parameters (pressure, temperature, speed, etc) needed could be more drastic for more elastic hydrogels than the conditions for more liquid-like materials. For the characterization of the mixtures rheological test will be carried out, and then ideal printing conditions will be determined by trial and error. If possible, a correlation between rheology and printing conditions will be made.

Controlling the printability of the materials requires understanding of physics and chemistry of the printing process. [4] In the 3D printing of pharmaceuticals, one of the most important parameters is the fidelity of the printed structure to the prepared CAD model.[16] Reproducibility is key to achieve an adequate quality level for the intended applications. Hence, attempts will be made to find connections between rheology and printability.

Particle size can be critical for the reproducibility, since this property affects layer thickness and the risk of segregation during layering. Water content may also be critical, since water is a potent plasticizer for many polymers. Consolidation of the printed pills will probably be needed as the method used for the printing will be PAM. It is expected that with just leaving the pills dry for at least 24 hours will be enough.

Later on, their pH behaviour test will be done as they have a pH dependent behaviour (Figure 16), due to the functional groups that conform their structure. Even though PEG and glycerol can accept protons below their pKa, the net-charge is still zero and thus they don't contribute to swelling by charge repulsion, they are just a medium for charge transfer. On the contrary, carboxymethyl cellulose (CMC) is an anionic cellulose derivative which's carboxymethyl groups are deprotonated when the pH is above their pKa (pKa = 4.30 [75]). CMC is supposed to collapse under acidic pH, preventing the drug release from the hydrogels. In acidic conditions, the hydrogel should be collapsed, holding the drug tightly. [76]

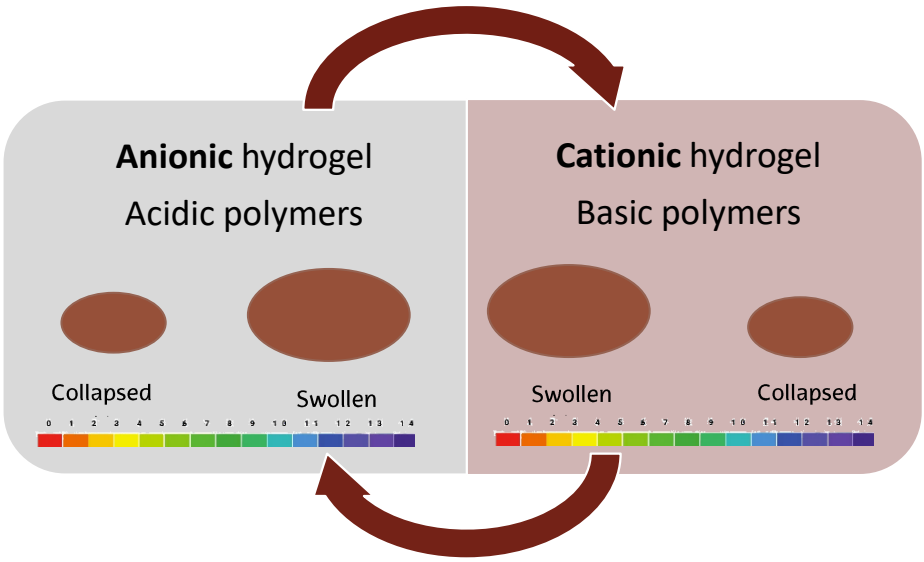

Figure 16. Scheme of hydrogels expected behaviours in different environments.

PEG is strongly dependent on pH and due to its nature; it contains a hydrophobic chain, composed of methylene groups interspersed with ether groups. The basicity of the R-O-R oxygen (pKa at 25°C→14.22 [77]) is what makes the hydrogels swell, leading to the release of a drug at high pH value and collapse at low pH values. [78], [79] Glycerol contains free -OH groups and the expected behaviour is similar to the PEG one (pKa = 14.4 [80]).

8. EXPERIMENTAL PROCEDURE

8.1 REAGENTS

The hydrogels contain 6 main reagents: water or glycerol as the base and main component of the hydrogel, CMC that is contained in all the hydrogels and PEG in those were the percentage of water is higher. The last two components are drugs: atenolol and HCTZ.

8.1.1 CMC

Carboxymethyl cellulose (Figure 17) is a cellulose-derivative polyanionic polysaccharide that contains abundant carboxyl groups in the polymer chain. It is known by its non-toxicity, biocompatibility and biodegradability. [76] The carboxymethyl groups that modify the cellulose make the polymer soluble in aqueous solutions. The substitution degree can range from 0.6 to 0.95. It has attracted attention in pharmaceutical applications lately. [61] CMC is water-soluble at neutral pH. Thanks to the carboxylic acid functionality, CMC is pH-sensitive. Hence, as an anionic polymer, it is usually used in order to prevent gastric degradation of drug. [81]

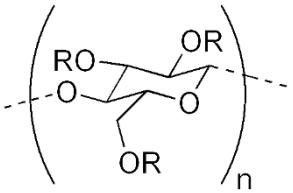

R= H or CH_2CO_2Na

Figure 17. CMC's molecular structure.

8.1.2 PEG

Polyethylene glycol (PEG) is a biocompatible and hydrophilic polyether compound that has many applications (Figure 18). PEG is referred to polymers with molecular weights lower than 100.000, whereas polymers with higher molecular weights are named polyethylene oxides (PEOs). [78] It is widely utilized in drug delivery due to its properties for evading the immune system and biocompatibility, although PEG is not biodegradable. [82]

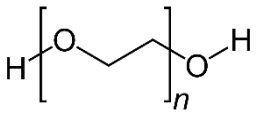

Figure 18. PEG's molecular structure.

8.1.3 GLYCEROL

Glycerol (Figure 19) is a trihydroxy alcohol with a structure of propane substituted at its three carbons with hydroxy groups. It has a role as a solvent in the prepared hydrogels. Glycerol has localized osmotic diuretic and laxative effects. [80]

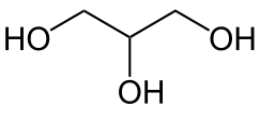

Figure 19. Glycerol's molecular structure.

8.1.4 ATENOLOL

Atenolol (Figure 20) is an ethanolamine compound that plays a beta-adrenergic antagonist role. Hence, this beta blocker medication is mainly used to treat high blood pressure and heart-associated chest pain. [83]

Beta receptors are present on heart cells. When adrenaline activates beta receptors, blood pressure and heart rate rise. Beta blockers, such as atenolol, prevent adrenaline from affecting the beta receptors in the blood vessels and heart. This causes the blood vessels to relax. By relaxing blood vessels, beta blockers help lower blood pressure and relieve chest pain, as well as reduce the heart's need for oxygen. [84]

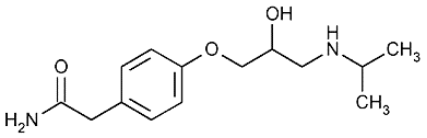

Figure 20. Atenolol molecular structure.

8.1.5 HCTZ

Hydrochlorothiazide (Figure 21) is a benzothiadiazide substituted in two positions by chloride and a sulphonamide. It acts like a diuretic and treats hypertension; it inhibits the sodium chloride co-transporter system on the distal convoluted tubules, which leads to a diuretic action and lowers blood pressure at the same time. [85]

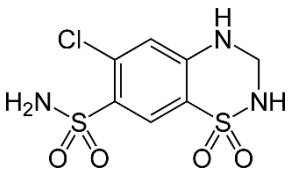

Figure 21. HCTZ molecular structure.

8.2 MIXTURES AND NOMENCLATURE

The nomenclature adopted for naming the samples prepared was intuitive (Figure 22). The hydrogel's base can be PEG or glycerol, so the first 3 letters were referred to the base. In case of having glycerol, for example, the name starts with GLY. Then the next letter was referred to the drug it contained. There were two possible drugs, being atenolol and HCTZ, so atenolol was represented by an A and HCTZ by an H. The numbers that follow this letter were referred to the percentage of the drug present on the hydrogel. In case of having both drugs in the same hydrogel both A and H appear on the name, each one followed by the percentage of drug.

PEGA2	GLYH12.5	GLYA12.5H6.25
• PEG base • 2 wt% Atenolol	• Glycerol base • 12.5 wt% HCTZ	• Glycerol base • 12.5 wt% Atenolol + 6.25 wt% HCTZ

Figure 22. Examples of the nomenclature used for the mixtures.

The mixtures prepared for this bachelor's degree are summarised in Table 5.

Table 5. Compilation of the mixtures prepared and their composition.

	MIXTURE (WT% COMPONENT)								
COMPONENTS	PEGA0	PEGA2	PEGA8	GLYA0	GLYA2	GLYA12.5	GLYH6.25	GLYH12.5	GLYA12.5H6.25
CMC	5	5	5	12,5	12,5	12,5	12,5	12,5	12,5
PEG 6000	20	20	20	-	-	-	-	-	-
H_20	75	73	67	5	5	5	5	5	5
GLYCEROL	-	-	-	82,5	80,5	70	76,25	70	63,75
ATENOLOL	-	2	8	-	2	12,5	-	-	12,5
HCTZ	-	-	-	-	-	-	6,25	12,5	6,25

8.3 GEL PREPARATION

The first step of the project was the preparation of the different mixtures (Figure 23). There were two well differentiated hydrogel bases: PEG and glycerol-based hydrogels. The preparation of the hydrogels was different depending on the base they had.

Starting with the PEG based ones, first PEG was added to a beaker. To melt the PEG, it was heated to 85ºC approximately, and when it turned transparent CMC and the necessary drug(s) were added. Each one of the mixtures will be explained in the following section. For stirring the mixtures, a rotor or a magnetic stirrer were used. Related to this, the rotor incorporated more air to the mix than the magnetic stirrer. Once all the reagents were well mixed, the beaker was taken off of the heating plate and the needed amount of water was added at once. It was mixed until the mixture was completely homogeneous and stored in a sealed glass vial.

Figure 23. Preparation process of a glycerol-based hydrogel. Close-up of the rotor mixing the hydrogel and its components. Glycerol based mixture.

With the glycerol-based hydrogels heat was not needed otherwise the process was similar.

8.4 RHEOLOGICAL MEASUREMENTS

8.4.1 MEASUREMENTS

Figure 24. Anton Paar rheometer used for all the rheological tests.

As explained in the introduction, 3 different rheological tests were carried out in order to elucidate the different hydrogel's structure and characteristics. In the next sections each of the measurements will be explained. For all these measurements an Anton Paar MC101 rheometer has been used (Figure 24). The measurements have been carried out with the parallel plate geometry of 25 mm of diameter.

The procedure for loading the sample to the rheometer was simple. First, the rheometer was set to 25 ºC where the zero gap was calibrated. Then, the upper geometry was elevated in order to place the mixture with a spatula between the plates. Then a gap value of 1mm was set for all the measurements and the sample was carefully trimmed to the geometry. Finally, the ring placed around the sample was filled with water for having reproducible humidity in the measurements and the lid was placed.

8.4.1.1 STRAIN SWEEP

A strain sweep is the first step in rheology because it gives information about the linear viscoelastic region where the structure of the hydrogel is not destroyed. The temperature was maintained at 25ºC and the frequency set to 1Hz in all the measurements. The strain values applied range from 0.001 % to 100 %, even though until around 0.1 % the values given by the rheometer are out of the sensibility range. However, this way the hydrogel had time to stabilise at the fixed temperature.

8.4.1.2 FREQUENCY SWEEP

Continuing with frequency sweeps, the parameter that is maintained constant is the strain whereas the frequency varies. The viscoelastic spectrum of the sample is obtained by these sweeps, which is used for further structural characterization.

In this case the strain value was selected where both G' and G'' were parallel and linear in the strain sweep, which depended on the previous measurement but it is a value under 10% strain (LVE conditions). The frequency was set from 100 Hz to 0.01 Hz.

8.4.1.3 TIME PROFILE

In time profiles different intervals can be differentiated. In the first interval, a low strain (1%) is applied to the sample in order to have a reference value of storage and loss modulus. Then, in the next interval, the value of the strain is drastically increased in order to break the gel's structure. The value is dependent on each of the mixtures because it depends on its structure's strength but it varied from 100 % to 1000 %. Ideally, in the last interval, storage and loss modulus should recover immediately to the values shown in the first interval once the high strain is not applied. Finally, the same low strain value is applied again and the structure's restoration kinetics are studied. If needed, more intervals can be programmed in the rheometer. All the experiments were performed at 25 ºC.

8.5 3D PRINTING

8.5.1 3D PRINTER: BIOPLOTTER

The Envisiontec 3D-Bioplotter® (Developer series) System is a suitable 3D printing device that serves for rapid prototyping. It can process a large number of materials, from soft hydrogels over polymer melts up to hard ceramics and metals, using 3D CAD models (Figure 25).

Figure 25. 3D Bioplotter printer from Envisiontec.

The Bioplotter uses air pressure to deposit multiple materials in three dimensions. The materials range from viscous pastes to liquids and are deposited using a syringe that moves in three dimensions. Applying air or mechanical pressure to the syringe, the material comes out of the cartridge until the pressure is not applied anymore. In addition, The device does not require a pre-processed filament, which is a big advantage over other 3D printing techniques.[86]

A material is dispensed from a cartridge through a needle tip from a 3-axis system to create a 3D object. The only requirement this technique has is that the material needs so somehow solidify. It could happen by chemical or physical reaction, for example.

It comes with a needle tip cleaning station that can be programmed to automatically clean the tip before and during the printing process. The tips compatible with the printer are Luer Lock needle tips, which inner diameters range from 0.1 mm to 1.2 mm. In the present work, the point used for printing all the mixtures had a diameter of 0.4 mm.

As the materials are printed from a cartridge, the printer is easier to clean than the ones that contain the filament in touch with it. The printer can be calibrated each time the tip, full cartridge or printing head is changed.

The hardware also has its advantages; there is full temperature control of the printing head, both in the parking positions, as well as during printing. For hydrogels the low temperature dispensing head is used (Figure 26), which temperature range is from 0 to 70ºC and its cartridge size is 30ml. [87]

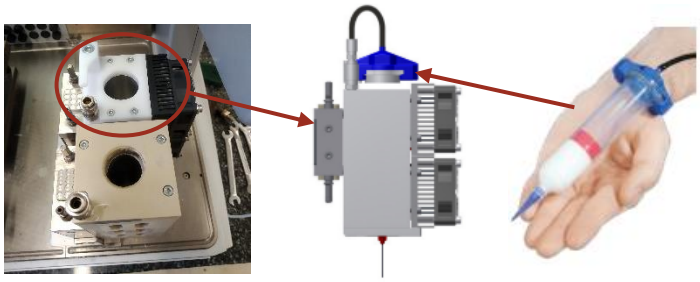

Figure 26. Low temperature dispensing head and cartridge. [87]

Finally, some of the limitations are that it does not use a screw to extrude the material like many other PAM printers, thus a pressure gradient can be expected. Furthermore, the temperature measured is the temperature of the mantle and not necessarily the temperature of the material at the tip.

8.5.1.1 PRINTING PROCEDURE

First, a virtual 3D design of an object using a design software (SolidWorks) was created. The model was then converted into an STL-format, which was needed for the printer. The format was then opened with another software (Perfactory) in order to slice the model in 2D horizontal layers that were then sent to the Bioplotter printer. Once a new project was created, the printing parameters were selected by trial and error until the printed sample resembles its design as close as possible. These parameters are summarized under "Printing parameters" section (*8.5.2 PRINTING DESIGN AND PARAMETERS*). When the project was finished, the actual print process began (Figure 27).

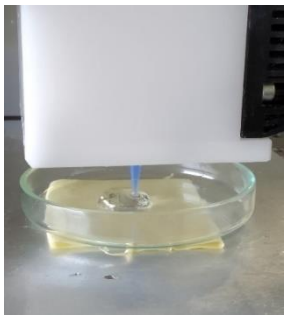

Figure 27. Layer by layer 3D printing process for a hydrogel.

The material was loaded into the cartridge, the selected tip was attached and it was mounted into the printer. Each time the cartridge was changed a calibration was needed (Figure 28). Once it was calibrated and all the parameters were as specified, the printing of the material begins.

Figure 28. Laser for needle calibration.

The print head was moved in the x-y axis to create the base and when it finished the layer the print head moved in the z axis to deposit the second layer of the material. This process continued until all the 3D object was completed.

Almost every 3D printed object required some sort of post-processing after it was printed. As mentioned in the introduction, the PAM printing process does not need high temperatures but requires an additional drying step in order to obtain stable pills. Drying and consolidation can be made in several conditions with variations in process types, temperature, and duration. [4] Shell formation could occur in the outer layer of the pills by this type of processes, leading to insufficient drying and poor mechanical properties. [88]

The post-processing in this case included drying and solidification at room temperature, which allowed the printed pill to gain sufficient physical strength. Post-processing can also improve aesthetics, which is relatively important for orally dosed printed pills.

8.5.2 PRINTING DESIGN AND PARAMETERS

The mixtures were printed following a cylindrical form (Figure 29) in order to obtain a pill and two different programs were required. *SolidWorks* was used for modelling the 3D design of the pill and *Perfactory RP* was used to slice the design into different layers (Figure 30). The slicing process was necessary for programming the Bioplotter.

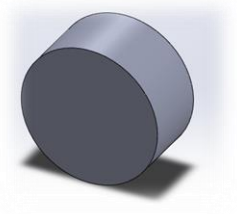

Figure 29. Design for the 3D printed pills.

The pills needed to be filled inside as well, so two different patterns were created (Figure 31) in order to be able to change it if the resolution of the material was good enough. The difference between the designs was the distance between strands. In the smaller one the distance was 1 mm whereas in the wider one it was the double. In each layer the orientation of the pattern was alternated making two different orientations possible, vertical and horizontal. Parallel strands were plotted in the first layer and in the following one, the direction of the strands was turned. This pattern created a fine mesh with good mechanical properties and geometrically well-defined porosity. This way the printed material acquired more orientations and adhesion between layers was enhanced.

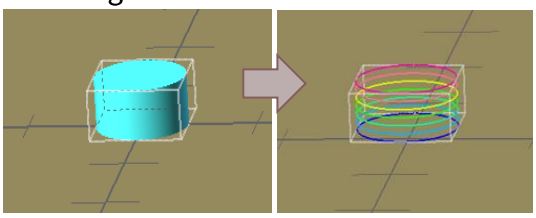

Figure 30. Sliced design in Perfactory.

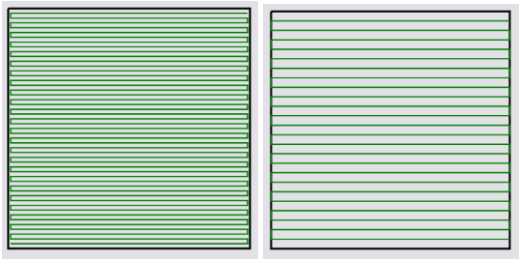

Figure 31. Designed patterns for the inner structure of the pills.

Now the printing parameters for each sample had to be searched. In this case they were experimentally obtained, meaning that parameters were changed until a successful print was obtained. The parameters are summarized in Table 6.

However, there were some logical changes that could be applied in the parameters. If the hydrogel was liquid like it needed less pressure to flow out of the cartridge compared with a more elastic hydrogel. Furthermore, increasing the speed results in less material deposited.

Increasing the temperature could help the material flow, but no important differences have been observed within the 5ºC change. Waiting time is related to the materials capacity to keep the shape. To finish with printing parameters discussion, hydrogels with lower restoration kinetics benefit from some seconds of waiting time between the layers.

Table 6. Printing parameters for each mixture prepared.

PRINTING PARAMETERS	PEGA0	PEGA2	PEGA8	GLYA0	GLYA2	GLYA12.5	GLYH6.25	GLYH12.5	GLYA12.5 H6.25
TEMPERATURE (ºC)	25	25	25	20	20	25	20	25	30
PRESSURE (bar)	0.6	4.7	1.5	2.8	3.5	4	3	1.2	4.5
SPEED (mm/s)	40	18	11	20	14	7	14	20	10
PRE-FLOW (s)	0	0.05	0.05	0	0.01	0	0.05	0	0.1
POST-FLOW (s)	0	0.1	0.1	0	0.01	0	0.1	0	0.1
WAIT TIME BETWEEN LAYERS (s)	1	5	5	0	0	0	5	5	5
NEEDLE OFFSET (mm)	0.33	0.33	0.33	0.33	0.33	0.33	0.33	0.33	0.33

8.6 PH BEHAVIOUR

The prepared formulations were intended to be used for oral drug delivery. Hence, a pH test that simulates gastric acid was performed in order to confirm whether the formulations were valid for the application or not.

For that a HCl buffer was prepared following the composition of a standard HCl buffer solution for a pH=1.2. For a realistic simulated digestion medium salts and digestive enzymes would be needed as well, but this test was only intended to investigate the pH-dependant behaviour of the formulations. [89]

After placing the samples into a polyethylene petri dish, 12 ml of the buffer were added to each sample and they were agitated in the incubator (Figure 32) for 30 minutes with constant movement and humidity. The temperature was kept at body temperature (37 ºC) throughout the whole period. [90]

Figure 32. Incubator for pH tests and sample lyophilizing process.

Once the 30 minutes were over, the samples were washed several times with water, lyophilized and stored in an evacuated desiccator until SEM characterization was carried out.

8.7 SEM

Scanning electron microscopy (SEM) is a technique that is based on the principle of optical microscopy in which the beam of light is replaced by an electron beam. It gives the possibility to obtain high resolution images with a magnification of 5x ~ 30,000x and up to 120,000x with digital zoom and examine different types of materials.

The instrument used is a Hitachi TM3030 Plus (Figure 33), which power of acceleration can vary between 1-30 kV. The acceleration of the electrons used was 10 kV. Accelerated electrons collide with gas molecules which dissociate into electrons, cations, and photons. The procedure is repeated several times. [91]

Figure 33. Hitachi TM3030Plus SEM device.

Scanning electron microscopy can be employed in various applications. Some examples are analysis of product design failures, surface defects, study of contaminants, characterization of the texture of the surface of a material and therefore morphological and structural study. [92]

8.7.1 SPUTTERING

The hydrogels to be analysed are not very conductive, thus a previous treatment of sputtering must be performed to increase the contrast during microscopy. For that, the printed pills were cut in half with a scalpel and mounted with paraffin wax on the sample holder before they were sputtered with gold to increase contrast. Samples of a non-conductive nature need to be used on conductive materials such as carbon tape, aluminium, copper, carbon or silver paint or aluminium sample holders. [93]

In the sputtering process, a material is coated with a conductive heavy metal by electrical ablation from the bulk material. The treatment consists of the radiation of energetic particles that erode the surface of the material exposed to the treatment. The energetic particles with which the surface of the sample is bombarded are gold, obtaining consequently a very thin layer of this material scattered on the surface of the hydrogel (Figure 34).

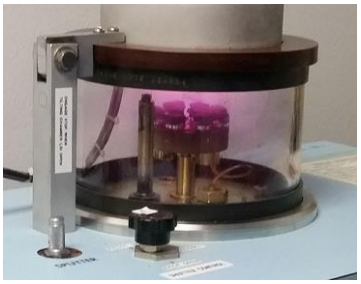

Figure 34. Gold sputtering process. [118]

A sputter coater Bio-Rad SC500 was used and the sputtering of the sample was done for 2 minutes with a voltage of 20 mA and 2 cm of distance.

9. RESULTS

9.1 GEL FORMATION

All the compounds added to the ink have groups that are either hydrogen bond donors or acceptors. Due to these groups, once the components are mixed and the mixture is let to rest, a network is formed.

As the bases for the mixtures are glycerol or water these will probably be the linkers for the rest of the components. In addition, the drugs are not completely solubilized in some of the mixtures so having big drug particles is probable. In those cases, the drug will interact with itself and only the molecules forming the surface will interact with the polymeric matrix. Atenolol is more soluble in water than HCTZ, meaning that the particles formed by atenolol will probably be smaller than the particles formed by HCTZ.

Taking all into account, a 2D scheme is proposed for the final formed network in Figure 35. Even though hydrogen bond donors and acceptors are marked in HCTZ and atenolol, it is probable that only the superficial molecules interact with the hydrogel's matrix, as they should form drug particles when they are added above their solubility limit.

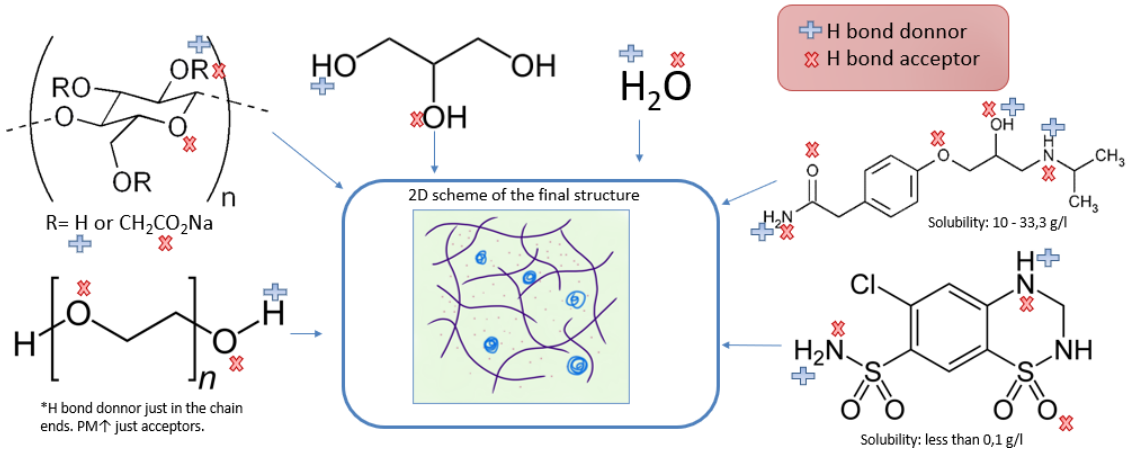

Figure 35. Representation of the hydrogen bond donors and acceptors present in the hydrogel's components and 2D scheme of the final structure. Small dots represent atenolol whereas blue big dots represent HCTZ particles. Purple lines represent the network formed by the polymeric matrix.

9.2 DESCRIPTION OF THE MIXTURES

A general description (Figure 36) of the samples prepared is compiled in Table 7. It is necessary to mention that the consistency of the mixtures changed over time, especially for the glycerol-based hydrogels. This tendency is explained by the rheology of the samples that will be explained in following sections.

Figure 36. All the samples prepared.

Table 7. Description of the samples right after their preparation.

MIXTURE (% COMPONENT)								
PEGA0	**PEGA2**	**PEGA8**	**GLYA0**	**GLYA2**	**GLYA12.5**	**GLYH6.25**	**GLYH12.5**	**GLYA12.5 H6.25**
Clear	Transparent	White, opaque	White, opaque	White, opaque	White paste, opaque	White, opaque	White, opaque	White, opaque
Blank	Viscous	More viscous. Effort to mix it homogeneously	Blank	Less viscous than PEGA2, same composition less drug.	Gum-like Not sticky Elastic	Liquid HCTZ not soluble	Liquid	Viscous
Less viscous than the formulations with the drug	Atenolol completely solved	Atenolol dispersed, no dissolved	Less viscous than the formulations with the drug	Atenolol dissolved	Atenolol dispersed	Not solubilized particles are clearly visible	Higher concentration of HCTZ	Atenolol and HCTZ dispersed
	Heterogeneous air bubbles. Mixed with rotor more bubbles	Not a lot of air bubbles			Prepared without heat (all glycerol-based mixtures)			Compared with the other mixtures it is not a gel, more liquid

Frequency sweeps of all mixtures are pretty similar following the behaviour shown in Figure 37. The information this measurement gives us is that after the printing process hydrogels remain as hydrogels and the internal structure is not altered.

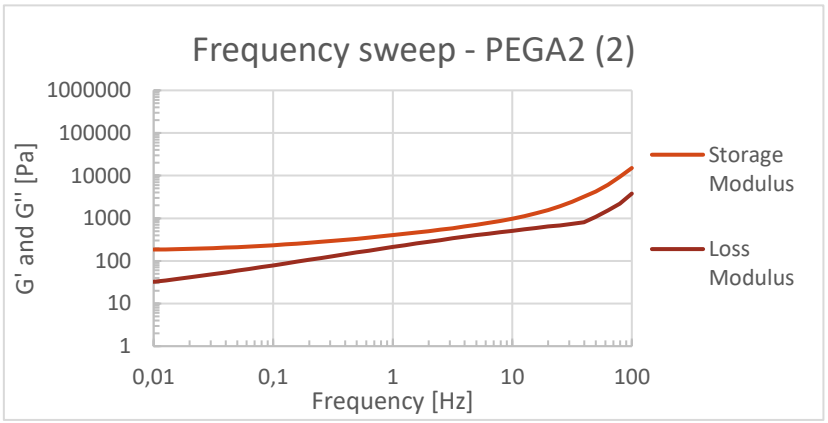

Figure 37. Example of these hydrogels' frequency sweep. All the samples follow the same behaviour varying G' and G'' values. Higher values in more elastic materials.

In addition, more elastic materials have higher G' modulus. When G' values are above G'', the hydrogel has a gel like behaviour, which is what is expected. In Figure 39 a comparison between G' values of the PEG based hydrogels is made where this behaviour can be seen. It is due to the solid content of the hydrogels. In PEGA2 atenolol is added below its solubility limit which makes the hydrogel more elastic compared with PEGA0. The effect is more drastic for PEGA8 where the drug is above its solubility limit. This effect can be related to the formulation containing atenolol particles, which are not fully solubilized, such that an increase in the G' value additionally to the effect shown in PEGA2 is observed.

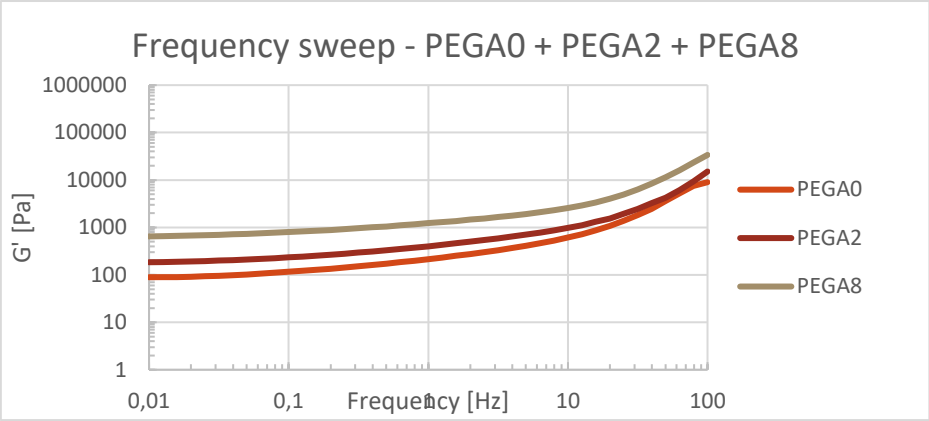

Figure 39. Frequency sweeps of the three PEG based hydrogels. The loss modulus is not represented as it follows Figure 54 scheme.

Similarly, in glycerol-based hydrogels frequency sweeps do not change much, except in the case of GLYA12.5 and GLYA12.5H6.25. In order to see the effect of the drug content, only the G' values will be compared with each other in Figure 38. They follow the same behaviour that has been discussed. More solid content equals more elastic material and higher modulus. Last, frequency sweeps confirm that the samples are still hydrogels after the printing process.

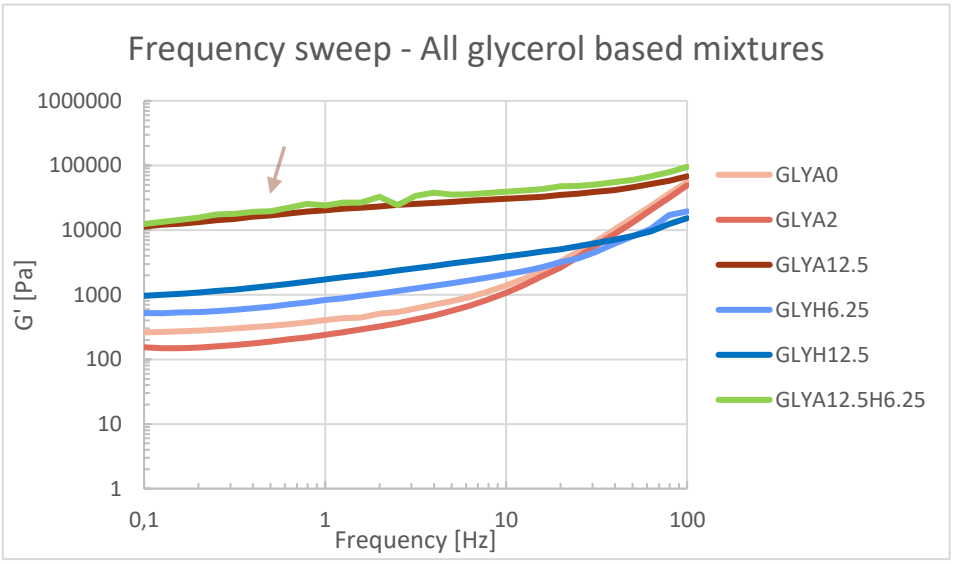

Figure 38. Storage modulus for all the glycerol-based samples in frequency sweeps.

In Figure 38 we can see that even though the expected behaviour is followed regarding elasticity, the hydrogel containing the higher concentration of atenolol has a huge increase in its G' value. Such an increase was not expected. It could be due to a bad dispersion of the drug in the hydrogel. However, what its clear is that the interaction between HCTZ or atenolol with the polymeric matrix is not the same. With the same concentration of HCTZ (GLYA12.5 and GLYH12.5) there is not such an increase in the storage modulus.

Notably, comparing frequency sweeps between PEG based and glycerol-based hydrogels for similar drug concentrations we can see that the behaviour is not the same (Figure 40).

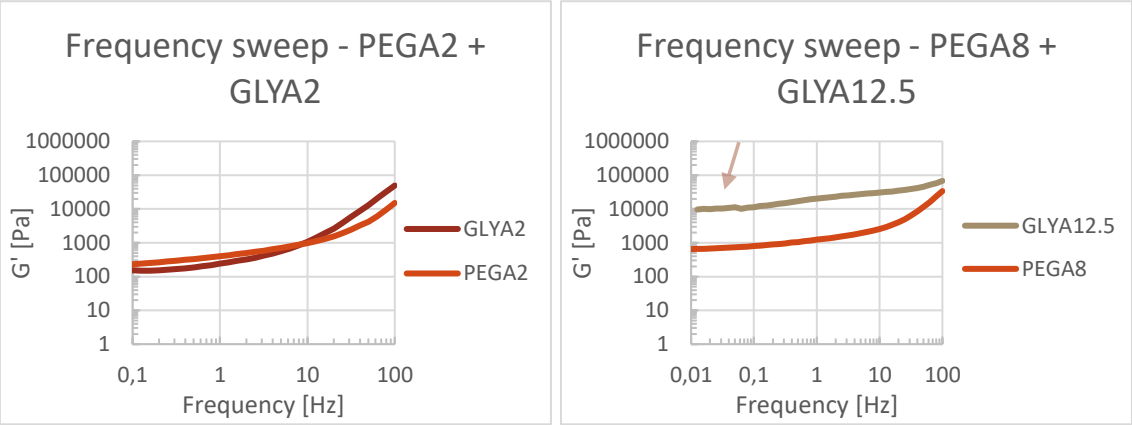

Figure 40. Comparation between PEG and glycerol-based hydrogels for similar drug concentrations.

In Figure 40 it was confirmed that the interaction between atenolol and the polymeric matrix is quite different. When it is below its solubility limit (GLYA2 and PEGA2) their behaviour and storage moduli are similar whereas at higher atenolol concentrations (GLYA12.5 and PEGA8), where the drug is above its solubility limit, the glycerol-based hydrogel experiences a bigger increase in the value. These behaviours are directly connected with the hydrogels network formation and it will be discussed later in the following section.

9.3 GELS UNDER STRESS

The behaviour of the hydrogels under stress has been tested for ensuring the printing process. Hydrogels show a predominantly solid-like behaviour as their G′ value is above their G″ value. However, in PAM extrusion-based 3D printing, when a certain pressure is applied to the sample, it needs to flow.

Starting by comparing the blanks with each other, when high values of strain (or stress) are applied to the samples, we can see a flow point in both mixtures, meaning that from this strain value onwards the hydrogel has a predominantly liquid-like behaviour. However, until that point the behaviour is predominantly solid-like.

We can already see some differences in PEG and glycerol-based hydrogels. PEG based ones have a larger linear viscoelastic region (LVE) than the glycerol-based ones, which lose their linear behaviour at low strain values as we can see in Figure 41. However, without any drug both mixtures have G' and G'' values in the same order of magnitude.

a)

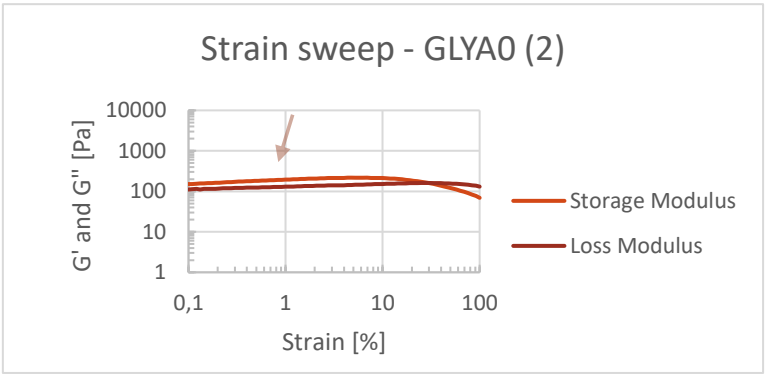

b)

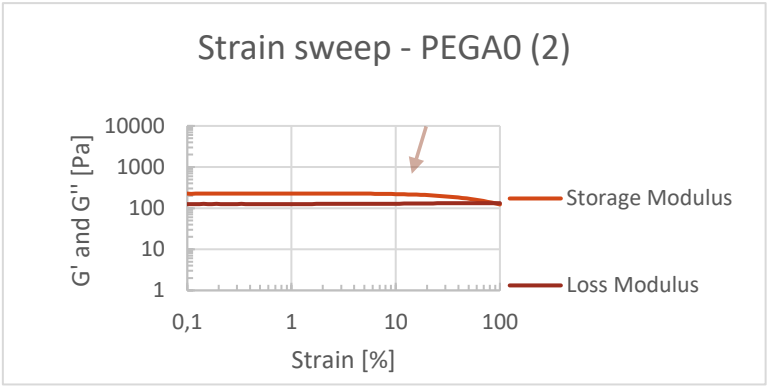

Figure 41. Comparison between the strain sweeps of the blanks a) GLYA0 and b) PEGA0. Faster linearity loss in GLYA0 and yield stress at lower strain values.

The behaviour shown in Figure 41 is needed for the ink to be printable by PAM as the crossover point is related to the yield stress that the sample needs for flowing in the printing process. This behaviour will be further investigated in the following sections.

9.4 STABILITY OF MIXTURES OVER TIME

Stability is key for pharmaceutical applications, so in this section the objective was to see if the mixtures prepared were stable or not over time. Comparing the same rheological tests measured with a defined period of time difference in between was the method used for this purpose.

Most of the samples showed a great stability over a couple days. For example, both PEGA2 strain sweeps point out that the behaviour is exactly the same as they overlap (Figure 42). The time the mixture has been stored in the refrigerator has not changed its properties. The same kind of stability was demonstrated for atenolol-based formulations PEGA0, PEGA8, GLYA2, GLYA12.5 and GLYA12.5H6.

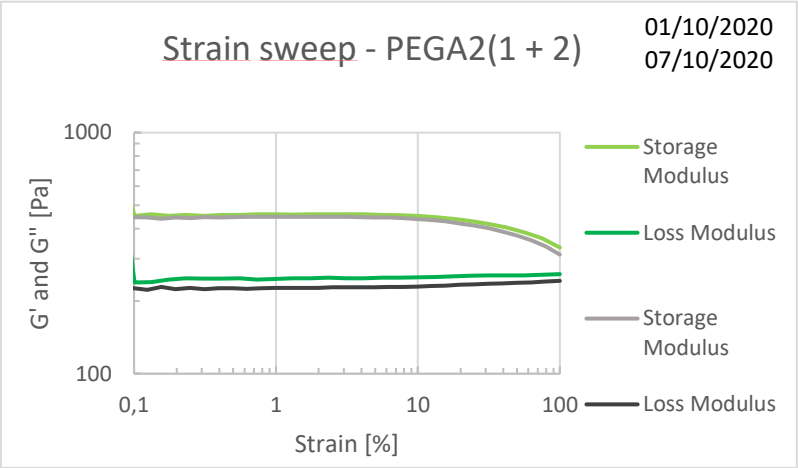

Figure 42. Strain sweep of the same sample with a week of difference between the measurements.

Conversely, HCTZ containing mixtures did not show such stable behaviours. To start with, GLYA0 has a behaviour that changes with time (Figure 43). The strain sweeps vary from one day to another and the behaviour also changes. Time profiles also show this change in the starting values.

a)

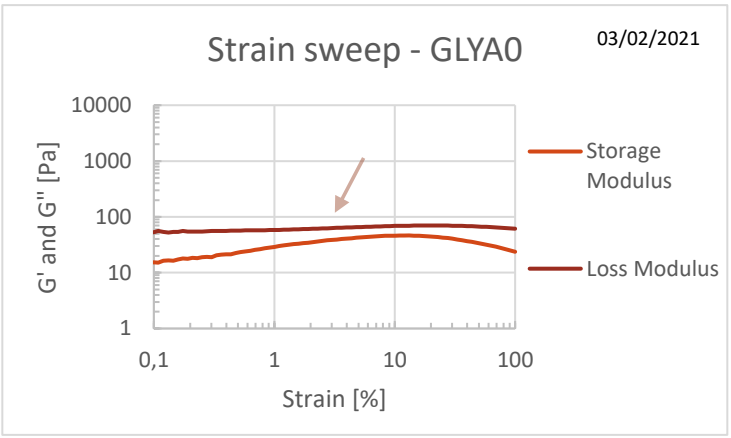

b)

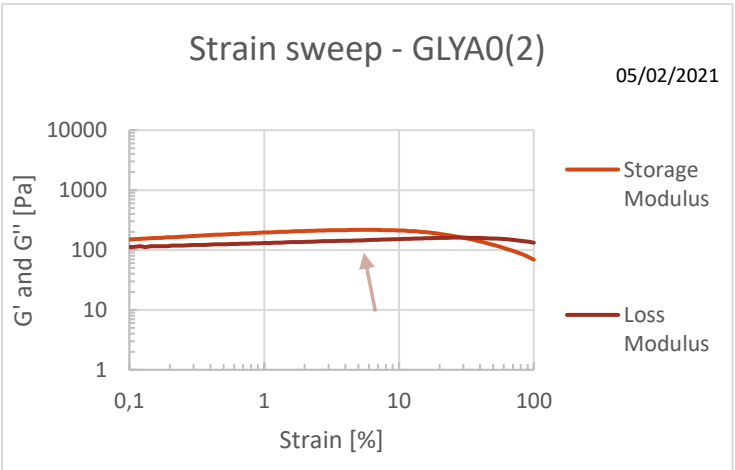

Figure 43. GLYA0 blank's strain sweeps. Liquid-like behaviour until stabilized. A) Measured the 03/02/21 and b) 05/02/21.

Second, GLYH6.25 (Figure 44) was very liquid at first, meaning that trimming the sample for the measurements was a bit difficult because as soon as it was trimmed it expanded again. The differences are obvious and the strain sweeps show different behaviours, changing from a predominantly liquid behaviour to a predominantly solid one.

It's probable that the dispersion of the HCTZ affects the measurements, varying the strain sweeps depending on the amount of HCTZ particles present in the sample for the measurement, even though it was mixed before the measurement to try to minimize the effect. The hydrogel needs a week or so to reach a stable rheological behaviour as we can see in the graphs above.

a)

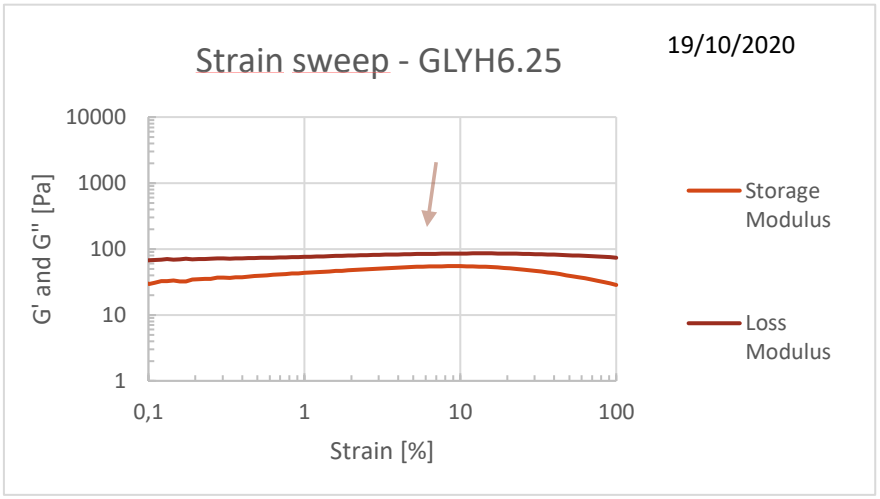

b)

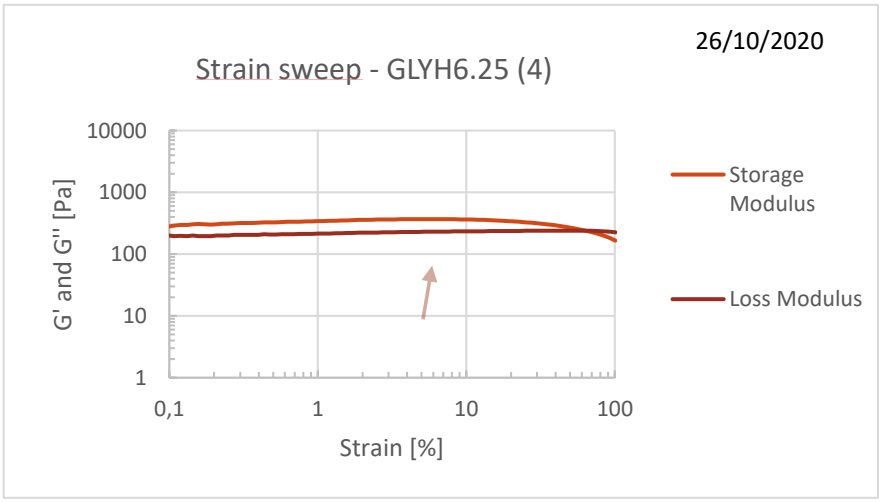

Figure 44. Strain sweeps of GLYH6.25 with a week of difference a) measured the 19/10/20 and b) 26/10/20. In a) the loss modulus is above the storage modulus whereas in b) the storage modulus is above. The behaviour of the same sample before and after being settled is completely different.

In GLYH12.5 the problem was similar as with GLYH6.25; the sample was to liquid to trim it properly at first. Likewise, the sample was homogenized before the measurements by stirring with a spatula. The concentration of HCTZ is doubled to the previous one, thus there should be more non-solubilized particles in the mixture, meaning a more solid content. Consequently, the sample became more elastic with time. There is a change in the order of magnitude of G' values from the first measurement to the last one, meaning that this mixture also needs a week or so to stabilize (Figure 45).

a)

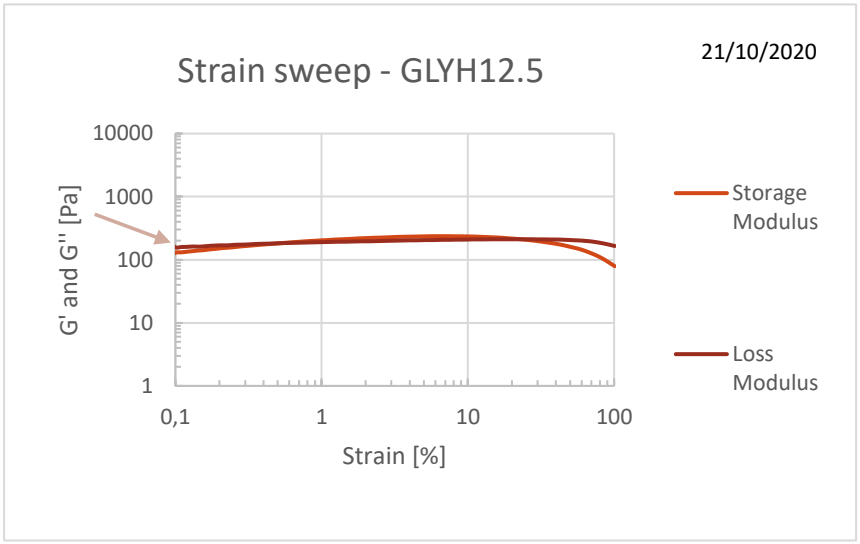

b)

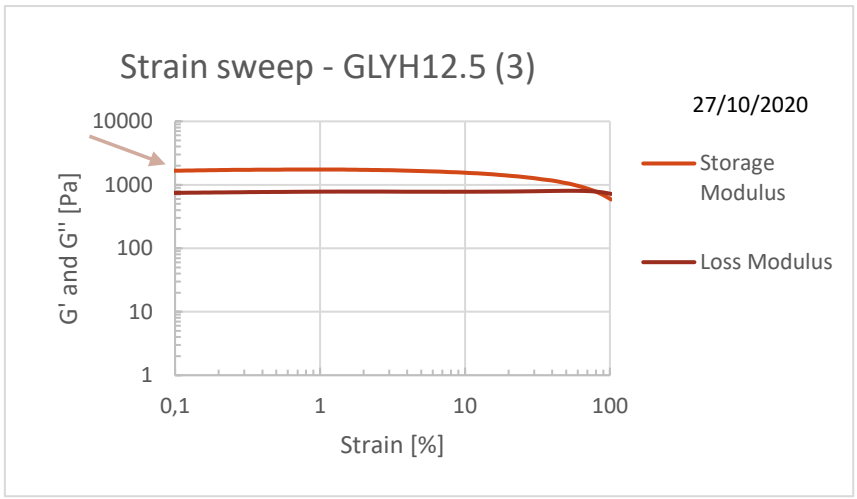

Figure 45. GLYH12.5's strain sweeps a) measured the 21/10/20 and b) 27/10/20. Notable difference with 6 days of difference between the measurements.

9.5 EFFECT OF THE DRUG INCORPORATION IN THE RHEOLOGICAL BEHAVIOUR OF HYDROGELS

Now that the stability of the mixtures has been discussed, comparing different compositions is the next step. By comparing the mixtures with each other we can see some patterns. All these comparisons were made under stable conditions.

The hydrogels are easily divided into two groups: first, PEG and water based and glycerol based. Thus, the comparation will be divided this way.

9.5.1 PEG BASED HYDROGELS

The difference between the PEG based hydrogels is that in PEGA2 the drug is below its solubility limit and in PEGA8 it is above it. The solubility of atenolol in water is 10 - 33,3 g/l. [94]

Starting by comparing PEGA0 and PEGA2 (Figure 46) adding the drug to the blank triggers a slight increase in both G′ and G″ values. Continuing with the comparation of PEGA2 and PEGA8 the change in the behaviour is similar. As the concentration of the drug increases the material becomes more elastic. In PEGA8 atenolol is above its solubility limit, thus solid particles are expected to appear in the hydrogel increasing both G′ and G″ modulus. From the blank (PEGA0) to PEGA8 there is an order of magnitude of difference.

Finally, the yield stress value (G′=G″) shifts to higher strains as the concentration of the drug increases. In addition, the linear behaviour is lost at lower strain values as the concentration increases. When we have longer linear behaviours the homogeneity of the dispersions is better than with shorter linear regions.

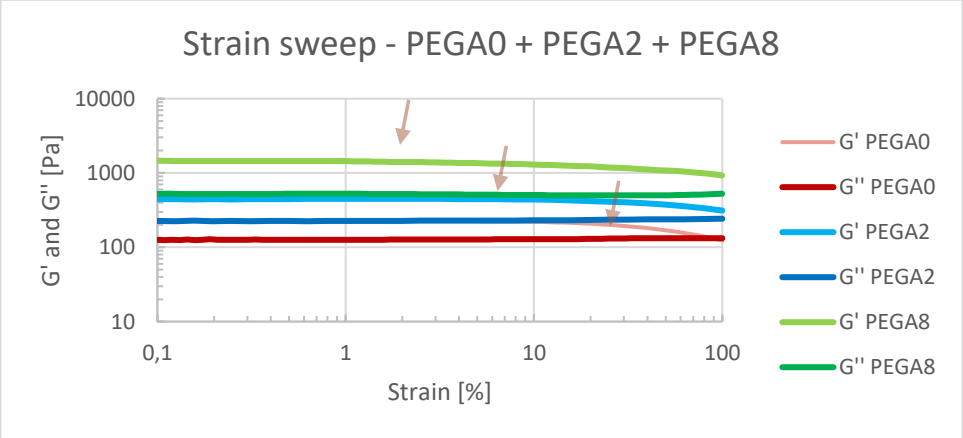

Figure 46. PEGA0, PEGA2 and PEGA8 strain sweeps. Slight variation in G′ and G″ values. Yield stress shifts to higher strains and the linear behaviour is lost at lower strain values as the concentration of the drug increases.

9.5.2 GLYCEROL BASED HYDROGELS

Now focusing on glycerol-based hydrogels, their composition varies the following way: the first 3 mixtures are similar to PEG based hydrogels where the percentage of atenolol increases progressively. GLYA0 is the blank that doesn't contain any drug, GLYA2 contains atenolol below its solubility limit and GLYA12.5 contains it above the solubility limit. Now starting to compare different compositions with each other, GLYA0, GLYA2 and GLYA12.5 follow the same behaviour as before. Adding the drug to the blank causes a slight increase in both G' and G'' values and the hydrogels behaviour is still similar in GLYA0 and GLYA2 (Figure 47).

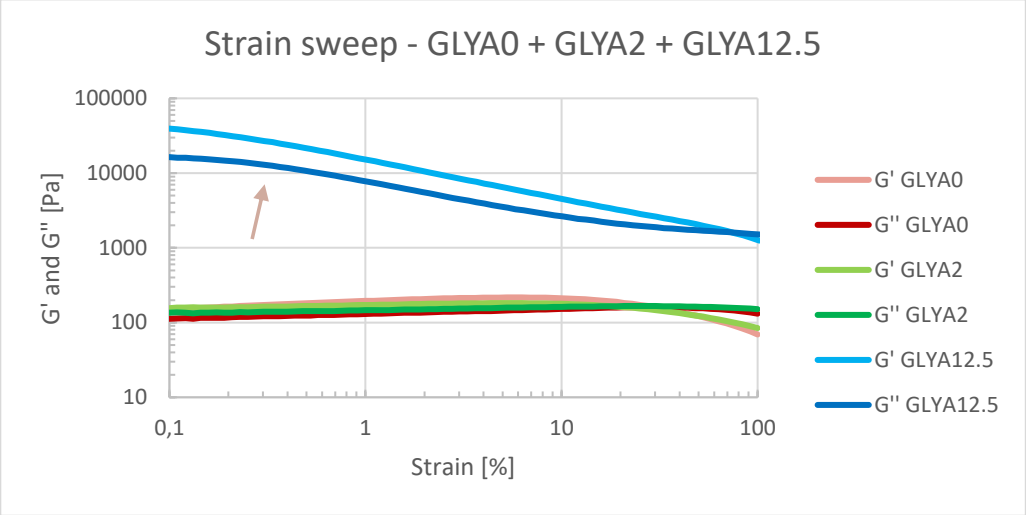

Figure 47. GLYA0, GLYA2, and GLYA12.5 strains sweeps. Slight G' and G'' increase in GLYA2 compared with GLYA0. Huge increase in GLYA12.5.

However, with GLYA12.5 the behaviour is much different. The increase on G' and G'' values is more drastic and it has a particular form that was not expected. As the concentration of atenolol is high, solid drug particles are dispersed into the hydrogel. When the sample is submitted to high strain values first the aggregation of drug particles is destroyed, and subsequently the crosslinked polymer network experiences the increasing amount of strain. Thus, the disproportionate increase is due to a bad dispersion of the drug particles in the hydrogel and the formation of a particle scaffold.

Focusing on HCTZ containing hydrogels, as the concentration of HCTZ increases the mixture becomes more elastic as we can see in the strain values of the GLYH6.25 and GLYH12.5 (Figure 48), explainable by the same reasons as the previous mixtures. In this case, both mixtures are above the solubility limit because HCTZ is less soluble than atenolol. HCTZs solubility is lower than 0.1g/L. [85] More solid content in the hydrogel helps having more elastic hydrogels with higher G' and G'' values. However, even though HCTZ mixture

are well above the solubility limit, they show a pronounced LVE region, reflecting a good dispersion of HCTZ particles within the hydrogel.

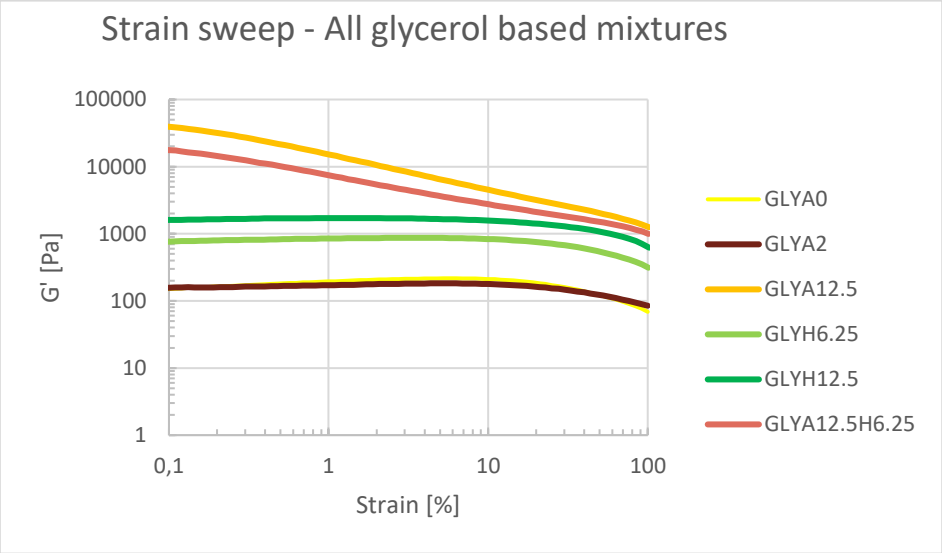

Figure 48. Strain sweep for GLYH6.25, GLYH12.5 and GLYA12.5H6.25.

At last, the mixture containing both drugs followed the expected behaviour. It combines the behaviour explained for GLYA12.5 which contained a high amount of atenolol particles dispersed and the behaviour of GLYH6.25 (

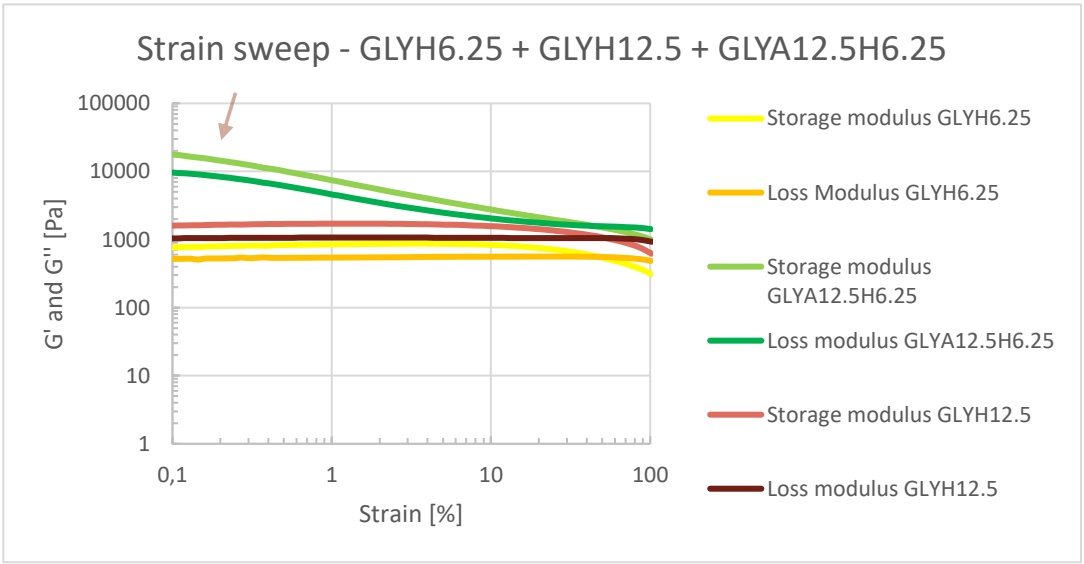

Figure 49). The bad dispersion that atenolol has in glycerol-based hydrogels is still present in GLYA12.5H6.25 but G' value seem to be countered by the incorporation of HCTZ.

Figure 49. Comparation between storage modulus of all the glycerol-based hydrogels.

9.6 REVERSIBILITY OF GELATION

By these measurements, the gel's restoration kinetics can be clearly seen. There is a difference between PEG and glycerol-based hydrogels as well as between mixtures with and without an API, so the comparison will be done this way. The mixtures made for the 3D printing application need to be reversible in order to be valid for the printing process. The hydrogels flow in the extrusion process and once the stress is not being applied, they need to recover their structure.

Ideally, in the last interval where low strain values are being applied again, storage and loss modulus should recover immediately the values shown in the first interval once the high strain is not being applied. This behaviour would be related to a good printability. If a hydrogel is extruded and deposited again by a layer-by-layer method, it would be ideal to recover the properties the hydrogel had before breaking its structure immediately.

9.6.1 WITHOUT DRUG

As we can see in Figure 50, the mixtures have quite a different recovery. Both of the blanks have G' values higher then G'', being predominantly solid-like and when a critical strain is applied, the network is broken and G'' gets higher values than G'. Then, when the strain is lowered again, both hydrogels recover higher G' values than G''.

Both hydrogels recover the starting properties. However, glycerol-based hydrogels need longer period of times to restore their structure whereas in the case of PEG based hydrogels the structure is recovered immediately.

a)

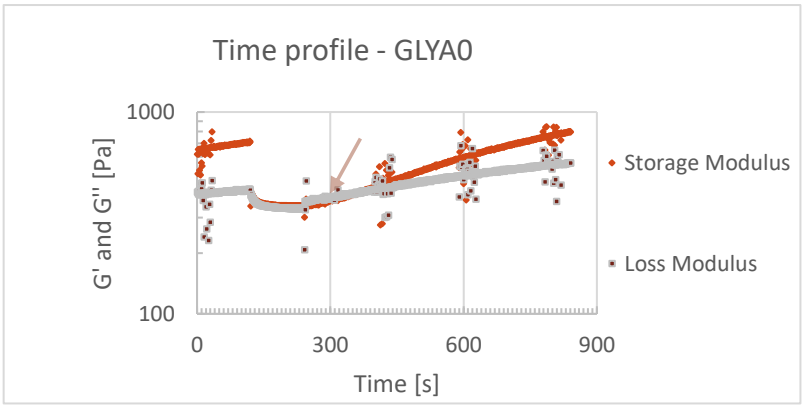

b)

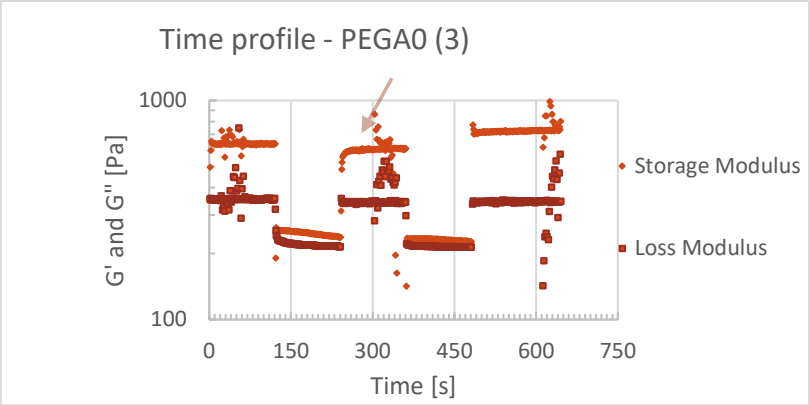

Figure 50. Comparation of time profiles of the blanks. A) represents GLYA0 and b) PEGA0.

9.6.2 WITH DRUG

The time profile for all PEG based hydrogels is favourable due to the hydrogels fast recovery when it is broken by high strain values. Best kinetics are observed for PEGA2, which has solubilized drug incorporated in the hydrogel. Atenolol particles could form hydrogen bonding interactions with the gel's matrix easily, explaining the fast recovery of the structure. However, it could also be that atenolol just doesn't inhibit the gel formation at such concentrations, because in the end it's very similar to PEGA0.

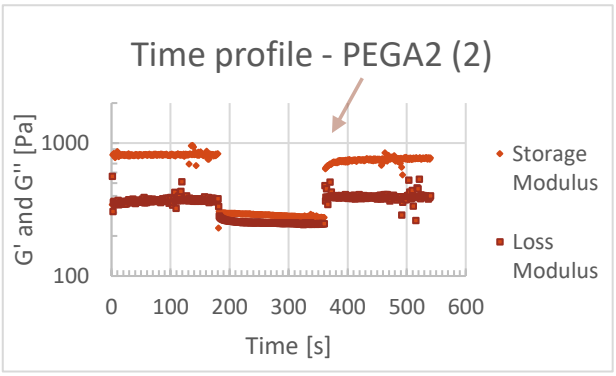

Figure 51. Time profile for PEGA2.

Two characteristics can be observed in Figure 51. First, the hydrogel recovers almost instantaneously to its initial values for G' and G'', giving the information of fast structure recovery. Second, the values reached are almost the same as the starting ones, meaning that the hydrogel doesn't lose its properties when high strain values are applied to it.

To conclude with this section, time profiles of glycerol-based hydrogels differed from the PEG based ones. They have slower restoration kinetics as shown in Figure 52.

a)

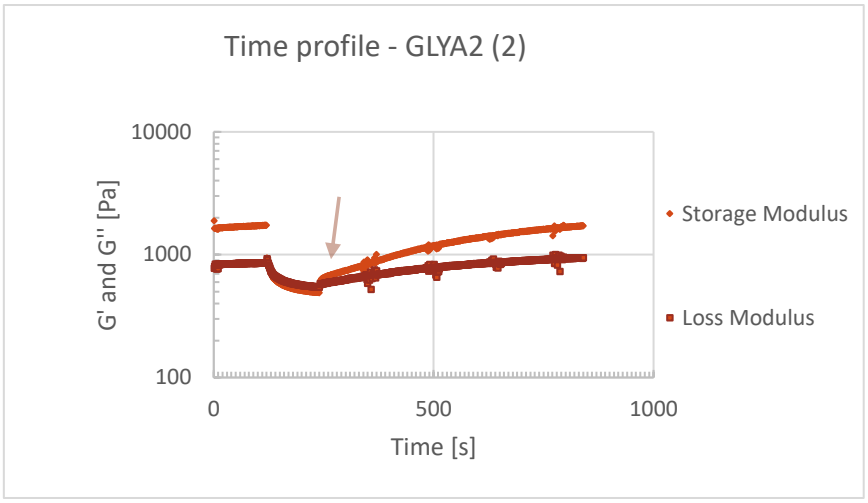

b)

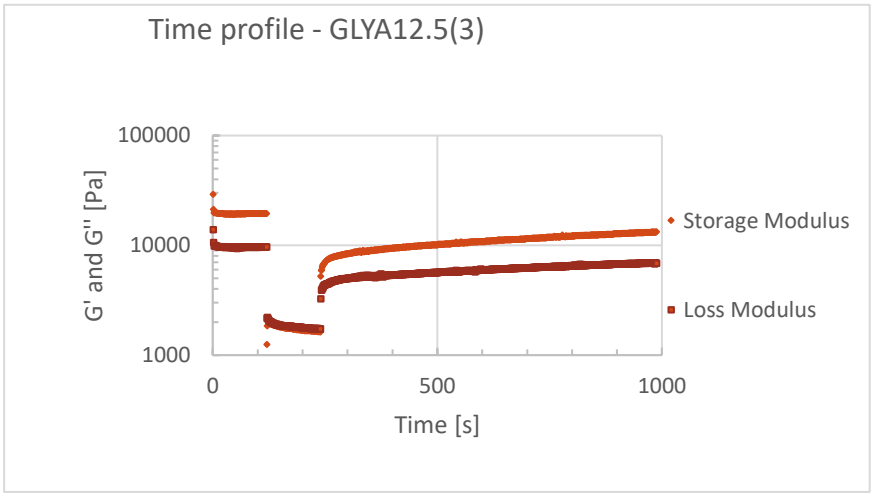

Figure 52. Time profile for GLYA2 and GLYA12.5 as an example for glycerol-based hydrogels a) referring to GLYA2 and b) to GLYA12.5. Slower restoration than with PEG based hydrogels. Better kinetics with higher drug concentration.

All the glycerol-based mixtures followed a similar behaviour as the example, but there are slight differences to the hydrogels containing a lower amount of drug. The behaviour of GLYA12.5 showed a faster restoration whereas GLYA2 has a behaviour more similar to the blank (GLYA0). The more immediate restoration in GLYA12.5 is probably due to the bad dispersion of the drug within the hydrogel.

9.7 PEG BASED VS GLYCEROL BASED HYDROGELS

Concluding with the rheological results, some general trends can be stated about each type of hydrogels (Figure 53). Each one has its advantages and disadvantages and their used is totally up to the user.

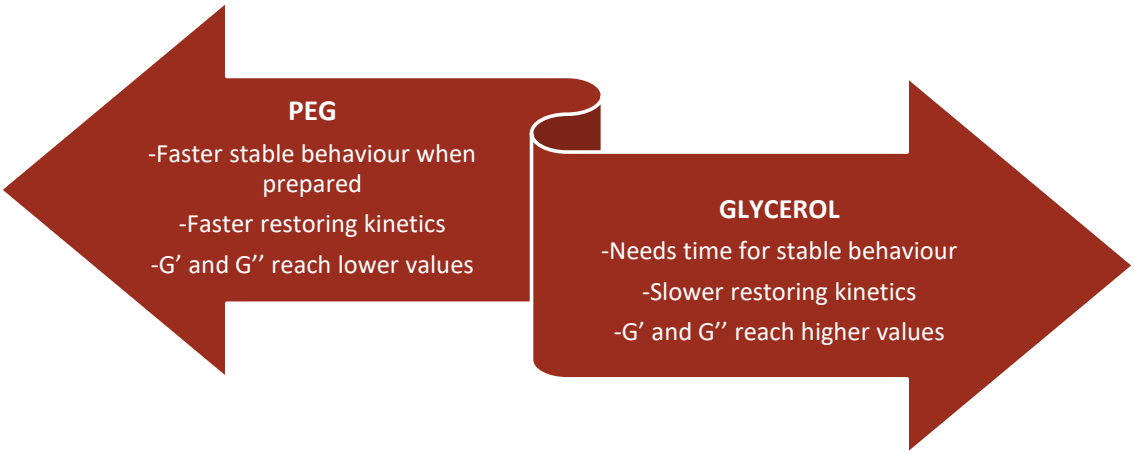

Figure 53. Comparison between PEG and glycerol-based hydrogels. Advantages and disadvantages.

In addition, the behaviour of each hydrogel varies with the API added as we have seen in this section, thus the interaction between the API and the hydrogel matrix does not seem to be the same in both cases. This has to be taken into account when the hydrogel is chosen depending on the rheological behaviour desired.

9.8 3D PRINTING

9.8.1 PRINTING MODEL FOR THE TIP

During the printing process, one of the most time-consuming parts has been the search of good printing parameters. They have been optimized by trial and error, which needed a large amount of tries. Thus, relating the rheological behaviours with printing conditions could be really interesting.

For this purpose, the following mathematical model has been applied to the experimental data. The intention is adapting the model to the data obtained by the rheological measurements and see if it fits correctly. If the model fits, parameters such as the pressure needed when printing could be easily predicted.

For the simulation of the model, the viscosity of a Newtonian material will be used where $\eta = \eta_o$(1). The strain sweeps made with the rheometer are related to the shear stress applied to the material in order to make it flow. Even if a Newtonian viscosity has not been measured, the complex viscosity has been. Thus, an assumption where η_o and η^* can be used indiscriminately will be made.

First, we need to put the stress (σ) as function of pressure (ΔP) in order to build a graph with the yield stress necessary to make the mixture flow and the values used for printing them. With this objective, we start from the stress equation where S_L is the lateral surface of a truncated cone, R_o is the radius of the tip on the upper part (Figure 54 and Figure 56) and F is the force exerted at the entrance of the tip. Therefore, the equation is as follows:

$$\sigma = \frac{F}{S_L} = \frac{\Delta P * surface\ area}{S_L} = \frac{\Delta P\ \pi\ R_0^2}{S_L} \quad (2)$$

As the lateral surface of a truncated cone is defined as shown in Figure 54, it can be substituted in the previous equation.

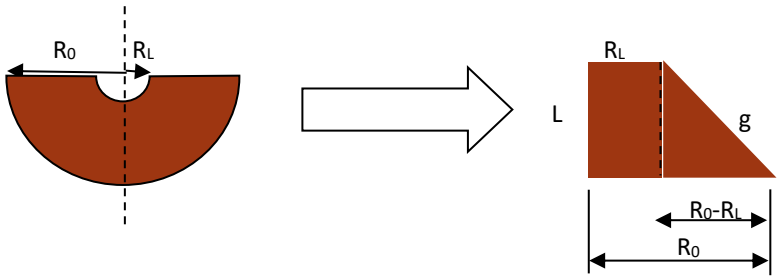

Figure 54. Parameters related to the lateral surface of a truncated cone.

$$S_L = \frac{2\pi R_L + 2\pi R_0}{2} g \quad (3) \qquad g = \sqrt{L^2 + (R_0 - R_L)^2} \quad (4)$$

$$S_L = \pi(R_0 + R_L)\sqrt{L^2 + (R_0 - R_L)^2} \quad (5)$$

Therefore, the stress as a function of pressure is as follows:

$$\sigma = \frac{\Delta P\ \pi\ R_0^2}{\pi(R_0 + R_L)\sqrt{L^2 + (R_0 - R_L)^2}} = \frac{\Delta P\ R_0^2}{(R_0 + R_L)\sqrt{L^2 + (R_0 - R_L)^2}} \quad (6)$$

With the relations made, the fit needs to be proven. .

Table 8 shows the parameters given by the printer, the calculated shear from the model explained and the shear stress values.

Table 8. Pressure values used to print the material in the Bioplotter, calculated shear stress values with the mathematical model and shear stress values from the strain sweeps of the mixtures.

	PEG A0	PEGA2	PEGA8	GLYA0	GLYA2	GLYA 12.5	GLY H6.25	GLY H12.5	GLYA12.5 H6.25
Pressure Bioplotter (Pa)	60000	470000	150000	280000	350000	400000	300000	120000	450000
Calculated shear stress (Pa)	1087	8516	2717	5073	6341	7247	5435	2174	8153
Yield stress point (Pa)	170	-	-	68,5	44,4	1630	215	783	987

In Figure 55 a critical value of shear stress has been defined (represented by the shear stress line). The stress values achieved in the printing process need to be below this line in order to make the hydrogels flow. Thus, the area shown below the line represents the printing area whereas the area above the line represents the clogging area.

Clogging occurs when the material blocks the small hole at the end of the nozzle, preventing the flow of the material. The clogging can be partial or total, either blocking the materials flow completely or just restricting it enough to cause problems. In both cases, the pressure is triggered.

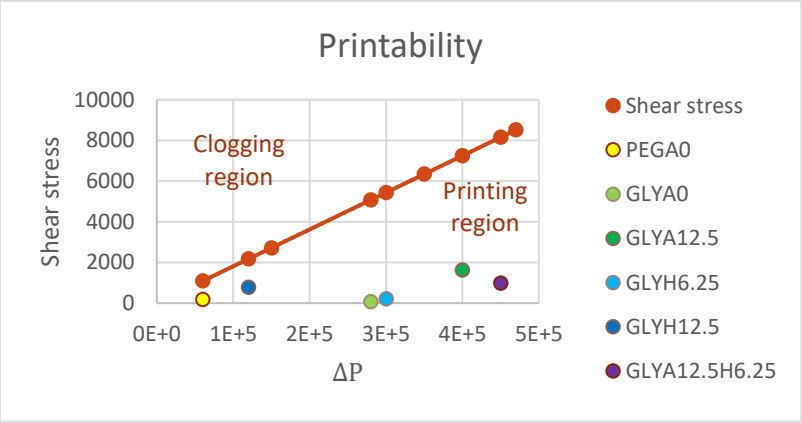

Figure 55. The line in this graph represents the limit shear stress value that need to be applied to the tip in the 3D printing process. The area below the line represents the printing zone whereas the area above represents the stress values where clogging occurs.

Once the printability of the samples has been tested, the calculation of the printing velocity has been made. This time the last values of the complex viscosity were taken in order to fill Equation 10's parameters, assuming it can be used as the Newtonian viscosity

value. Another assumption made here was that the speed of the tip set on the Bioplotter could be compared with the flow of material that what coming out of the tip.

The first thing we need to do is express the viscosity as a function of speed and the stress as function of pressure. First, starting by putting the viscosity as a function of speed, the equation obtained from the book "dynamics of polymeric liquids" [103] that describes the viscosity of a material in a truncated cone will be used, which represents the form of the point used for the PAM 3D printing (Figure 56). [96]

$$Q = \frac{\pi\,\Delta P\,R_0^4\,R_X}{8\eta L} \quad (7) \qquad R_X = \left[1 - \frac{1 + \frac{R_0}{R_L} + \left(\frac{R_0}{R_L}\right)^2 - 3\left(\frac{R_0}{R_L}\right)^3}{1 + \frac{R_0}{R_L} + \left(\frac{R_0}{R_L}\right)^2}\right] \quad (8)$$

In addition, the flow rate Q can be also defined as $Q = \pi r_q V$ (9), where V is the caudal of material per time unit (mm³/s) that comes out of the tip. Replacing this in the previous equation by replacing the Q term we obtain:

$$\pi r_q V = \frac{\pi\,\Delta P\,R_0^4\,R_X}{8\eta L} \quad (10)$$

Now, taking into account that we are interested in the flow at the exit of the tip the r_q parameter is equal to R_L, which can also be substituted (Figure 56). As π is present in both sides it is cancelled, simplifying the equation. Then, the viscosity is set as a function of the speed so that it can be replaced.

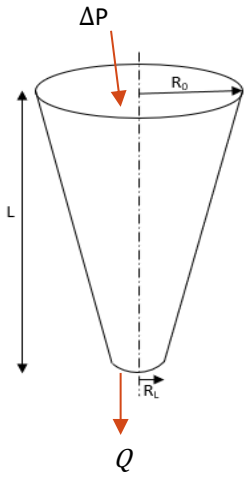

Figure 56. Parameters related to the tip.

$$R_L V = \frac{\Delta P\,R_0^4\,R_X}{8\eta L} \quad (11) \rightarrow \quad \eta = \frac{\Delta P\,R_0^4\,R_X}{8VLR_L^2} \quad (12)$$

Once the viscosity is obtained as a function of velocity it is substituted into the equation of a Newtonian material's viscosity. Finally, the speed (V) is cleared from the equation and calculated (Table 9).

$$\eta = \eta_o \ (13) \quad \rightarrow \quad \frac{\Delta P\,R_0^4\,R_X}{8VLR_L^2} = \eta_o \ (14) \quad \rightarrow \quad V = \frac{\Delta P\,R_0^4\,R_X}{8LR_L^2\eta_0} \quad (15)$$

Table 9. Prediction of printing speed by the mathematical model.

	PEGA0	PEGA2	PEGA8	GLYA0	GLYA2	GLYA12.5	GLYH6.25	GLYH12.5	GLYA12.5 H6.25
Complex viscosity (Pa·s)	29,5	62,9	170	36,1	37,1	372	125	236	357
V Bioplotter (mm/s)	40	18	11	20	14	7	14	20	10

V predicted (mm/s)	28729	105545	12463	109557	133255	15188	33900	7182	17804

This time the model did not work properly as it was expected. It is clearly visible that the model cannot be used with the parameters measured in the experiments done in this work. Furthermore, the assumptions made in order to predict the parameters are not correct as the values obtained for the speed are not realistic at all.

9.8.2 POST-PROCESSING

The post processing of the sample is required in order to achieve a final stable product. The method for drying the sample was simple, storing them at room temperature for at least a week in a petri dish covered by a lid. The difference from the freshly printed pill to the dried one can be seen in Figure 57.

Figure 57. GLYH12.5 freshly printed on the left and dried on the right.

9.8.3 RESOLUTION CRITERIA

At first, we though that fast restoration kinetics were needed in order to have good resolutions. It seems logical that if the polymeric matrix restores itself fast, the appearance of the printed object would be more accurate to the designed model. However, materials time profiles and the pills printed did not show this behaviour. First, in the case of PEG based

a)

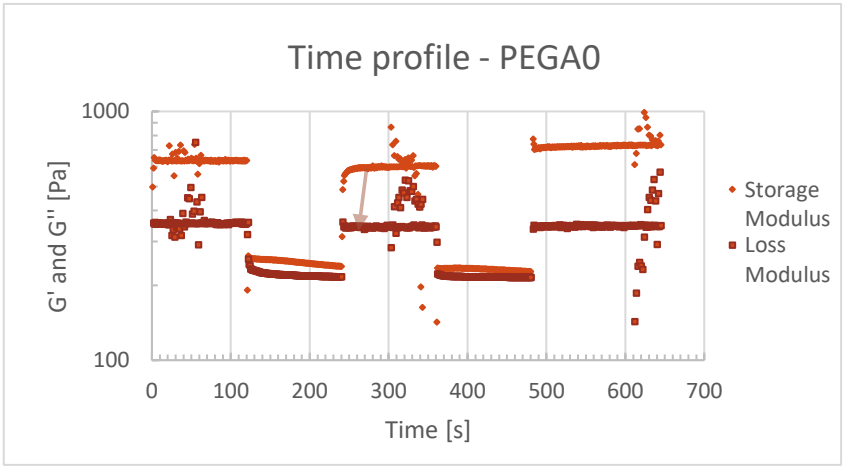

samples, their time profiles show instantaneous restoration kinetics as can be seen in Figure 58.

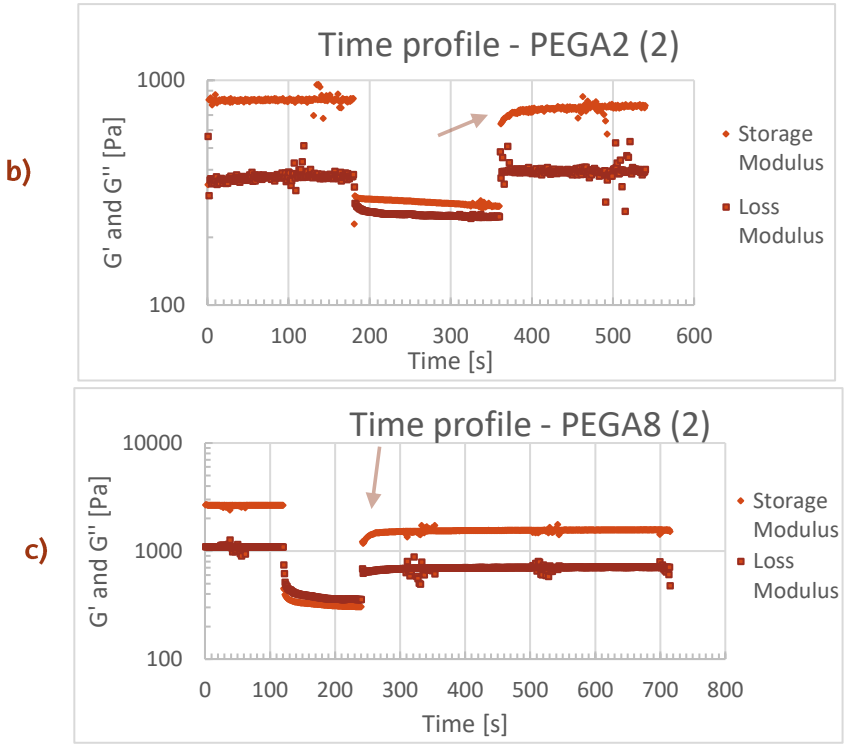

Figure 58. Time profiles of the three PEG based hydrogels. a) PEGA0, b) PEGA2 and c) PEGA8.

With these immediate recovering networks good resolutions were expected but only PEGA8 showed it as we can see in Figure 59.

Analysing the same with the glycerol-based mixtures, they show slower restoration kinetics as we can see in Figure 60.

Figure 59. PEGA0 (left), PEGA2 (middle) and PEGA8 (right).

a)

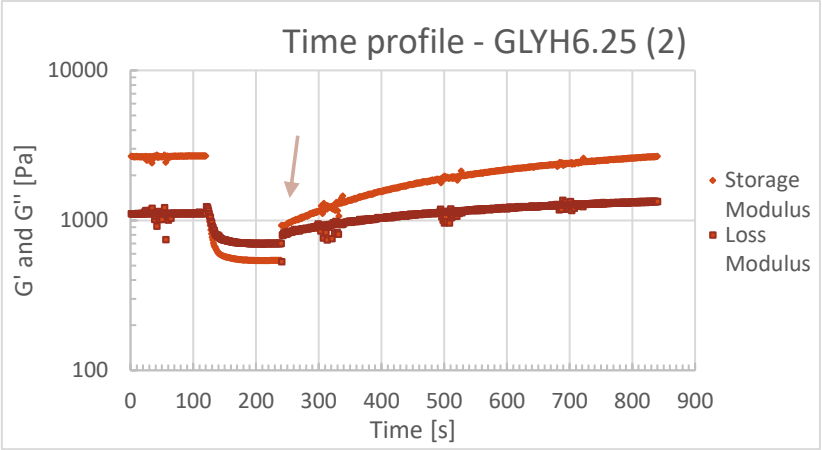

b)

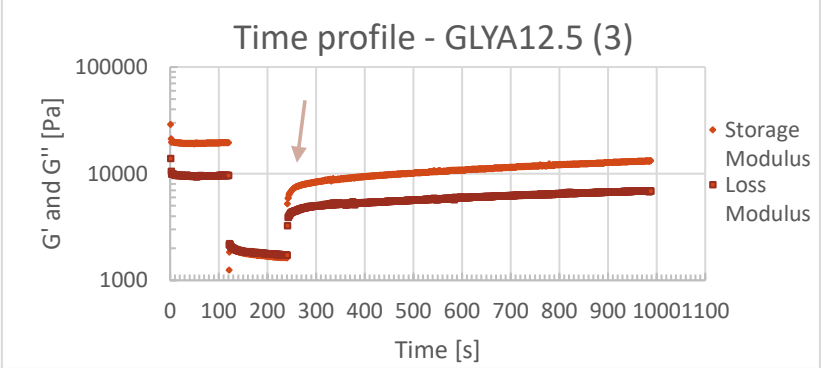

c)

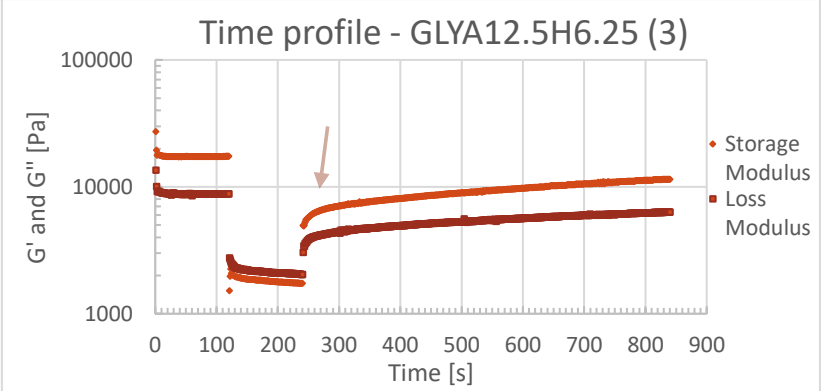

Figure 60. Time profile examples for glycerol-based mixtures. a) GLYH6.25, b) GLYA12.5 and c) GLYA12.5H6.25.

In this case, only GLYA12.5 and GLYA12.5H6.25 shoed good restorations kinetics as we can see in Figure 61, but both formulations show slower restoration kinetics then PEG based hydrogels.

By interpretating these results, it seems that all the samples with good resolution present a G' values over 1000 Pa, regardless the recovery kinetics. Thus, the recovery profile does not seem to be critical for the resolution.

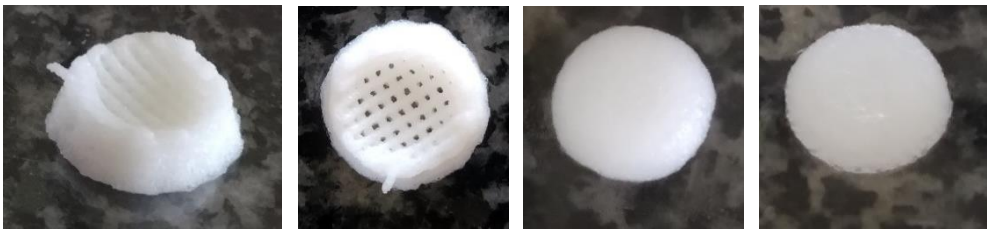

Figure 61. Printed pills for GLYA12.5H6.25, GLYA12.5, GLYH6.25 and GLYH12.5 from left to right.

9.9 MORPHOLOGICAL CHARACTERIZATION

The last step for the thesis was the evaluation of the morphology of the printed pills and the influence of acidic pH on it by scanning electron microscope (SEM), to estimate the behaviour of the pills in the stomach. As explained in the experimental procedure, each pill was submerged in an HCl buffer (pH=1.2) for 30 minutes and slightly agitated. By SEM a comparison can be made between the samples before and after their exposure to acidic pH. Characteristics such as porosity and surface morphology can be studied by SEM technique.

9.9.1 SEM OF UNTREATED GLYA12.5

The first SEM characterization was done with GLYA12.5 after it was printed and dried. The samples were cut with a scalpel and the cross section was observed.

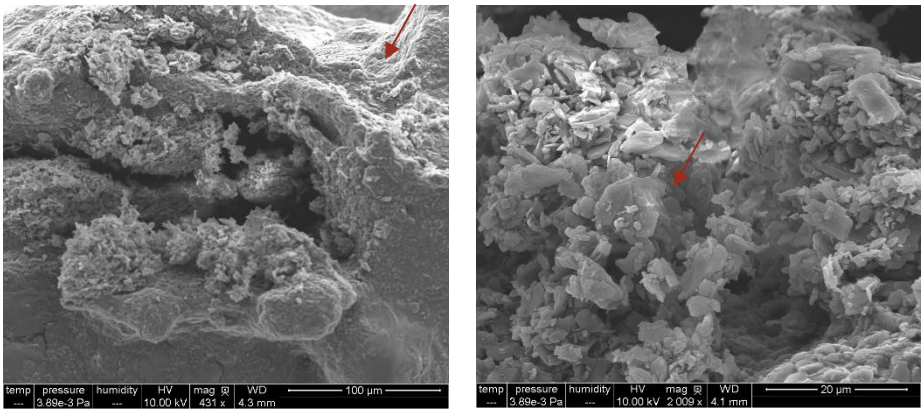

Figure 62. SEM micrograph of Atenolol crystals present on the surface of the hydrogel.

As we can see in Figure 62, the surface of the hydrogel seems heterogeneous and not smooth. With the SEM technique, crystals are visible in the cross section of GLYA12.5, which were present in all the sample but seem to be more localized near the pores.

Under higher magnification, smaller pores can also be seen. Their size seems to be from 20 to around 100 μm, thus being heterogeneous. The formation of these pores could be due to the evaporation of solvent, which should be water in this case, when vacuum is applied to the sample. Last, the pores seem to be interconnected with each other as can be seen in Figure 63.

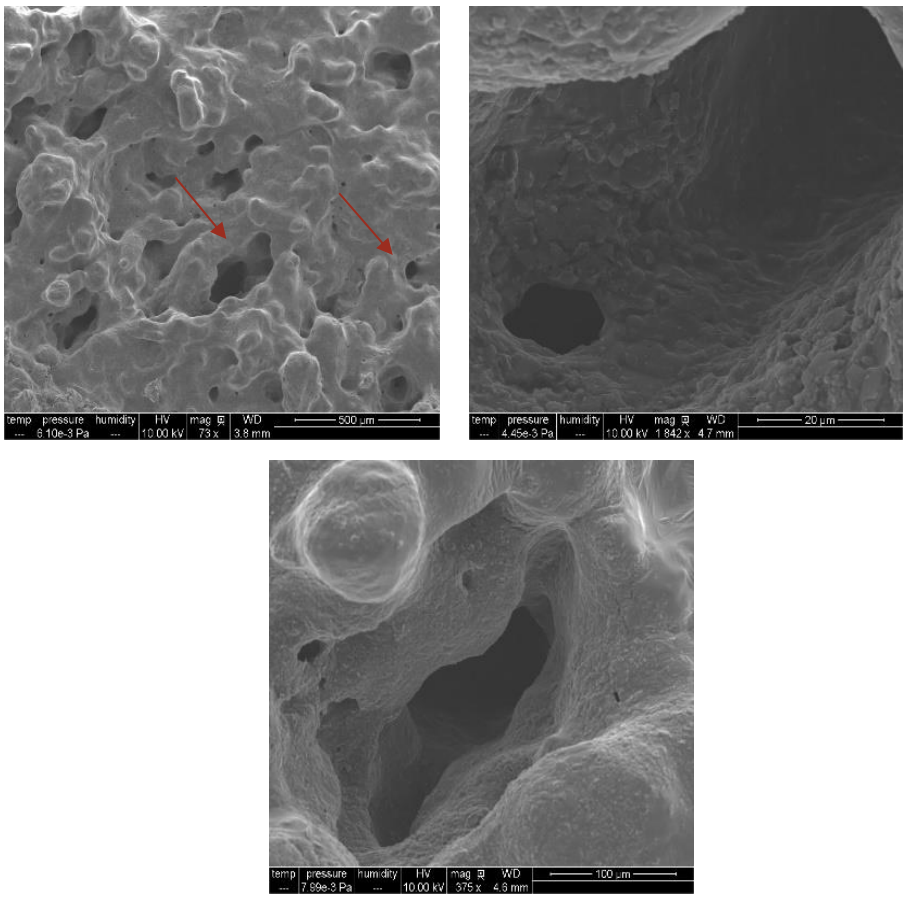

Figure 63. SEM micrograph of interconnecting pores on GLYA12.5 mixture.

When comparing with GLYA0 (Figure 65) it can be assumed that the crystals are probably formed by atenolol, as the blank does not contain any.

9.9.2 SEM OF GLYA12.5 AFTER PH TEST AND LYOPHILIZATION

Moving on to comparing the sample before and after the pH test. The sample is clearly affected by the acidic environment or lyophilization as it is eroded on the surface. Seems that it started to erode from the outer layer as it shows roughness and fibrous appearance but the centre of the cross section is still pretty similar to the SEM images of GLYA12.5 before the pH test. The surface texture could be due to both pH and lyophilization processes. Notably, atenolol crystals are not visible this time (Figure 64).

The hydrogel should have collapsed under low pH values due to the CMC contained in it, protecting the drug, but it seems that all the atenolol has been dissolved on the surface. Nonetheless, the fibrous appearance could be due to collapsed CMC chains. Methods such as vacuum can also affect the structure and properties of the finished pills as well as shrinkage.

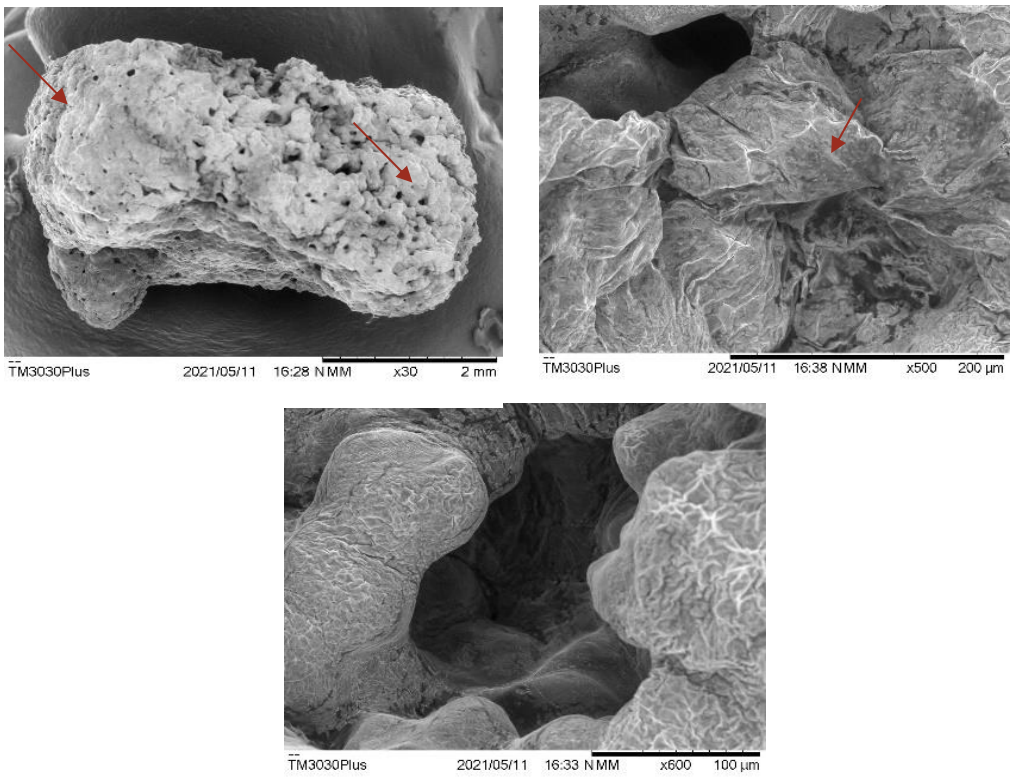

Figure 64. SEM micrograph of the cross section of GLVA12.5 after the pH test and vacuum. Atenolol crystals are not visible. Different size pores visible.

9.9.3 SEM OF GLVA0 AFTER PH TEST AND LYOPHILIZATION

Then, SEM characterization of a blank was made in order to compare the effect of the drug in the hydrogel. In this case the material seems much different to the previous ones as we can see in Figure 65.

The surface of the blank is much smoother compared with the previous glycerol-based hydrogel. There are no pores in it, cracks appeared instead, probably due to the evaporation of solvent under vacuum and the lyophilization process. It seems like without drug the gel seems to be collapsed as it was expected when subjecting CMC to acidic pH.

Thus, dispersion of atenolol could promote pore formation under acidic pH, due to dissolution taking into account that the hydrogel containing 12.5% of atenolol did not show any crystals after the pH test.

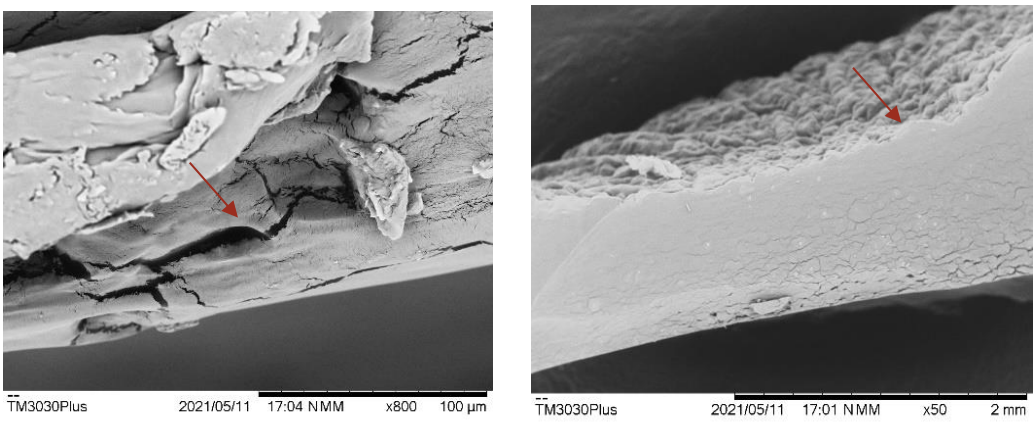

Figure 65. SEM micrograph of GLYA0 blanks cross section.

9.9.4 SEM OF PEGA0 AFTER PH TEST AND LYOPHILIZATION

Last, SEM characterization of the other blank was made. It looked more fibrous than the previous samples. Furthermore, this sample seems to be highly eroded with very large pores that could almost be described as channels. Different sized pores are clearly visible, up to 1 mm in diameter, which differentiates this composition from the glycerol-based blank that contained almost none.

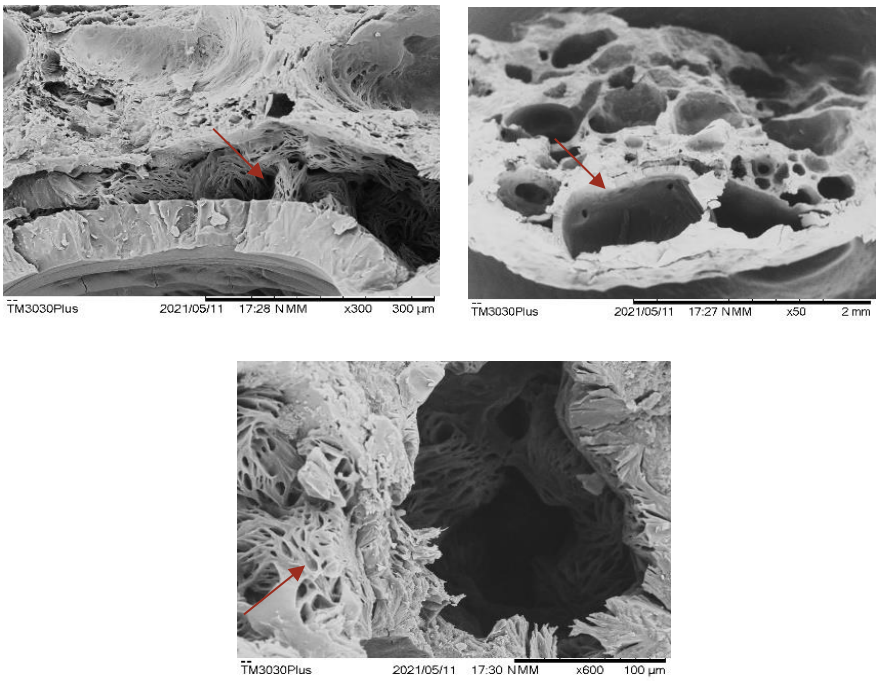

Figure 66. SEM micrograph of PEGA0 cross section SEM. Porous material.

It needs to be taken into account that PEG based hydrogels contain a higher percentage of water in their structure, thus, when the lyophilization is done or vacuum is applied, it can be vaporized leaving the hydrogel fibrous as in Figure 66.

To conclude with the morphological characterization section, it seems like the adhesion between layers is quite good for the samples characterized, as there are not any visible fault lines. However, it could be due to the cutting process as well, which alters the surface of the material. Atenolol is clearly visible as a solid in the materials before exposing it to acidic pH.

In glycerol-based materials interconnected pores seem to appear only in drug containing hydrogels, whereas in PEG-based hydrogel pores appeared without any drug contained. Thus, there is a morphological difference between the two materials even though with rheology tests they seem similar.

Keeping in mind that the CMC containing hydrogel should retain its cargo at acidic pH, in GLYA12.5 it seems that it is not a suitable formulation for that purpose. The PEG-samples contain much more water which can be removed by lyophilization resulting in a much more porous material, which might be unsuitable for retaining the drug as well.

Further SEM characterization of the remaining samples is needed in order to confirm the results obtained and the theories hypothesised until now.

10.1 CONCLUSION

After doing rheological and morphological characterizations some conclusions can be obtained. First, thanks to the formulation modification and rheological characterization, it was possible to print drug containing hydrogels with different drugs and concentrations. In addition, rheology allowed us to discuss the interactions between polymeric matrixes. It has been shown that atenolol above its solubility limit forms homogeneous hydrogels except in the case of glycerol base. In GLYA12.5 the dispersions seem not to be homogeneous, thus increasing the G' and G'' values of the mixture unexpectedly probably due to the atenolol particle scaffold formed.

It is probable that the rheological behaviour of the samples is dependent on the hydrogels structure and on the concentration of the API loaded; as well as on the actual API's chemical structure. Comparing GLYA12.5 and GLYH12.5 for example, they are above atenolol's solubility limit and their rheological behaviour is different. Same happens by comparing PEGA8 and GLYA12.5 where the behaviour is different again, being API-matrix interaction dependent.

Although the drug formulations were suitable for 3D printing, further research is needed to determine the most optimal printing parameters for each formulation easier, and not by trial and error. The objective is to achieve accurate dimensions and resolution, and thus dosing. In fact, even though all the formulations were printable, only glycerol-based formulations that contained high drug concentrations showed good resolution (GLYA12.5 and GLYA12.5H6.25).

It has also been shown that the restoration of the hydrogels network does not play such an important role as it was expected at the begging. Even though PEG-based hydrogels had better restoration kinetics, more CAD design accurate pills were obtained with the glycerol-based ones. Hence, a printability criterion has been obtained, where hydrogels with G' values above 1000 Pa have better resolutions.

The mathematical model does not adjust to the parameters used in this thesis, probably due to the assumptions made. However, it has been shown that the pressure parameters used in the Bioplotter for the extrusion of the material are directly correlated to the material's rheology, specifically to the yield stress value.

By the morphological characterization of the printed pills before and after the pH test and lyophilization processes showed that the CMC's pH responsiveness is good as it was expected, but not enough for the purpose of protecting the drug from dissolving in the stomach. By comparing GLYA12.5 before and after the pH test, it has been shown that the

atenolol contained dissolved in the acidic environment, even though CMC collapsed in such pH (pH=1.2) and thus, it should have stopped the drug liberation.

Last, by SEM it has also been shown that even though the rheological properties of the two blanks (PEG- and glycerol-based) were similar, their behaviour in acidic pH is really different. PEG-based hydrogels seem to be more affected than the glycerol based blank, which seemed to be collapsed.

10.2 CONCLUSIONES

Tras realizar caracterizaciones reológicas y morfológicas se pueden obtener algunas conclusiones. En primer lugar, gracias a la modificación de la formulación y caracterización reológica, fue posible imprimir fármacos que contenían hidrogeles con diferentes fármacos y concentraciones. Además, la reología nos permitió discutir las interacciones entre matrices poliméricas. Se ha demostrado que el atenolol por encima de su límite de solubilidad forma hidrogeles homogéneos excepto en el caso de la base de glicerol. En GLYA12.5 las dispersiones parecen no ser homogéneas, aumentando así los valores G' y G" de la mezcla inesperadamente probablemente debido al andamiaje de partículas de atenolol formado en estas mezclas.

Es probable que el comportamiento reológico de las muestras dependa de la estructura de los hidrogeles y de la concentración del API cargado; además de la estructura química del API. Comparando GLYA12.5 y GLYH12.5 por ejemplo, están por encima del límite de solubilidad de atenolol y su comportamiento reológico es diferente. Lo mismo sucede al comparar PEGA8 y GLYA12.5 donde el comportamiento es diferente de nuevo, siendo dependiente de la interacción API-matriz.

Aunque las formulaciones de fármacos eran adecuadas para la impresión 3D, se necesita más investigación para determinar los parámetros de la impresora óptimos para cada formulación sin el método de prueba y error, con el objetivo de lograr dimensiones y resolución precisas, y por lo tanto una dosificación precisa. De hecho, a pesar de que todas las formulaciones eran imprimibles, sólo las formulaciones a base de glicerol que contenían altas concentraciones de fármacos mostraron buena resolución (GLYA12.5 y GLYA12.5H6.25).

También se ha demostrado que la restauración de la red de hidrogeles no juega un papel tan importante como se esperaba en un principio. A pesar de que los hidrogeles basados en PEG tenían una mejor cinética de restauración, se obtuvieron píldoras más precisas al diseño CAD con las basadas en glicerol. Por lo tanto, se ha obtenido un criterio

de imprimibilidad, donde se requiere que los hidrogeles presenten valores de G' por encima de 1000 Pa para tener buenas resoluciones.

El modelo matemático no se ajusta a los parámetros utilizados en esta tesis, probablemente debido a las suposiciones realizadas. Sin embargo, se ha demostrado que los parámetros de presión utilizados en la Bioplotter para la extrusión del material están directamente correlacionados con la reología del material, específicamente con el valor de esfuerzo de fluencia.

Por la caracterización morfológica de las pastillas impresas antes y después de la prueba de pH y los procesos de liofilización se pudo observar que la capacidad de respuesta del pH del CMC es tan buena como se esperaba, pero no sirve para el propósito de proteger el medicamento de disolverse en el estómago. Al comparar GLYA12.5 antes y después de la prueba de pH, se ha demostrado que el atenolol contenido se disuelve en el ambiente ácido, a pesar de que el CMC colapsara en dicho pH (pH = 1.2) y, por lo tanto, debería haber protegido el medicamento.

Por último, por SEM también se ha observado que aunque las propiedades reológicas de los dos blancos (basados en PEG y glicerol) eran similares, su comportamiento en pH ácido es diferente. El hidrogel basado en PEG parece más afectado que el basado en glicerol, que parece colapsado.

11. OUTLOOK AND FUTURE WORK

The basic characterization of the mixtures prepared has been completed in this thesis, although there is still a lot of work to do. The following steps in the project can be divided in further physical characterization, morphology studies and 3D printing (Figure 67).

Regarding physical characterization, a try will be made quantifying hydrogen bonding interactions of each mixture by rheology. For this purpose, strain and frequency sweeps will be made at different temperatures and frequencies. In addition, DMTA measurements will also be made (See *11.1 HYDROGEN BONDING* and *11.2 DMTA*).

Morphology-wise, further SEM characterization needs to be done in order to finish with the mixtures prepared in this work. In the future there is also the intention of printing more complex polypills. Hence, chitosan-based hydrogels are being prepared with the purpose of achieving a floating polypill. This objective is further explained in the next section (See *11.3 CHITOSAN AND BICARBONATE MIXTURES*).

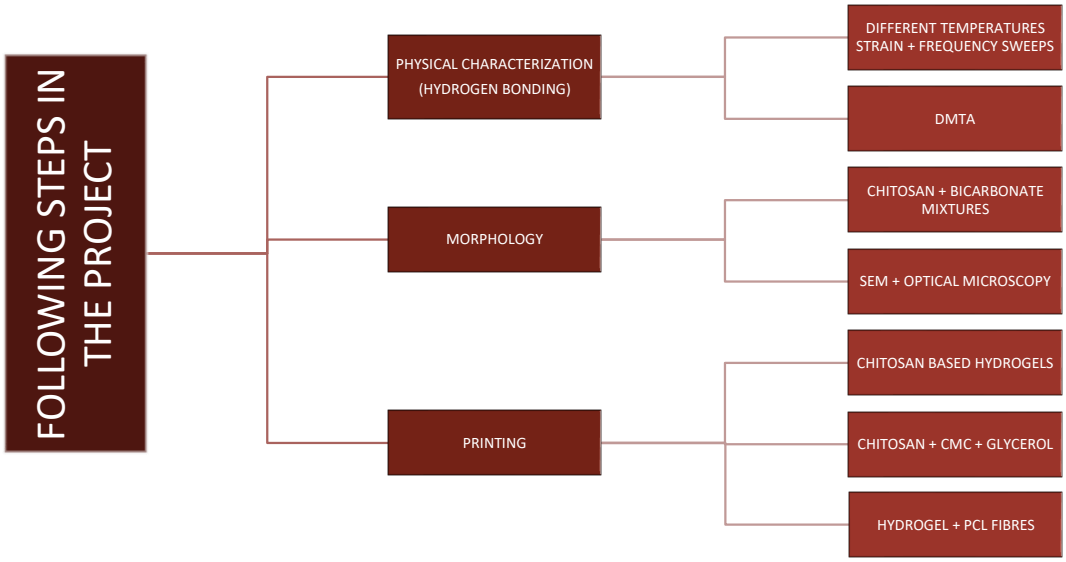

Figure 67. Scheme of the remaining work.

11.1 HYDROGEN BONDING

The objective of multifrequency tests was quantifying the strength of hydrogen bonding present in each mixture as the composition changed from one to another. Slight changes on G' values on both strain and frequency sweeps are expected due to hydrogen bonding, which is both frequency and temperature dependent. Due to the time had for the thesis, only a samples characterization was completed. Thus, there is not enough information about this method.

First, strain sweeps were measured at 3 different frequencies: 0.1, 1 and 10 Hz. Each frequency was also measured at 2 different temperatures, -10 and 50ºC. The behaviour expected is the hydrogel being more elastic at -10 ºC as it should be frozen. Furthermore, comparing the sweeps at one of the temperatures, 50ºC for example, it is expected to have higher values following: 0,1Hz‹1Hz‹10Hz as the frequency is inversely proportional to the experimental time (Figure 68).

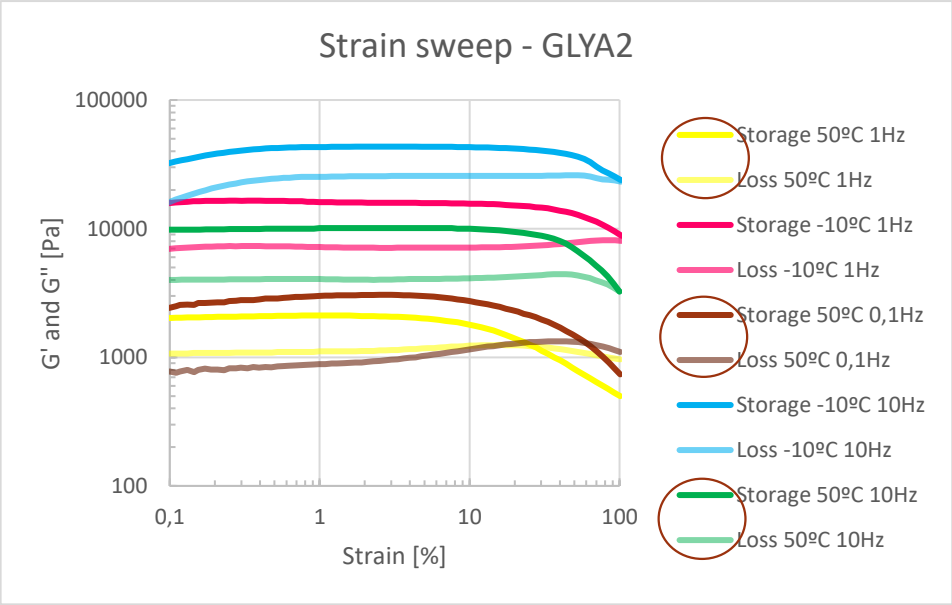

Figure 68. Strain sweeps for GLYA2 at 3 frequencies: 0.1, 1 and 10 Hz. Each frequency measured at -10 and 50ºC.

On the contrary of what was expected, the G' values followed 10Hz›0,1Hz›1Hz. This behaviour is not explainable by hydrogen bonding. Hence, DMTA should be used in order to confirm the results obtained by rheology. Anyways, there is still no more data available.

Last, the expected temperature related behaviour has been confirmed as we can see in Figure 69.

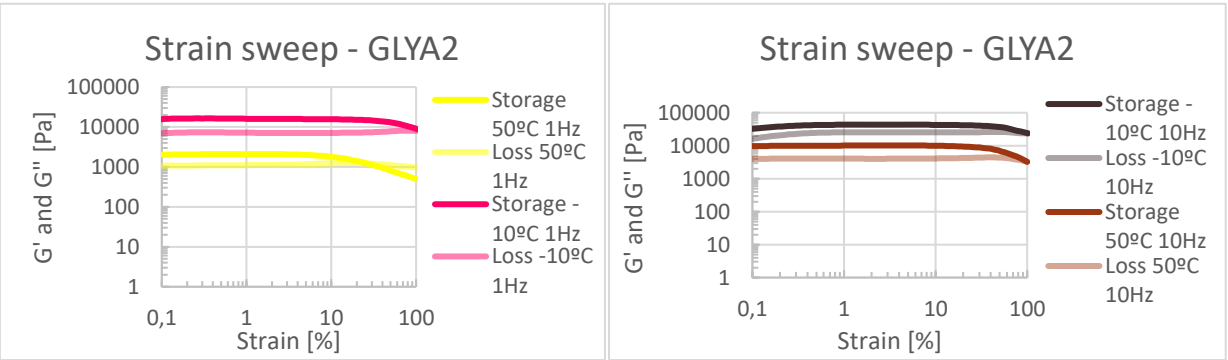

Figure 69. GLYA2 strain sweeps at 1(left) and 10 Hz (right). Each frequency has been measured at -10 and 50ºC. G' values are higher for the frozen sample.

At -10ºC the sample was frost and more elastic behaviour was observed in the three frequencies measured. At 50ºC the sample has enough energy to contain movement. Hence, hydrogen bond formation and break are easier than in the frozen state where its more rigid.

11.2 DMTA

Dynamic mechanical thermal analysis (DMTA) of GLYH12.5 has made with the purpose of confirming rheology tests made for the quantification of hydrogen bonding (Figure 70). In addition, DMTA can be used to test the mechanical properties of a hydrogel. When the temperature is continuously changing, the material is exposed to oscillatory shear. [97] The obtained data is used to find out characteristic phase changes such as the occurring of melting and crystallization or the glass transition. Unfortunately, no reproducible results were obtained yet.

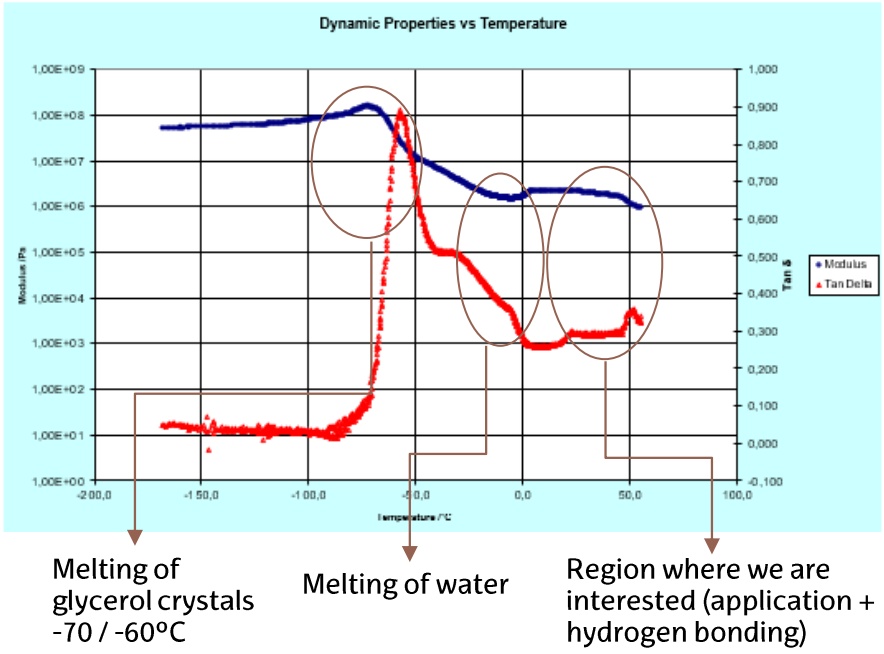

Figure 70. DMTA of GLYH12.5.

On the measured DMTA two main transitions can be seen: from -70 to -60ºC the melting of glycerol vrystals appears. Later on a shoulder can be seen from -20 to 0ºC that is related to the melting of whater. Howerver, the region where we are interested in is the region above 0ºC, where the application of the technnique takes place.

11.3 CHITOSAN AND BICARBONATE MIXTURES

The last step in the thesis was the preparation of chitosan-based hydrogels. The idea is achieving printing a pill with two differentiated parts. One of them would be the mixtures prepared in this thesis and the other one a chitosan-based gas liberating system in order to fabricate floatable oral drug delivery systems.

In effervescent or gas generating systems (Figure 72), the generation of air bubbles causes buoyancy. These floating systems use matrices developed using swellable polymers such as polysaccharides like chitosan and effervescent agents such as sodium bicarbonate. [33] In these systems, the dosage form floats on the gastric liquid in the stomach due to the release of carbon dioxide. Two-layer or multi-layer systems have been designed where gas generating agents are added into some of the layers, which allows to prepare drug and excipients independently. [98], [99] They are usually prepared by a low-density polymer, and effervescent compound; sodium bicarbonate, for example.

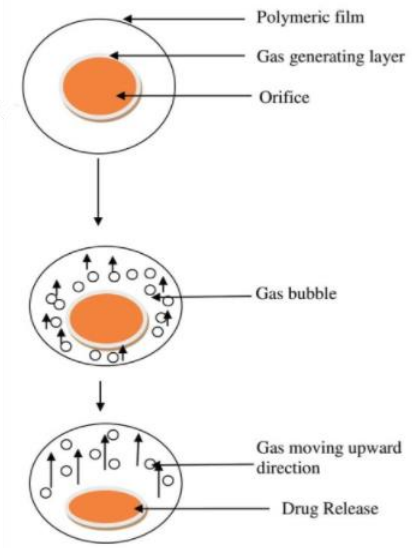

Figure 72. Mechanism of floatation of effervescent systems via CO2 liberation. [119]

These systems utilize the effervescent reaction when the hydrogel comes into contact with the low pH gastric juice. Then, when the liquid penetrates into the tablet, the system produces carbon dioxide gas and makes the tablet starts to float. Acids, bicarbonates and carbonates (the effervescent compounds) react in gastric acid forming CO_2. [100]

$$NaHCO_3 + HCl \rightarrow NaCl + H_2O + CO_2$$

First, chitosan flakes were dissolved in aqueous acetic acid. They were agitated for more than 24h to ensure that all the chitosan was dissolved. Then, they were syringe crosslinked by dropwise addition into ethanolic NaOH. Sodium carbonate was added in order to make a CO_2 gas liberating system, which makes the chitosan hydrogel float (Figure 71).

This way chitosan hydrogel spheres were obtained. Chitosan (Figure 73) is a cationic polysaccharide with a variable number of N-glucosamine and N-acetyl-glucosamine groups. The presence of primary amine of glucosamine residue makes chitosan as a pH-responsive polycation. Thus, it can be found swollen in basic environment and collapsed in acidic ones. Its searched characteristics for oral drug delivery are biodegradability and biocompatibility. [101]

The intention is seeing if this material is printable or not but it has not been tried yet.

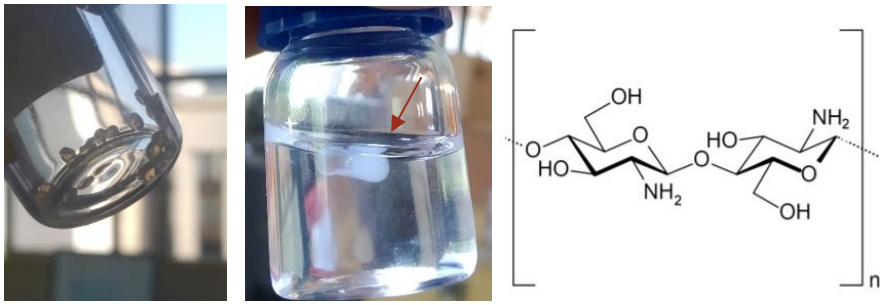

Figure 73. Chitosan based hydrogels obtained and its molecular structure.

12.REFERENCES

[1] "Opportunities, Challenges, and Policy Implications of Additive Manufacturing 3D Printing United States Government Accountability Office," 2015.

[2] B. C. Gross, J. L. Erkal, S. Y. Lockwood, C. Chen, and D. M. Spence, "Evaluation of 3D printing and its potential impact on biotechnology and the chemical sciences," *Anal. Chem.*, vol. 86, no. 7, pp. 3240–3253, 2014, doi: 10.1021/ac403397r.

[3] "What is 3D Printing? - Technology Definition and Types - TWI." https://www.twi-global.com/technical-knowledge/faqs/what-is-3d-printing (accessed Jun. 20, 2021).

[4] J. Norman, R. D. Madurawe, C. M. V. Moore, M. A. Khan, and A. Khairuzzaman, "A new chapter in pharmaceutical manufacturing: 3D-printed drug products," *Adv. Drug Deliv. Rev.*, vol. 108, pp. 39–50, 2017, doi: 10.1016/j.addr.2016.03.001.

[5] W. E. Katstra, R. D. Palazzolo, C. W. Rowe, B. Giritlioglu, P. Teung, and M. J. Cima, "Oral dosage forms fabricated by Three Dimensional Printing(TM)," *J. Control. Release*, vol. 66, no. 1, pp. 1–9, May 2000, doi: 10.1016/S0168-3659(99)00225-4.

[6] I. Gibson, D. Rosen, B. Stucker, and M. Khorasani, *Additive Manufacturing Technologies*. Springer International Publishing, 2021.

[7] S. Ahadian *et al.*, "Micro and nanoscale technologies in oral drug delivery," 2020, doi: 10.1016/j.addr.2020.07.012.

[8] M. P. Chhaya, P. S. P. Poh, E. R. Balmayor, M. Van Griensven, J. T. Schantz, and D. W. Hutmacher, "Additive manufacturing in biomedical sciences and the need for definitions and norms," *Expert Rev. Med. Devices*, vol. 12, no. 5, pp. 537–543, Sep. 2015, doi: 10.1586/17434440.2015.1059274.

[9] "3D printing and traditional manufacturing processes." https://www.sculpteo.com/blog/2019/07/16/comparison-between-3d-printing-and-traditional-manufacturing-processes-for-plastics-3 (accessed Jun. 20, 2021).

[10] A. Goyanes, A. B. M. Buanz, A. W. Basit, and S. Gaisford, "Fused-filament 3D printing (3DP) for fabrication of tablets," *Int. J. Pharm.*, vol. 476, no. 1, pp. 88–92, Dec. 2014, doi: 10.1016/j.ijpharm.2014.09.044.

[11] M. Hofmann, "3D printing gets a boost and opportunities with polymer materials," *ACS Macro*

Lett., vol. 3, no. 4, pp. 382–386, 2014, doi: 10.1021/mz4006556.

[12] D. G. Yu, L. M. Zhu, C. J. Branford-White, and X. L. Yang, "Three-dimensional printing in pharmaceutics: Promises and problems," *J. Pharm. Sci.*, vol. 97, no. 9, pp. 3666–3690, Sep. 2008, doi: 10.1002/jps.21284.

[13] M. Vaezi, H. Seitz, and S. Yang, "A review on 3D micro-additive manufacturing technologies," *International Journal of Advanced Manufacturing Technology*, vol. 67, no. 5–8. Springer London, pp. 1721–1754, Nov. 25, 2013, doi: 10.1007/s00170-012-4605-2.

[14] M. Alomari, F. H. Mohamed, A. W. Basit, and S. Gaisford, "Personalised dosing: Printing a dose of one's own medicine," *Int. J. Pharm.*, vol. 494, no. 2, pp. 568–577, Oct. 2015, doi: 10.1016/j.ijpharm.2014.12.006.

[15] B. T. Peek, "Accuracy of Tablet Splitting by Elderly Patients," *JAMA J. Am. Med. Assoc.*, vol. 288, no. 4, pp. 451–452, Jul. 2002, doi: 10.1001/jama.288.4.451.

[16] M. A. Azad, D. Olawuni, G. Kimbell, A. Z. M. Badruddoza, M. S. Hossain, and T. Sultana, *Polymers for extrusion-based 3D printing of pharmaceuticals: A holistic materials–process perspective*, vol. 12, no. 2. 2020.

[17] B. Wendel, D. Rietzel, F. Kühnlein, R. Feulner, G. Hülder, and E. Schmachtenberg, "Additive processing of polymers," *Macromolecular Materials and Engineering*, vol. 293, no. 10. John Wiley & Sons, Ltd, pp. 799–809, Oct. 10, 2008, doi: 10.1002/mame.200800121.

[18] D. T. Pham and R. S. Gault, "A comparison of rapid prototyping technologies," *Int. J. Mach. Tools Manuf.*, vol. 38, no. 10–11, pp. 1257–1287, Oct. 1998, doi: 10.1016/S0890-6955(97)00137-5.

[19] "How Does Powder-Based 3D Printing Work? | Help Center | i.materialise." https://imaterialise.helpjuice.com/design-printing/powder-based-3d-printing (accessed Jun. 20, 2021).

[20] "VAT Photopolymerisation | Additive Manufacturing Research Group | Loughborough University." https://www.lboro.ac.uk/research/amrg/about/the7categoriesofadditivemanufacturing/vatphotopolymerisation/ (accessed Jun. 20, 2021).

[21] J. Goole and K. Amighi, "3D printing in pharmaceutics: A new tool for designing customized drug delivery systems," *International Journal of Pharmaceutics*, vol. 499, no. 1–2. Elsevier B.V., pp. 376–394, Feb. 29, 2016, doi: 10.1016/j.ijpharm.2015.12.071.

[22] A. J. Capel, R. P. Rimington, M. P. Lewis, and S. D. R. Christie, “3D printing for chemical, pharmaceutical and biological applications,” *Nature Reviews Chemistry*, vol. 2, no. 12. Nature Publishing Group, pp. 422–436, Dec. 01, 2018, doi: 10.1038/s41570-018-0058-y.

[23] B. K. Lee, Y. H. Yun, J. S. Choi, Y. C. Choi, J. D. Kim, and Y. W. Cho, “Fabrication of drug-loaded polymer microparticles with arbitrary geometries using a piezoelectric inkjet printing system,” *Int. J. Pharm.*, vol. 427, no. 2, pp. 305–310, May 2012, doi: 10.1016/j.ijpharm.2012.02.011.

[24] K. Vithani, A. Goyanes, V. Jannin, A. W. Basit, S. Gaisford, and B. J. Boyd, “An Overview of 3D Printing Technologies for Soft Materials and Potential Opportunities for Lipid-based Drug Delivery Systems,” *Pharmaceutical Research*, vol. 36, no. 1. Springer New York LLC, pp. 1–20, Jan. 01, 2019, doi: 10.1007/s11095-018-2531-1.

[25] C. Y. Liaw and M. Guvendiren, “Current and emerging applications of 3D printing in medicine,” *Biofabrication*, vol. 9, no. 2. Institute of Physics Publishing, p. 024102, Jun. 07, 2017, doi: 10.1088/1758-5090/aa7279.

[26] C. Li *et al.*, “Recent progress in drug delivery,” *Acta Pharmaceutica Sinica B*, vol. 9, no. 6. Chinese Academy of Medical Sciences, pp. 1145–1162, Nov. 01, 2019, doi: 10.1016/j.apsb.2019.08.003.

[27] A. Melocchi, F. Parietti, A. Maroni, A. Foppoli, A. Gazzaniga, and L. Zema, “Hot-melt extruded filaments based on pharmaceutical grade polymers for 3D printing by fused deposition modeling,” *Int. J. Pharm.*, vol. 509, no. 1–2, pp. 255–263, Jul. 2016, doi: 10.1016/j.ijpharm.2016.05.036.

[28] “Short fiber reinforced composites for fused deposition modeling.” https://www.infona.pl/resource/bwmeta1.element.elsevier-e273710d-f73e-3ac5-bcfe-62ea5c7ff15b (accessed Jun. 20, 2021).

[29] M. A. Alhnan, T. C. Okwuosa, M. Sadia, K. W. Wan, W. Ahmed, and B. Arafat, “Emergence of 3D Printed Dosage Forms: Opportunities and Challenges,” *Pharmaceutical Research*, vol. 33, no. 8. Springer New York LLC, pp. 1817–1832, Aug. 01, 2016, doi: 10.1007/s11095-016-1933-1.

[30] S. A. Khaled, J. C. Burley, M. R. Alexander, and C. J. Roberts, “Desktop 3D printing of controlled release pharmaceutical bilayer tablets,” *Int. J. Pharm.*, vol. 461, no. 1–2, pp. 105–111, Jan. 2014, doi: 10.1016/j.ijpharm.2013.11.021.

[31] J. Firth, A. W. Basit, and S. Gaisford, “The role of semi-solid extrusion printing in clinical practice,” in *AAPS Advances in the Pharmaceutical Sciences Series*, vol. 31, Springer Verlag, 2018, pp. 133–151.

[32] A. Abramson *et al.*, “HHS Public Access,” vol. 25, no. 10, pp. 1512–1518, 2020, doi:

10.1038/s41591-019-0598-9.A.

[33] M. J. Bhandwalkar, P. S. Dubal, A. K. Tupe, and S. N. Mandrupkar, “REVIEW ON GASTRORETENTIVE DRUG DELIVERY SYSTEM,” vol. 13, no. 12, 2020.

[34] L. M. Ensign, R. Cone, and J. Hanes, “Oral drug delivery with polymeric nanoparticles: The gastrointestinal mucus barriers,” *Adv. Drug Deliv. Rev.*, vol. 64, no. 6, pp. 557–570, 2012, doi: 10.1016/j.addr.2011.12.009.

[35] R. Arévalo-Pérez, C. Maderuelo, and J. M. Lanao, “Recent advances in colon drug delivery systems,” *Journal of Controlled Release*, vol. 327. Elsevier B.V., pp. 703–724, Nov. 10, 2020, doi: 10.1016/j.jconrel.2020.09.026.

[36] J. F. Reinus and D. Simon, *Gastrointestinal anatomy and physiology: The essentials*. Wiley Blackwell, 2014.

[37] L. Liu, W. Yao, Y. Rao, X. Lu, and J. Gao, “pH-Responsive carriers for oral drug delivery : challenges and opportunities of current platforms,” vol. 7544, 2017, doi: 10.1080/10717544.2017.1279238.

[38] M. N. Martinez and G. L. Amidon, “A mechanistic approach to understanding the factors affecting drug absorption: A review of fundamentals,” *J. Clin. Pharmacol.*, vol. 42, no. 6, pp. 620–643, Jun. 2002, doi: 10.1177/00970002042006005.

[39] M. Vertzoni *et al.*, “Impact of regional differences along the gastrointestinal tract of healthy adults on oral drug absorption: An UNGAP review,” *Eur. J. Pharm. Sci.*, vol. 134, pp. 153–175, Jun. 2019, doi: 10.1016/j.ejps.2019.04.013.

[40] M. T. Cook, G. Tzortzis, D. Charalampopoulos, and V. V. Khutoryanskiy, “Microencapsulation of probiotics for gastrointestinal delivery,” *Journal of Controlled Release*, vol. 162, no. 1. pp. 56–67, Aug. 20, 2012, doi: 10.1016/j.jconrel.2012.06.003.

[41] V. V. Khutoryanskiy, “Supramolecular materials: Longer and safer gastric residence,” *Nature Materials*, vol. 14, no. 10. Nature Publishing Group, pp. 963–964, Sep. 23, 2015, doi: 10.1038/nmat4432.

[42] T. G. Iversen, T. Skotland, and K. Sandvig, “Endocytosis and intracellular transport of nanoparticles: Present knowledge and need for future studies,” *Nano Today*, vol. 6, no. 2, pp. 176–185, 2011, doi: 10.1016/j.nantod.2011.02.003.

[43] S. Bazban-shotorbani, M. M. Hasani-sadrabadi, A. Karkhaneh, and V. Serpooshan, “Revisiting structure-property relationship of pH-responsive polymers for drug delivery applications,” *J.*

Control. Release, vol. 253, pp. 46–63, 2017, doi: 10.1016/j.jconrel.2017.02.021.

[44] S. Hua, "Advances in Oral Drug Delivery for Regional Targeting in the Gastrointestinal Tract - Influence of Physiological, Pathophysiological and Pharmaceutical Factors," *Frontiers in Pharmacology*, vol. 11. Frontiers Media S.A., p. 524, Apr. 28, 2020, doi: 10.3389/fphar.2020.00524.

[45] A. M. Pedersen, A. Bardow, S. B. Jensen, and B. Nauntofte, "Saliva and gastrointestinal functions of taste, mastication, swallowing and digestion," *Oral Diseases*, vol. 8, no. 3. Oral Dis, pp. 117–129, 2002, doi: 10.1034/j.1601-0825.2002.02851.x.

[46] "Differences in Small & Large Intestines | Children's Pittsburgh." https://www.chp.edu/our-services/transplant/intestine/education/about-small-large-intestines (accessed Jun. 21, 2021).

[47] "The Digestive Process: The Large Intestine | University Hospitals." https://www.uhhospitals.org/health-information/health-and-wellness-library/article/adult-diseases-and-conditions-v1/the-digestive-process-the-large-intestine (accessed Jun. 21, 2021).

[48] B. Homayun, X. Lin, and H. J. Choi, "Challenges and recent progress in oral drug delivery systems for biopharmaceuticals," *Pharmaceutics*, vol. 11, no. 3, 2019, doi: 10.3390/pharmaceutics11030129.

[49] C. B. Fox, J. Kim, L. V. Le, C. L. Nemeth, H. D. Chirra, and T. A. Desai, "Micro/nanofabricated platforms for oral drug delivery," *J. Control. Release*, vol. 219, pp. 431–444, 2015, doi: 10.1016/j.jconrel.2015.07.033.

[50] T. Pelaseyed *et al.*, "The mucus and mucins of the goblet cells and enterocytes provide the first defense line of the gastrointestinal tract and interact with the immune system," *Immunological Reviews*, vol. 260, no. 1. Blackwell Publishing Ltd, pp. 8–20, 2014, doi: 10.1111/imr.12182.

[51] Y. Han *et al.*, "Multifunctional oral delivery systems for enhanced bioavailability of therapeutic peptides/proteins," *Acta Pharm. Sin. B*, vol. 9, no. 5, pp. 902–922, 2019, doi: 10.1016/j.apsb.2019.01.004.

[52] S. J. Buwalda, T. Vermonden, and W. E. Hennink, "Hydrogels for Therapeutic Delivery : Current Developments and Future Directions," 2017, doi: 10.1021/acs.biomac.6b01604.

[53] N. A. Peppas, J. Z. Hilt, A. Khademhosseini, and R. Langer, "Hydrogels in Biology and Medicine: From Molecular Principles to Bionanotechnology**," 2006, doi: 10.1002/adma.200501612.

[54] N. A. Peppas and J. Klier, "Controlled release by using poly(methacrylic acid-g-ethylene glycol)

hydrogels," *J. Control. Release*, vol. 16, no. 1–2, pp. 203–214, Jun. 1991, doi: 10.1016/0168-3659(91)90044-E.

[55] Z. Shariatinia and A. M. Jalali, "International Journal of Biological Macromolecules Chitosan-based hydrogels : Preparation , properties and applications," *Int. J. Biol. Macromol.*, vol. 115, pp. 194–220, 2018, doi: 10.1016/j.ijbiomac.2018.04.034.

[56] K. R. Kamath and K. Park, "Biodegradable hydrogels in drug delivery," *Adv. Drug Deliv. Rev.*, vol. 11, no. 1–2, pp. 59–84, Jul. 1993, doi: 10.1016/0169-409X(93)90027-2.

[57] N. Michida, M. Hayashi, and T. Hori, "Comparison of event related potentials with and without hypnagogic imagery," *Psychiatry Clin. Neurosci.*, vol. 52, no. 2, pp. 145–147, 1998, doi: 10.1111/j.1440-1819.1998.tb00997.x.

[58] B. Amsden, "Solute diffusion within hydrogels. Mechanisms and models," *Macromolecules*, vol. 31, no. 23, pp. 8382–8395, Nov. 1998, doi: 10.1021/ma980765f.

[59] L. A. Sharpe, A. M. Daily, S. D. Horava, and N. A. Peppas, "Therapeutic applications of hydrogels in oral drug delivery," *Expert Opinion on Drug Delivery*, vol. 11, no. 6. Informa Healthcare, pp. 901–915, 2014, doi: 10.1517/17425247.2014.902047.

[60] S. W. Kim, Y. H. Bae, and T. Okano, "Hydrogels: Swelling, Drug Loading, and Release," *Pharmaceutical Research: An Official Journal of the American Association of Pharmaceutical Scientists*, vol. 9, no. 3. Pharm Res, pp. 283–290, 1992, doi: 10.1023/A:1015887213431.

[61] Y. Hu *et al.*, "A double-layer hydrogel based on alginate-carboxymethyl cellulose and synthetic polymer as sustained drug delivery system," *Sci. Rep.*, vol. 11, no. 1, pp. 1–14, Dec. 2021, doi: 10.1038/s41598-021-88503-1.

[62] P. Robles-Martinez *et al.*, "3D printing of a multi-layered polypill containing six drugs using a novel stereolithographic method," *Pharmaceutics*, vol. 11, no. 6, 2019, doi: 10.3390/pharmaceutics11060274.

[63] "FICHA TECNICA CADUET 10 mg/10 mg COMPRIMIDOS RECUBIERTOS CON PELICULA." https://cima.aemps.es/cima/dochtml/ft/67326/FT_67326.html (accessed Jun. 20, 2021).

[64] R. Fernández-García, M. Prada, F. Bolás-Fernández, M. P. Ballesteros, and D. R. Serrano, "Oral Fixed-Dose Combination Pharmaceutical Products: Industrial Manufacturing Versus Personalized 3D Printing," *Pharmaceutical Research*, vol. 37, no. 7. Springer, pp. 1–22, Jul. 01, 2020, doi: 10.1007/s11095-020-02847-3.

[65] R. Schlosser, “Fixed-Dose and Fixed-Ratio Combination Therapies in Type 2 Diabetes,” *Canadian Journal of Diabetes*, vol. 43, no. 6. Elsevier B.V., pp. 440–444, Aug. 01, 2019, doi: 10.1016/j.jcjd.2019.05.005.

[66] F. Moriarty, K. Bennett, and T. Fahey, “Fixed-dose combination antihypertensives and risk of medication errors,” *Heart*, vol. 105, no. 3, pp. 204–209, Feb. 2019, doi: 10.1136/heartjnl-2018-313492.

[67] D. Q. Wu and C. C. Chu, “Biodegradable hydrophobic-hydrophilic hybrid hydrogels: Swelling behavior and controlled drug release,” *J. Biomater. Sci. Polym. Ed.*, vol. 19, no. 4, pp. 411–429, Apr. 2008, doi: 10.1163/156856208783719536.

[68] E. Larrañeta, S. Stewart, M. Ervine, R. Al-Kasasbeh, and R. F. Donnelly, “Hydrogels for hydrophobic drug delivery. Classification, synthesis and applications,” *Journal of Functional Biomaterials*, vol. 9, no. 1. MDPI AG, Jan. 24, 2018, doi: 10.3390/jfb9010013.

[69] D. Desai, J. Wang, H. Wen, X. Li, and P. Timmins, “Formulation design, challenges, and development considerations for fixed dose combination (FDC) of oral solid dosage forms,” *Pharmaceutical Development and Technology*, vol. 18, no. 6. Informa Healthcare, pp. 1265–1276, 2013, doi: 10.3109/10837450.2012.660699.

[70] K. Z. Vardakas, F. Athanassaki, V. Pitiriga, and M. E. Falagas, “Clinical relevance of in vitro synergistic activity of antibiotics for multidrug-resistant Gram-negative infections: A systematic review,” *Journal of Global Antimicrobial Resistance*, vol. 17. Elsevier Ltd, pp. 250–259, Jun. 01, 2019, doi: 10.1016/j.jgar.2019.01.004.

[71] M. M. Jiménez, M. J. Fresno, and A. Ramírez, “The influence of cosolvent polarity on the flow properties of hydroalcoholic gels. Empirical models,” *Chem. Pharm. Bull.*, vol. 53, no. 9, pp. 1097–1102, Sep. 2005, doi: 10.1248/cpb.53.1097.

[72] T. Instruments, “Understanding Rheology of Structured Fluids,” *TA instruments*, pp. 1–11, 2021.

[73] J. D. Ferry, “Viscoelastic properties of polymers,” *Viscoelastic properties of polymers*. 1980, doi: 10.1149/1.2428174.

[74] R. Fernández-García, M. Prada, F. Bolás-Fernández, M. P. Ballesteros, and D. R. Serrano, “Oral Fixed-Dose Combination Pharmaceutical Products: Industrial Manufacturing Versus Personalized 3D Printing,” *Pharmaceutical Research*, vol. 37, no. 7. Springer, pp. 1–22, Jul. 01, 2020, doi: 10.1007/s11095-020-02847-3.

[75] “Carboxymethylcellulose Sodium.”

https://www.drugfuture.com/chemdata/Carboxymethylcellulose-Sodium.html (accessed Jun. 21, 2021).

[76] S. Javanbakht and A. Shaabani, "Carboxymethyl cellulose-based oral delivery systems," *International Journal of Biological Macromolecules*, vol. 133. Elsevier B.V., pp. 21–29, 2019, doi: 10.1016/j.ijbiomac.2019.04.079.

[77] "Ethylene glycol(107-21-1) MSDS Melting Point Boiling Point Density Storage Transport." https://www.chemicalbook.com/ProductMSDSDetailCB7852707_EN.htm (accessed Jun. 21, 2021).

[78] L. Pietrelli, "Effect of MW and pH on poly(ethylene glycol) adsorption onto carbon," *Adsorption*, vol. 19, no. 5, pp. 897–902, 2013, doi: 10.1007/s10450-013-9503-x.

[79] D. Aydinoɨlu, "Investigation of pH-dependent swelling behavior and kinetic parameters of novel poly(acrylamide-co-acrylic acid) hydrogels with spirulina," *E-Polymers*, vol. 15, no. 2, pp. 81–93, 2015, doi: 10.1515/epoly-2014-0170.

[80] T. Kusukawa, G. Niwa, T. Sasaki, R. Oosawa, W. Himeno, and M. Kato, "Observation of a hydrogen-bonded 3d structure of crystalline glycerol," *Bull. Chem. Soc. Jpn.*, vol. 86, no. 3, pp. 351–353, 2013, doi: 10.1246/bcsj.20120300.

[81] T. Yoshida, T. C. Lai, G. S. Kwon, and K. Sako, "PH-and ion-sensitive polymers for drug delivery," *Expert Opinion on Drug Delivery*, vol. 10, no. 11. NIH Public Access, pp. 1497–1513, 2013, doi: 10.1517/17425247.2013.821978.

[82] J. J. F. Verhoef and T. J. Anchordoquy, "Questioning the use of PEGylation for drug delivery," *Drug Delivery and Translational Research*, vol. 3, no. 6. NIH Public Access, pp. 499–503, Dec. 2013, doi: 10.1007/s13346-013-0176-5.

[83] N. Rouge *et al.*, "Comparative pharmacokinetic study of a floating multiple-unit capsule, a high-density multiple-unit capsule and an immediate-release tablet containing 25 mg atenolol," *Pharm. Acta Helv.*, vol. 73, no. 2, pp. 81–87, 1998, doi: 10.1016/S0031-6865(97)00050-2.

[84] "Atenolol: Side Effects, Dosage, Uses, and More." https://www.healthline.com/health/atenolol/oral-tablet (accessed Jun. 15, 2021).

[85] A. Florence *et al.*, "Powder study of hydrochlorothiazide form II," *Acta Crystallogr. Sect. E Struct. Reports Online*, vol. 61, no. 9, pp. o2798–o2800, Sep. 2005, doi: 10.1107/S1600536805023640.

[86] "Impresora 3D 3D-Bioplotter de EnvisionTEC | Precios y características en Imprimalia 3D."

http://imprimalia3d.com/services/3d-bioplotter (accessed Jun. 16, 2021).

[87] "Table of content," *Electroencephalogr. Clin. Neurophysiol.*, vol. 60, no. 6, pp. 595–599, 1985, doi: 10.1016/0013-4694(85)91127-7.

[88] I. El Aita, J. Breitkreutz, and J. Quodbach, "On-demand manufacturing of immediate release levetiracetam tablets using pressure-assisted microsyringe printing," *Eur. J. Pharm. Biopharm.*, vol. 134, pp. 29–36, Jan. 2019, doi: 10.1016/j.ejpb.2018.11.008.

[89] E. S. Material, "Electronic Supplementary Material (ESI) for Food & Function . This journal is O The Royal Society of Chemistry 2020 Preparation of simulated digestion mediums First , simulated salivary , gastric and intestinal fluids were prepared for later step . The ," pp. 2020–2021, 2020.

[90] Y. Piao and B. Chen, "Self-assembled graphene oxide-gelatin nanocomposite hydrogels: Characterization, formation mechanisms, and pH-sensitive drug release behavior," *J. Polym. Sci. Part B Polym. Phys.*, vol. 53, no. 5, pp. 356–367, 2015, doi: 10.1002/polb.23636.

[91] "Features and applications of Hitachi tabletop microscope TM3030Plus | SI NEWS : Hitachi High-Tech GLOBAL." https://www.hitachi-hightech.com/global/sinews/technical_explanation/07071/ (accessed Jun. 17, 2021).

[92] "Microscopía electrónica de barrido (SEM), ¿para qué me sirve? | Atria." https://www.atriainnovation.com/microscopia-electronica-de-barrido-sem-utilidades/ (accessed Jun. 17, 2021).

[93] R. Behrisch, "Introduction and overview," 1981, pp. 1–8.

[94] "Atenolol Fichas de datos de seguridad." Accessed: Jun. 17, 2021. [Online]. Available: www.edqm.eu.

[95] R. B. Bird, R. C. Armstrong, and O. Hassager, "Dynamics_of_polymeric_liquids_(Vol._1._Fluid_mechanics)_(1987)(2nd_ed.)(en)(649s).pdf." .

[96] R. B. Bird, R. C. Armstrong, and O. Hassager, "DYNAMICS OF POLYMERIC LIQUIDS VOLUME 1 FLUID MECHANICS SECOND EDITION."

[97] "Dynamic Mechanical Thermal Analysis on Polymer Nanocomposites." https://www.azom.com/article.aspx?ArticleID=15320 (accessed Jun. 23, 2021).

[98] R. Garg and G. Gupta, "Progress in Controlled Gastroretentive Delivery Systems," *Trop. J. Pharm. Res.*, vol. 7, no. 3, pp. 1055–1066, 2008, doi: 10.4314/tjpr.v7i3.14691.

[99] R. S. Kesarla, P. A. Vora, B. K. Sridhar, G. Patel, and A. Omri, “Formulation and evaluation of floating tablet of H2-receptor antagonist,” *Drug Dev. Ind. Pharm.*, vol. 41, no. 9, pp. 1499–1511, 2015, doi: 10.3109/03639045.2014.959969.

[100] ahmed a goyal dan sharma, “Effervescent Floating Drug Delivery System,” vol. 3, no. 2, p. 29, 2014.

[101] H. H. Chang, N. C. Cheng, Y. C. Ethan Li, J. H. Wang, and T. H. Young, “pH-responsive characteristics of chitosan-based blends for controlling the adhesivity of cells,” *J. Taiwan Inst. Chem. Eng.*, vol. 111, pp. 34–43, Jun. 2020, doi: 10.1016/j.jtice.2020.04.022.

[102] Z. K. J. Ferguson, *Applied Fluid Rheology*. Elsevier Applied Science, 1991.

[103] R. Pugliese, B. Beltrami, S. Regondi, and C. Lunetta, “Polymeric biomaterials for 3D printing in medicine: An overview,” *Ann. 3D Print. Med.*, vol. 2, p. 100011, Jun. 2021, doi: 10.1016/j.stlm.2021.100011.

[104] C. D. Han, “Rheology in Polymer Processing,” *Acad. Press*, 1976.

[105] “Rod Climbing - The Weissenberg Effect | Non-Newtonian Fluid Dynamics Group.” https://nnf.mit.edu/home/billboard/topic-5 (accessed Jun. 21, 2021).

[106] J. M. Dealy and T. K. P. Vu, “The Weissenberg effect in molten polymers,” *J. Nonnewton. Fluid Mech.*, vol. 3, no. 2, pp. 127–140, Nov. 1977, doi: 10.1016/0377-0257(77)80045-1.

[107] R. A. Figueiredo, C. M. Oishi, A. M. Afonso, I. V. M. Tasso, and J. A. Cuminato, “A two-phase solver for complex fluids: Studies of the Weissenberg effect,” *Int. J. Multiph. Flow*, vol. 84, pp. 98–115, Sep. 2016, doi: 10.1016/j.ijmultiphaseflow.2016.04.014.

[108] R. Hernández, “Diapositivas de la asignatura materiales macromoleculares 2,” *UPV / EHU*, vol. Tema 1, no. Reología, p. 16, 2021.

[109] A.Collier, “Thechniques in Rheological Measurements,” *Chapman Hall*, 1993.

[110] W. W. Graessley, *Polymeric Liquids and Networks: Dynamics and Rheology*. Garland Science, 2008.

[111] “Bosch Packaging Services modifica la línea de termoconformado.” https://www.elempaque.com/temas/Bosch-Packaging-Services-modifica-la-linea-de-termoformado-para-el-envasado-de-pastillas-Emser+102560?pagina=2 (accessed Jun. 10, 2021).

[112] “Medicamentos impresos en 3D: ¿por qué son el futuro de la medicina personalizada? - 3Dnatives.” https://www.3dnatives.com/es/medicamentos-impresos-en-3d-140520202/ (accessed Jun. 10, 2021).

[113] “3D Printer Supports vs. Rafts vs. Brims: What are they and when to use them? « Home 3D Print Guide.” https://home3dprintguide.com/3d-printer-supports-vs-rafts-vs-brims-what-are-they-and-when-to-use-them/ (accessed Jun. 10, 2021).

[114] M. I. Maksud, M. N. Nodin, and S. Hassan, “UTILIZING RAPID PROTOTYPING 3D PRINTER FOR FABRICATING FLEXOGRAPHIC PDMS PRINTING PLATE,” vol. 11, no. 12, 2016, Accessed: Jun. 20, 2021. [Online]. Available: www.arpnjournals.com.

[115] “The GI Tract | Drawing of the GI tract, with labels pointing… | Flickr.” https://www.flickr.com/photos/nihgov/25083237542 (accessed Jun. 09, 2021).

[116] “Most nutrient absorption takes place in small intestine.” https://public.wsu.edu/~rlee/biol103/lect06/sld014.htm (accessed Jun. 10, 2021).

[117] “(PDF) Stimuli-Responsive Polysaccharide-Based Hydrogels.” https://www.researchgate.net/publication/299456933_Stimuli-Responsive_Polysaccharide-Based_Hydrogels (accessed Jun. 20, 2021).

[118] “Gold Sputtering - Houston Electron Microscopy.” https://houstonem.com/gold-sputtering.html (accessed Jun. 22, 2021).

[119] “View of OVERVIEW ON FLOATING DRUG DELIVERY SYSTEM | International Journal of Applied Pharmaceutics.” https://innovareacademics.in/journals/index.php/ijap/article/view/28774/16224 (accessed Jun. 12, 2021).

[120] “(PDF) Hydrodynamic Stability of Newtonian and Non-Newtonian Fluids.” https://www.researchgate.net/publication/251857805_Hydrodynamic_Stability_of_Newtonian_and_Non-Newtonian_Fluids (accessed Jun. 13, 2021).

[121] “Mouse dissection for Principles of Biology.” Accessed: Jun. 10, 2021. [Online]. Available: http://biology.about.com/gi/dynamic/offsite.htm?site=http://www.geocities.com/virtualbiology/necropsy.html.

13. APPENDIX

13.1 RHEOLOGICAL MEASUREMENTS

Viscoelasticity behaviours of polymers affect to the processing of the material as well as the behaviour of the material during its application. The tests made are strain and frequency sweeps as well as time profiles of the materials. Parallel plates are often used for gels and pastes, but could also be used for melted polymers, being a useful rheometer assembly. [102]

All the tests were carried out placing the material between two parallel plates (Figure 74), trimming the sample to obtain a cylinder shape of 1mm height between the plates. This flow unidirectional and it is based on a simple shear flow. In this kind of flows the material's layers slide one on top of each other and the deformation is minimized to one of the axes. [103] This is the base of most of the viscosity measurement devices.

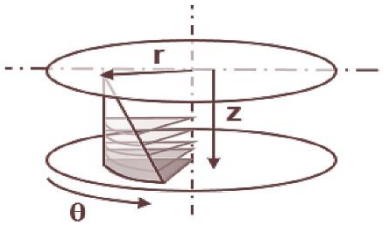

Figure 74. Schematic representation of parallel plates system for a rheometer. [108]

Regarding the flow of the material between two plates the direction of the flow is the angle, due to the movement of one of the plates over the static one. The gradient is formed in the z direction, creating a vector from one of the plates to the other one perpendicularly. Finally, the neutral direction is r, referring to the circle radius. The parameters measured in these measurements are torque and angular speed. [104]

It is also important to have in mind the Weissenberg effect (Figure 75) in these measurements. This effect shows if the material is being subjected to deformations at high speeds and the level of entanglement of the polymer is high, giving the material some elasticity. [105] This viscoelastic effect happens due to the memory of the chains at high speeds and the normal force that is formed. The material does not have enough time to reach a new equilibrium state so it tries to go back to the state it was before the external deformation. [106] Because of its viscoelastic nature, normal forces appear to the direction of the flow that cause these viscoelastic behaviours (Weissenberg and Barus effects, for example). [107] The normal forces that

Figure 75. Weissenberg effect example in a high molecular weight PIB and low molecular weight polyisobutylene solution. [120]

cause these effects are higher as the material is more elastic (G'›G''). The sample could also be expulsed outside the parallel plates at high speeds. [106]

The parallel plates method has two advantages over other measurement types: first, it allows to manipulate the distance between the plates (height) depending on the material's thickness. Second, the flow of the material between parallel plates allows to do oscillatory measurements, key to obtain the material's viscoelasticity spectrum, which gives a lot of information about the material's behaviour. [107] Viscoelasticity is dependent on the time, so in all the measurements one of the parameters taken into account is the time.

13.2 SPECIFIC TESTS

13.2.1 STRAIN SWEEP

Measuring the strain amplitude dependence of the storage and loss moduli (G', G'') is a good first step taken in characterizing viscoelastic behaviour because it will establish the material's linearity. The linear viscoelastic region (LVE) indicates the range in which the test can be carried out without destroying the structure of the sample. It is the region depicted on the left side of the diagram, the range with the lowest strain values (Figure 76). [72]

The measurement is carried out by incrementing the strain (or stress) value gradually at a determined frequency value that stays constant. [108] Other parameters such as temperature are also determined and maintained constant as well.

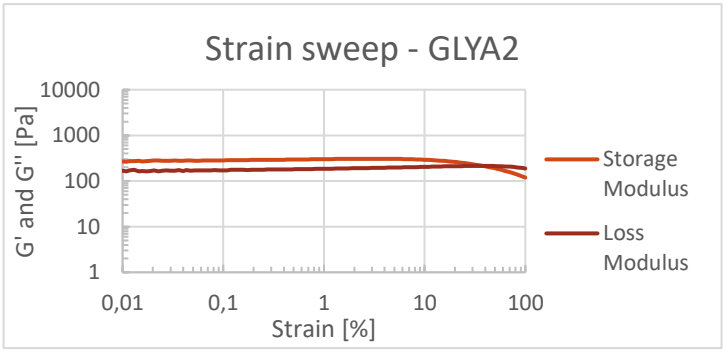

Figure 76. Example of a strain sweep. The linear behaviour extents until a strain value of 10% approximately. The flow point is also visible.

The sweeps can also be used for determining the flow point, independently to if test was performed as a strain sweep (with controlled shear deformation) or a stress sweep (with controlled shear stress). The material becomes progressively more fluid-like, the moduli decline, and G'' exceeds G' eventually. [104]

The flow point or yield stress is the value of the shear stress at the crossover point where both G' and G'' have the same value. At higher shear, the viscous portion will

dominate and the sample flows. Both values (LVE limit and flow point) are dependent on the measuring conditions. [73] The flow point is especially important for the 3D printing application as the material needs to be exposed to higher stress (or strain) values than the flow point in order to be able to extrude the material. Below those values, the material could clog the point.

In the region between yield point and flow point G' is higher than G". Within this yield zone, the initial structural strength of the LVE region has already decreased but the sample still predominantly solid. If a sample shows G" values higher than G' in the linear region (the character of a fluid) it may have a yield point but not a flow point because it is always liquid. [72]

The linear region of the experiment is related to the mechanical properties of the material. Comparing the value of G' with the elastic modulus of a mechanical stress-strain measurement the value is the same, even though the terms don't mean the same. [108]

13.2.2 FREQUENCY SWEEP

After the fluid's linear viscoelastic region has been defined by a strain sweep, its structure can be further characterized using a frequency sweep at a strain below the critical strain so that the measurements are comparable with each other. This provides more information about the effect of colloidal forces, referred to the interactions among particles or droplets and it allows to predict how the viscoelastic properties of the sample vary over time. [72] The viscoelastic spectrum (Figure 77) of the sample is obtained with this measurement. Changes in the material's structure have strong influence over the viscoelastic spectrum. [73]

In frequency sweeps, measurements are made over a range of oscillation frequencies at a constant oscillation amplitude and temperature. [108] For this measurement the strain or stress applied to the sample is constant and the value of the frequency varies in the specified range. [109] Below the critical strain, the elastic modulus G' is often nearly independent of frequency, as would be expected from a structured or solid-like material. The more frequency dependent the elastic modulus is, the more fluid-like is the material. [110]

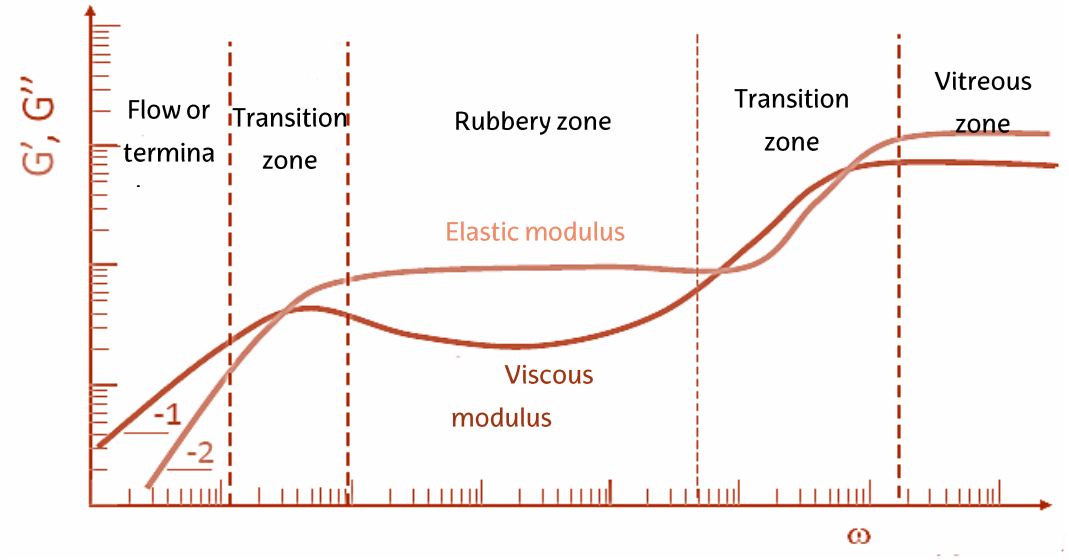

Figure 77. Scheme of a complete frequency sweep where the different parts are pointed out. [108]

The final values of the graphs usually tend to increase due to the lack of mobility liberty. This increase means that in the strain point chosen the G' and G'' values were not totally parallel or the strain value is very low. These values are not reliable.

13.2.3 TIME PROFILE

The time profile has been used for breaking the gel by applying a high strain for some time and then releasing that high strain to control if the gel reforms itself. [73] Once the strain goes back to lower values the gel can restore its properties totally or partially (Figure 78).

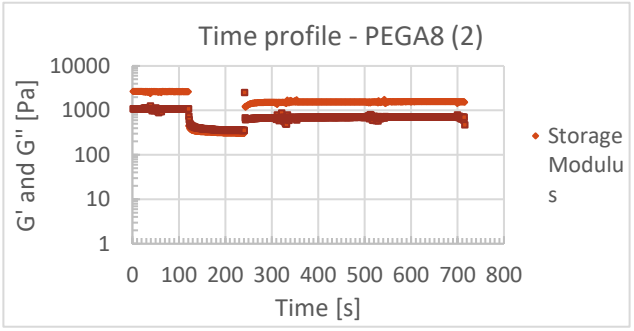

Figure 78. Example of a time profile. Three intervals can be easily differentiated.

By this kind of measurements, we can clearly see the gel's restoration kinetics. It is important that before the high strain is applied lower values of strain are applied to stabilize the gel. This way the gel starts forming a plateau value that serves as the reference value to justify the recovery once it is broken.